8-2005

Computational Investigations of Collision Induced Absorption

Timothy Carl Lillestolen
University of Tennessee, Knoxville

To the Graduate Council:

I am submitting herewith a dissertation written by Timothy Carl Lillestolen entitled "Computational Investigations of Collision Induced Absorption." I have examined the final electronic copy of this dissertation for form and content and recommend that it be accepted in partial fulfillment of the requirements for the degree of Doctor of Philosophy, with a major in Chemistry.

Robert J. Hinde, Major Professor

We have read this dissertation and recommend its acceptance:

Jeffrey Kovac, John Turner, J. Larese, James Mancillas

Accepted for the Council:
Dixie L. Thompson

Vice Provost and Dean of the Graduate School

(Original signatures are on file with official student records.)

To the Graduate Council:

I am submitting herewith a dissertation written by Timothy Carl Lillestolen entitled "Computational Investigations of Collision Induced Absorption". I have examined the final paper copy of this dissertation for form and content and recommend that it be accepted in partial fulfillment of the requirements for the degree of Doctor of Philosophy, with a major in Chemistry.

Robert J. Hinde, Major Professor

We have read this dissertation
and recommend its acceptance:

Accepted for the Council:

Vice Chancellor and Dean of
Graduate Studies

Computational Investigations of Collision Induced Absorption

A Dissertation
Presented for the
Doctor of Philosophy
Degree
The University of Tennessee, Knoxville

Timothy Carl Lillestolen
August 2005

Dedication

This work is dedicated in loving memory to my mother, Kathy Lillestolen. My first teacher, she instilled in me a joy of learning and a vast curiosity for the workings of the world. Without her loving guidance and influence, I would have never made it as far as I have. Thank you.

Acknowledgments

First and foremost, I would like to thank my father for his love and support throughout my life and academic career. He deserves as much of the credit for finishing this degree as I do. I would also like to thank the rest of my family for their continued love and encouragement: Jon, Robert, Shari, Chris, and especially Farmor.

I wish to thank my adviser, RJ Hinde, for his guidance throughout my graduate career and for helping to mold me as a scientist. His enthusiasm for science, coupled with an extraordinary amount of patience, made the five years I spent in his group a truly enjoyable experience.

There are many others in the chemistry department I would like to thank: Dr. Kovac for putting up with my sense of humor for four years; Dr. Larese for his guidance and computational might; John Turner for many interesting conversations over frosty beverages; past and present members of the Hinde group: Phil Stimac, James Mancillas, Lee Warren, Ben-hui Yang, Eugene DePrince and Patrick Moehlen; and all of my other friends in the department.

Abstract

The focus of this dissertation is the computational determination of collision induced absorption spectra. We have focused on two different types of collision induced absorption: that of translational absorption and that of broadening of atomic spectral lines. We have focused on generating high quality ab initio potential energy and dipole moment surfaces, and using these surfaces to calculate fully quantum mechanical absorption spectra for the systems of interest, He-Xe and Na-He.

In the case of He-Xe we have calculated the potential energy and dipole moment surface using the coupled cluster single and doubles method, with a perturbative triples correction, using large correlation consistent basis sets, midbond functions, and an effective core potential on Xenon. We find our potential to be in excellent agreement with several empirical He-Xe potentials in the literature. Using these calculated surfaces, we generate fully quantum mechanical translational absorption spectra for the dimer at 298 K and 1000 K. Our results at 298 K are in good agreement with experimental results. We have also performed an analysis of the functional derivative of the absorption coefficient with respect to the dipole moment at both of these temperatures, and used these derivatives to analyze differences between the spectra calculated using our ab initio potentials, and the spectra computed by other researchers. Finally, we have presented results for the transition dipole moment integrals of the pure rotational transitions of of He-Xe dimers, in order to compare with future theoretical and experimental results.

We have also calculated the potential energy curves for the ground and low-lying excited states of the Na-He dimer using a multi-configurational ab initio approach and large correlation consistent basis sets. We have calculated the ground state dipole moment of the dimer, and used linear response theory to calculate the transition dipole moments between the ground and excited states. We have used these surfaces to calculate a fully quantum mechanical translational absorption spectrum for the ground state of Na-He at 300 K and 1000 K, which is in reasonable agreement with previous theoretical results. We have also used these surfaces to calculate the broadening of the Na-D line due to atomic helium at 1000 K. We present results for the wings of the broadened line, which we find in reasonable agreement with other theoretical results.

Contents

List of Tables

List of Figures

Chapter 1

Motivation

1.1 Absorption Spectra of Extra-Solar Objects with Substellar Masses

Our interest in collision-induced absorption spectra stems from the recent discoveries of brown dwarfs and extra-solar gas giants by the astrophysical community. In 1995, the first confirmed brown dwarf, Gliese 229B, was discovered[32]. Brown dwarfs, a class of substellar-mass objects, were posited to exist as early as 1963[4], but remained elusive due to the cool nature of the objects. Because brown dwarfs begin their lives as stars, they are able to sustain hydrogen fusion for a time but eventually burn out and are unable to maintain surface temperatures of greater than 3000 K. The result of this is that the brown dwarf cools over time, losing much of its luminosity[4,10]. This is further complicated by the chemistry that begins to take place at lower temperatures. As the brown dwarf cools, molecules such as methane, water, ammonia, and carbon monoxide begin to become prevalent in the upper atmosphere causing further reduction in the luminosity by absorbing light emitted from the core of the dwarf[31].

The relatively cool temperatures of brown dwarfs ($\sim$ 800 K to $\sim$ 3000 K) means that many of the molecules that are unable to exist in stars, such as water, carbon monoxide, methane and ammonia, are prevalent in their atmospheres, as well as high concentrations of molecular hydrogen and atomic helium[4]. Thus, in the near-infrared region (1000-2000 nm), the spectra are dominated by these molecules, and it was in fact the presence of methane in the spectra of Gliese 229B that confirmed its classification as a brown dwarf. The visible region of the spectrum, however, is relatively sparse in terms of absorbers, due to the "rainout" or condensation of the heavier metals at low temperatures[10]. Thus, in the brighter dwarfs that have been observed, including GL 229B, the visible region of the spectra is dominated by the lighter alkali metals, mainly lithium, sodium, and potassium.

The near-infrared region of the spectra for these dwarfs is relatively well understood, and can be effectively modeled using a mixture of water, methane, and hydrogen for wavelengths longward of 1000 nm[11]. The visible region, however, is much more difficult. Prominent in this region are the Na D-line ($\sim$ 589 nm) and the K I line ($\sim$ 770 nm), both occurring due to their respective $n^2S \rightarrow n^2P$ transitions ($n = 3$ Na, $n = 4$ K). These lines, however, are significantly broadened (c.f. figure 1.1) and assume the role of the continuum in the region of 400 to 1000 nm, due to the lack of other absorbers in this region[1,10,12]. It is thus important to understand the origins of this line-broadening in order to accurately model the atmosphere of a brown dwarf.

Since brown dwarfs form in much the same manner as stars, they have very similar elemental compositions. They are primarily composed of hydrogen, which exists in molecular form in the atmosphere, and helium. The two elements combine to contribute 99.9% of a brown dwarf's mass, with hydrogen making up 91% of that mass[10]. For this reason, molecular hydrogen and atomic helium are the prime candidates to examine for the broadening of the Na and K spectral lines.

We have chosen to begin our study with the broadening of the Na-D line by atomic helium. This is the simplest case, and while it may not contribute as much to the broadening as molecular hydrogen[1,12], it is an excellent starting point for an investigation of the problem. For the atmospheric conditions thought to exist in a brown dwarf[11], that of moderate pressure *, the theory of collision induced absorption for two atoms has been worked out in detail[22]. At these pressures the absorption occurs due to pairs of atoms that exist in the gas, which exist mostly in free states of nuclear motion, and can be treated using methods similar to those of atomic collision theory[5,20]. We can therefore calculate a fully quantum-mechanical absorption coefficient for this system, that can be used to both better understand the visible spectra of brown dwarfs and as a benchmark for recent[1,12] and future calculations.

In order to study the Na-He problem, it is necessary to have accurate potential surfaces for both the ground and excited states of the dimer, as well the transition dipole moments between ground and excited states. The absorption spectrum will be very sensitive to the difference potential between the ground and excited states[28], and therefore we decided to perform our own ab initio calculations of these values. Since this involves calculating three potential surfaces and two transition dipole moment surfaces for a system that has an odd number of electrons and significant multi-reference character (c.f. Chapters 2,5), we decided to test that our implementation of the theory was correct on a system where accurate experimental data existed.

*We define a moderate pressure to be between the low pressure regime where Doppler broadening is significant and the high pressure regime where multiple encounters between atoms are frequent[22,28].

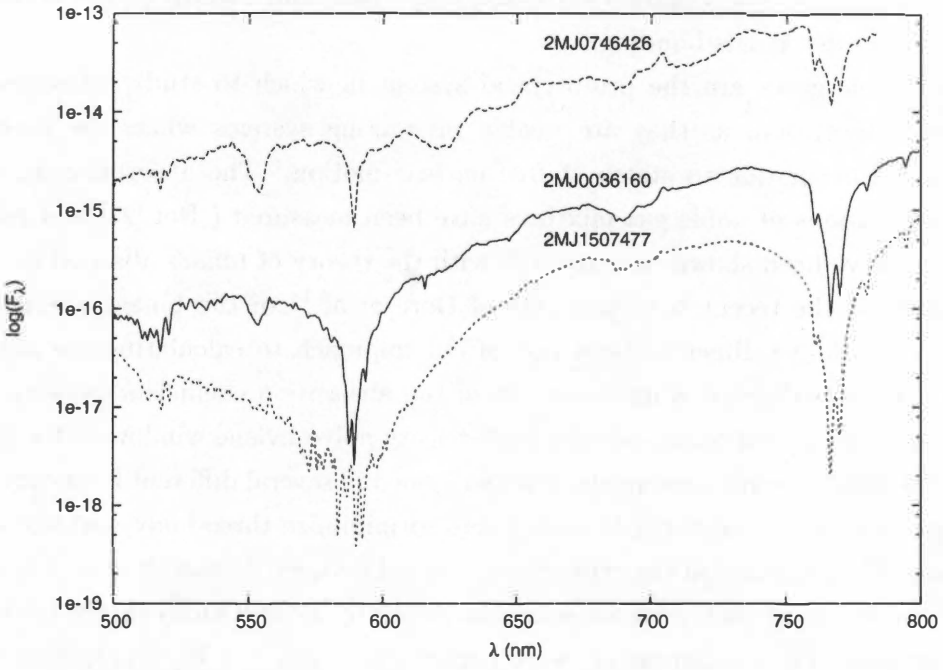

Figure 1.1: Visible spectrum of several brown dwarfs. The spectra of 2MJ003610 and 2MJ0746246 have been offset by a factor of 10 and 100, respectively. The data was obtained by Reid et al.[38] and has been smoothed according to the procedure discussed in section 5.7. The Na D-line is located at 589 nm, and the K I line at 770 nm.

1.2 Translational Absorption

The simplest case of collision-induced absorption is that of a mixture of monatomic gases. At moderate pressures, a pure monatomic gas will not absorb radiation in the microwave or far infrared regions, due to the inversion symmetry that exists between two like atoms. When two dissimilar monatomic gases are mixed, however, a weak absorption band appears in the far infrared. In the low density limit, where contributions from three body and higher order interactions can be neglected, this translational band occurs due to appearance of a weak transient dipole moment that appears when two dissimilar atoms collide. The dipole moment occurs due to the standard exchange, dispersion, and overlap effects found in the treatment of van der Waals bonding.

The noble gases are the prototypical system in which to study collision-induced translational absorption, as they are weakly interacting systems where the majority of absorption will occur due to states of free nuclear motion. The absorption spectra for various combinations of noble gas mixtures have been measured (Ref [22] and references therein), and have been shown to agree well with the theory of binary absorption.

We chose the recent measurements of Dore et al.[18] of the binary absorption coefficient for the He-Xe dimer to be a test of our approach to calculating the absorption coefficient. They performed a measurement of the absorption coefficient between 10 and 600 cm^{-1} using a 1 m cell equipped with high density polyethylene windows. Due to experimental limitations, the measurements were performed in several different frequency ranges, with the pressure being adjusted in each range to minimize three-body and higher order interactions. The pressures in the experiments ranged between 35 and 60 atm. The number density of the atoms at each pressure was determined by using a virial expansion to determine the density. The measurements were performed at 298 $\pm$ 1 K. The quality of these measurements (error estimated to be about 10%, mainly from uncertainties in the virial treatment) makes them an excellent test for our method of calculating the collision induced absorption.

The determination of these absorption coefficients provide an excellent testing ground for evaluating the accuracy of current methods in determining both potential energy surfaces and dipole moment surfaces. We also chose the He-Xe problem because ab initio potentials had not yet been determined in the literature. This is largely due to the size of the xenon atom; with 54 electrons it is difficult to perform an all electron calculation, as the velocity of the inner core electrons is so large that they must be treated relativistically. Recently, however, Peterson et al.[35] introduced a relativistic effective core potential, along with correlation consistent basis sets, which allow us to accurately treat the xenon atom using non-relativistic quantum chemical methods.

Finally, the analysis of the He-Xe absorption coefficient by Frommhold et al.[24], pro-

vides us with a final method which we can test our approach. Frommhold et al. used a parameterized Hartree-Fock Dispersion potential determined from experimental scattering data by Aziz et al.[3], and the spectra of Dore et al.[18] to determine the best fit to a parameterized form of the dipole moment function. The first test of our approach will be to reproduce the results of Frommhold et al., after which we can compare our calculations of both the potentials and dipole moments as well as the spectrum, in order to assess the accuracy of our results.

With the successful completion of the calculation of the He-Xe absorption coefficient, we will then have confidence that our method is suitable for the calculation of the Na-He absorption coefficient, for which reliable experimental data is not available. This confidence is important, as we are interested in using ab initio quantum chemical methods to determine properties of weakly interacting systems, and then using these results to calculate the absorption properties of these systems. This is especially important for astrophysical problems, as replicating the conditions found in the atmospheres of extra-solar objects may not be possible or practical in a laboratory environment, making accurate theoretical results even more important. Finally, we expect that if our approach works well in the case of Na-He, we should be able to calculate the ab initio properties of Na-H_2 which is isoelectronic with Na-He. The extension of this method to the case of the K I line would also be possible.

Chapter 2

Introduction to Electronic Structure Theory

2.1 Introduction

Electronic structure theory is the theory of how electrons "move" in atoms or molecules. In order to describe the electronic structure of an ensemble of electrons, moving in a field of nuclei, it is necessary to turn to quantum mechanics. The theory of quantum mechanics states that because the mass of an electron is so small, it is not localized at any point in space, but is better thought of as a distribution in space, which can be obtained from the wavefunction. The wavefunction for a stationary state of a collection of M nuclei and N electrons can be determined by solving Schrödinger's time-independent wave equation:

$$\hat{H}\Psi = E\Psi. \tag{2.1}$$

In this equation, $\hat{H}$ is the non-relativistic Hamiltonian operator:

$$\begin{aligned}\hat{H} = -\frac{\hbar^2}{2m_e}\sum_{i=1}^{N}\nabla_i^2 \;-\; &\frac{\hbar^2}{2M_A}\sum_{A=1}^{M}\nabla_A^2 - \sum_{i=1}^{N}\sum_{A=1}^{M}\frac{Z_A}{4\pi\epsilon_0 r_{iA}} \\ &+ \sum_{i=1}^{N}\sum_{j>i}^{N}\frac{e^2}{4\pi\epsilon_0 r_{ij}} + \sum_{A=1}^{M}\sum_{B>A}^{M}\frac{Z_A Z_B e^2}{4\pi\epsilon_0 R_{AB}}\end{aligned} \tag{2.2}$$

where A, B refer to nuclei; i, j refer to electrons; m_e is the mass of an electron; M_A is the mass of nucleus A; ∇^2 is the Laplacian operator; Z_A is the atomic number of nucleus A; e is the charge of the electron; r_{ij} is the distance between electrons i and j; r_{iA} is the distance between electron i and nucleus A; R_{AB} is the distance between nuclei A and B; ϵ_0 is the permittivity of vacuum; and $\hbar$ is Planck's constant divided by 2π.

The first two terms in $\hat{H}$ are the kinetic energy operators for the electrons and nuclei, while the third term describes coulombic attraction between electrons and nuclei, and the final two terms describe the interelectronic repulsion and the repulsion between nuclei, respectively. Rewriting this equation in atomic units (cf section **2.1.1** Szabo and Ostlund[44]) we obtain:

$$\hat{H} = -\sum_{i=1}^{N} \frac{1}{2}\nabla_i^2 - \sum_{A=1}^{M} \frac{1}{2M_A}\nabla_A^2 - \sum_{i=1}^{N}\sum_{A=1}^{M} \frac{Z_A}{r_{iA}} + \sum_{i=1}^{N}\sum_{j>i}^{N} \frac{1}{r_{ij}} + \sum_{A=1}^{M}\sum_{B>A}^{M} \frac{Z_A Z_B}{R_{AB}}. \tag{2.3}$$

Equation 2.1 is certainly not trivial to solve using the Hamiltonian operator described in eqn 2.3. In order to simplify our problem, we invoke one of the central approximations of quantum chemistry, the Born-Oppenheimer approximation[30]. This approximation hinges on the difference in mass between nuclei and electrons. The nucleus is much more massive than an electron, and hence moves very slowly compared to the electron. We can then consider that when the nucleus moves, the electron has more than enough time to re-equilibrate its distribution about the nucleus, and hence the nucleus appears fixed in space to the electron. This approximation allows us to approximately separate the motions of the electrons from those of the nuclei, and write the overall molecular wavefunction as:

$$\Psi = \psi_{nuc}\psi_{elec} \tag{2.4}$$

where ψ_{elec} depends parametrically on the nuclear positions and is an eigenfunction of an electronic Hamiltonian that also depends on nuclear positions:

$$\hat{H}_{elec}\psi_{elec} = E_{elec}\psi_{elec} \tag{2.5}$$

with:

$$\hat{H}_{elec} = -\sum_{i=1}^{N} \frac{1}{2}\nabla^2 - \sum_{i=1}^{N}\sum_{A=1}^{M} \frac{Z_A}{r_{iA}} + \sum_{i=1}^{N}\sum_{j>i}^{N} \frac{1}{r_{ij}}. \tag{2.6}$$

It is important to note that the electronic wavefunction, ψ_{elec}, is a parametric function of the nuclear coordinates, and the effective potential energy felt by the nuclei is given by:

$$E = E_{elec} + \sum_{A=1}^{M}\sum_{B>A}^{M} \frac{Z_A Z_B}{R_{AB}}. \tag{2.7}$$

2.2 Wavefunctions

Although the electronic Hamiltonian in eqn 2.6 depends on only the spatial coordinates of the electrons, it is still necessary to specify an electron's spin in order to completely describe

it. A wavefunction for an N-electron system must then be a function of $4N$ coordinates, three of which are the spatial coordinates (x_i, y_i, z_i), and the fourth is the spin coordinate. We shall denote the spin coordinate as ω, and define two eigenfunctions of the $\hat{s}_z$ spin operator:

$$\begin{aligned} \hat{s}_z\alpha(\omega) &= \frac{1}{2}\alpha(\omega) \\ \hat{s}_z\beta(\omega) &= -\frac{1}{2}\beta(\omega), \end{aligned} \tag{2.8}$$

which allows us to associate a spin with each electron depending on our choice of spin eigenfunction. We then denote the spatial coordinates of electron i as $\mathbf{r}_i$ and the combination of spatial and spin coordinates of this electron as $\mathbf{x}_i$. The N-electron wavefunction is then a function of the coordinates, $\mathbf{x}_i$, of all N electrons. The simplest form of an N-electron wavefunction might then be a product of one electron spin-orbitals:

$$\psi_{elec}(\mathbf{x}_1, \mathbf{x}_2, \ldots, \mathbf{x}_N) = \chi_1(\mathbf{x}_1)\chi_2(\mathbf{x}_2)\ldots\chi_K(\mathbf{x}_N) \tag{2.9}$$

where $\chi(\mathbf{x})$ is a spin-orbital, comprised of the product of a spatial orbital, $\phi(\mathbf{r})$, and a spin function. We assume that the spatial orbitals $\{\phi_1, \phi_2, \ldots, \phi_N\}$ form an orthonormal set. It is important to note that for any given set of K spatial orbitals, $\phi(\mathbf{r})$, we can form a set of $2K$ spin-orbitals, i.e. $\phi(\mathbf{r})\alpha(\omega)$ and $\phi(\mathbf{r})\beta(\omega)$.

The function defined by eqn 2.9 is called a Hartree product; although its simplicity is appealing, it has the serious drawback that it violates the anti-symmetry principle that governs the electronic wavefunction. Electron are fermions; hence upon interchanging any pair of electrons the wavefunction must change sign. In order to enforce this requirement while retaining much of the simplicity of the Hartree product, we introduce the Slater determinant:

$$\psi_{elec}(\mathbf{x}_1, \mathbf{x}_2, \ldots, \mathbf{x}_N) = (N!)^{-1/2} \begin{vmatrix} \chi_i(\mathbf{x}_1) & \chi_j(\mathbf{x}_1) & \cdots & \chi_k(\mathbf{x}_1) \\ \chi_i(\mathbf{x}_2) & \chi_j(\mathbf{x}_2) & \cdots & \chi_k(\mathbf{x}_2) \\ \vdots & \vdots & \ddots & \vdots \\ \chi_i(\mathbf{x}_N) & \chi_j(\mathbf{x}_N) & \cdots & \chi_k(\mathbf{x}_N) \end{vmatrix} \tag{2.10}$$

where $(N!)^{-1/2}$ is a normalization factor. This wavefunction has N electrons in N spin-orbitals, without specifying which electron is in which orbital. From the properties of determinants, we can see that upon interchange of any two rows (which interchanges a pair of electrons) the determinant changes sign. Also, if any two columns are the same (two electrons occupying the same spin-orbital) the determinant is zero. This wavefunction then obeys both the anti-symmetry principle and the Pauli-exclusion principle. The Slater

determinant is often expressed in the form:

$$\psi_{elec}(\mathbf{x}_1, \mathbf{x}_2, \ldots, \mathbf{x}_N) = |\chi_i(\mathbf{x}_1)\chi_j(\mathbf{x}_2)\ldots\chi_k(\mathbf{x}_N)\rangle \tag{2.11}$$

where we only show the diagonal elements of the Slater determinant, and the normalization factor has been suppressed for convenience.

2.3 Hartree-Fock Approximation

Solving the electronic Schrödinger equation, eqn 2.5, using the electronic Hamiltonian, eqn 2.6, and the Slater determinant is a very difficult mathematical problem. In fact, except for the one-electron problem it is not exactly solvable. For this reason, it is desirable to find approximate methods for the solution of this equation. The starting point for many quantum chemical methods is the Hartree-Fock approximation. We assume that the wavefunction can be written as a single Slater determinant:

$$\psi_{HF}(\mathbf{x}_1, \mathbf{x}_2, \ldots, \mathbf{x}_N) = |\chi_i(\mathbf{x}_1)\chi_j(\mathbf{x}_2)\ldots\chi_k(\mathbf{x}_N)\rangle \tag{2.12}$$

where the spatial part of each spin-orbital is taken as a linear combination of basis functions:

$$\phi_i = \sum_j c_{i,j}\Phi_j \tag{2.13}$$

and the $c_{i,j}$ are expansion coefficients to be determined. The basis functions Φ_j are collectively termed the one-electron basis set (a term that is often shortened to simply "basis set"); they are often taken to be the product of atom-centered Gaussian-type functions[8] and spherical harmonic functions, because this simplifies the computation of the coulomb and exchange integrals defined below. However, other choices for the one-electron basis set are possible[44].

In order to determine the expansion coefficients, we use the variational theorem[30], which states that:

$$E_0 \leq E_0^{approx} = \langle\psi_T|\hat{H}|\psi_T\rangle \tag{2.14}$$

where $\hat{H}$ is the full electronic Hamiltonian and E_0 is the true ground state energy.

Therefore the best wavefunction of the form given in eqn 2.12 is the one which gives the lowest possible energy. The Hartree-Fock method optimizes the wavefunction, eqn 2.12, by minimizing the energy with respect to the variational parameters, $c_{i,j}$, subject to the constraint that the spin-orbitals are orthonormal. For closed shell systems, where we have an even number of electrons, it is common to make a further approximation. We assume that all of our electrons are spin-paired, i.e. we have an equal number of α and β

electrons with the spatial degrees of freedom of each pair described by a single orbital. This is commonly termed the restricted Hartree-Fock (RHF) approximation. Making the RHF approximation, we substitute equations 2.6 and 2.12 into eqn 2.14 to obtain:

$$E_{RHF} = 2\sum_{i=1}^{N/2} h_{ii} + \sum_{i=1}^{N/2}\sum_{j=1}^{N/2}(2J_{ij} - K_{ij}) \tag{2.15}$$

where we have defined

$$h_{ii} \equiv \left\langle \phi_i(1) \left| -\frac{1}{2}\nabla_1^2 - \sum_{A=1}^{M} \frac{Z_A}{r_{1A}} \right| \phi_i(1) \right\rangle \tag{2.16}$$

as the one electron integrals that describe the kinetic energy of an electron in spatial orbital ϕ_i, and the coulombic interaction between it and the nuclei;

$$J_{ij} \equiv \left\langle \phi_i(1)\phi_j(2) \left| \frac{1}{r_{12}} \right| \phi_i(1)\phi_j(2) \right\rangle \tag{2.17}$$

as the Coulomb integral which describes the average coulombic interaction between spatial orbitals ϕ_i and ϕ_j ; and

$$K_{ij} \equiv \left\langle \phi_i(1)\phi_j(2) \left| \frac{1}{r_{12}} \right| \phi_j(1)\phi_i(2) \right\rangle \tag{2.18}$$

as the exchange integral for spatial orbitals ϕ_i and ϕ_j, which arises from the antisymmetric nature of the trial wavefunction and does not have a classical interpretation. The effect of the exchange integral is that it creates a region around each electron that effectively repels electrons with the same spin, thus correlating their motions. The indices describing the Coulomb and exchange integrals have only $N/2$ values because we require a pair of electrons (one spin-up and one spin-down) to occupy each spatial function ϕ. The Hartree-Fock equations ultimately reduce to an eigenvalue equation for each spatial orbital:

$$f\phi_i = \epsilon_i\phi_i \tag{2.19}$$

where we define the Fock operator, f as:

$$f = h + v^{HF} \tag{2.20}$$

In eqn 2.20 the core operator h includes all of the one-electron terms in the electronic Hamiltonian; when h acts on spatial orbital ϕ_i, it multiples that orbital by the quantity h_{ii}

defined in eqn 2.16:

$$h\phi_i = h_{ii}\phi_i. \tag{2.21}$$

The operator v^{HF} contains the effects of all of the two-electron terms in the electronic Hamiltonian, and is called the Hartree-Fock potential. This potential depends on all of the other spin-orbitals, and thus eqn 2.19 is a non-linear eigenvalue equation that must be solved iteratively. The typical method for solving this set of equations is the self consistent field (SCF) method[44]. One first makes a guess at the initial spin-orbitals, calculates the average field seen by each electron, thereby defining the form of the Hartree-Fock potential v^{HF}, and then solves the eigenvalue equation for a new set of spin-orbitals. These spin-orbitals are then used as the new guess, which changes the form of the Hartree-Fock potential, and the procedure is repeated until the spin-orbitals give a consistent result (i.e. a set of spin-orbitals yield the same spin-orbitals upon substitution into eqn 2.19). This procedure yields a set of orthonormal spin-orbitals χ_i, with orbital energies ϵ_i. The occupied spin-orbitals are those with the $N/2$ lowest orbital energies, while we term the remaining spin-orbitals virtual orbitals. The Hartree-Fock wavefunction is then the Slater determinant that is formed from the occupied spin-orbitals, and is the best single determinant variational approximation to the ground state of the system.

The method we have described above is termed the restricted Hartree Fock method. This method assumes that we have a closed shell system, where we require that each spatial orbital is occupied by two electrons that are spin-paired. However, many systems of chemical interest are not closed shell molecules. It is therefore worthwhile to mention two other Hartree-Fock approximations that are equipped to deal with open shell systems. The first is the unrestricted Hartree Fock (UHF) method. In UHF, the restriction that electrons are paired into spatial orbitals is relaxed, and every electron is allowed to occupy its own individual spatial orbital, leading to a system of equations that treats the α and β spin-orbitals separately. However, the UHF wavefunction is not an eigenfunction of the squared spin angular momentum operator, $\hat{S}^2$, which means that Slater determinants formed from the best spin-orbitals satisfying the UHF equations may be spin contaminated, or contain terms with higher order spin multiplicities than that of the system that is being studied.

The restricted open Shell Hartree Fock (ROHF) wavefunction keeps the constraint that most of the electrons are paired into spatial orbitals, but allows for unpaired α electrons. This constrains the wavefunction to be an eigenfunction of $\hat{S}^2$ so that it does not suffer from spin contamination. Due to the nature of the calculation, however, the α electrons in doubly occupied orbitals will have a slightly different potential than the β electrons in these orbitals because of the exchange operator. This forces the ROHF wavefunction to be higher in energy than a UHF wavefunction because the spatial orbitals for the doubly occupied orbitals in ROHF are constrained to be the same. In general, due to the variational nature

of the problem the UHF energy will always be lower than or equal to the energies obtained using R(O)HF methods.

2.4 Configuration Interaction

Because Hartree-Fock is a single determinant theory, it neglects correlation between electrons with different spin, which can lead to a poor description of the electronic structure. We can reconcile this by adding more determinants to our trial function, and using the variational principle to once again minimize the energy with respect to our trial function. The simplest method of doing this is to use configuration interaction (CI) theory. For simplicity, we once again assume that we have a closed shell system, although the theory is equally applicable to open shell systems. We assume that to a first approximation, our system is adequately described by a single determinant, and that determinant is the Hartree-Fock determinant. We then have a set of $2K$ spin-orbitals, the lowest N of which are occupied in the HF wavefunction. We can then form a linear combination of determinants that includes our HF determinant, as well as all the determinants that can be created with N electrons in $2K$ spin-orbitals. This can be done systematically in the following manner. The ground state is written:

$$|\Psi_{HF}\rangle = |\chi_1\chi_2\cdots\chi_a\chi_b\cdots\chi_N\rangle. \tag{2.22}$$

We can then create a set of determinants where we have promoted an electron in spin-orbital χ_a to a virtual spin-orbital χ_r, referred to as singly-excited determinants:

$$|\Psi_a^r\rangle = |\chi_1\chi_2\cdots\chi_r\chi_b\cdots\chi_N\rangle. \tag{2.23}$$

It follows that by promoting two electrons to virtual states, we obtain a doubly-excited determinant:

$$|\Psi_{ab}^{rs}\rangle = |\chi_1\chi_2\cdots\chi_r\chi_s\cdots\chi_N\rangle. \tag{2.24}$$

By continuing this series, we can then create $\binom{2K}{N}$ determinants from the HF determinant, that all involve the promotion of various numbers of electrons ranging from zero to N. By then taking a linear combination of these determinants:

$$|\Psi_{CI}\rangle = c_0|\Psi_{HF}\rangle + \left(\frac{1}{1!}\right)\sum_{ar} c_a^r|\Psi_a^r\rangle + \left(\frac{1}{2!}\right)\sum_{abrs} c_{ab}^{rs}|\Psi_{ab}^{rs}\rangle + \ldots \tag{2.25}$$

and variationally optimizing the coefficients, we obtain an exact wavefunction for our system, within a given one-electron basis set, that includes all electron correlation. The lowest eigenvalue of the Hamiltonian, E_{exact}, given by this wavefunction will correspond to the exact non-relativistic ground state energy within the Born-Oppenheimer approximation and

the limitations of the one-electron basis set. We often term the quantity:

$$E_{corr} = E_{exact} - E_{HF} \tag{2.26}$$

where E_{HF} is the Hartree-Fock energy, the correlation energy. Configuration interaction, in the limit of N excitations and an infinite one-electron basis, is a formally exact theory. However, the incompleteness of the basis set expansion will lead to a basis set truncation error. In addition, as the system size increases, the number of determinants needed to describe the exact wavefunction increases factorially with the number of electrons and basis functions, and thus it is impossible to include them all. For this reason, the CI expansion is generally truncated after a finite number of excitations, leading to CISD (singles and doubles), CISDT (singles, doubles and triples), CISDTQ etc. Unfortunately, truncating the CI series leads to a lack of size-consistency. For example, a CISD calculation of two H_2 molecules separated at large distances does not give twice the CISD energy of a single H_2 molecule. For this reason, CI must be used with care, especially when considering the dissociation of a molecular or super-molecular system.

2.5 Multi-Configurational Self-Consistent Field

The above treatment of configuration interaction assumes that a single determinant, $|\Psi_{HF}\rangle$, is a suitable approximation to the exact wavefunction ($c_0 \approx 1$ in eqn 2.25). However, for many systems of chemical interest this may not be the case, as multiple determinants in the CI expansion may contribute significantly to the exact wavefunction. This is important in systems where, for example, there exist low-lying excited states that have considerable mixing with the ground state. For these systems, a single determinant reference function is inadequate to describe our trial function, and a multi-configurational trial function must be used. The multi-configurational self-consistent field method (MCSCF)[41,44] is a truncated CI expansion:

$$|\Psi_{MCSCF}\rangle = \sum_I c_I |\Psi_I\rangle \tag{2.27}$$

where we simultaneously optimize the expansion coefficients, c_I, as well as the spin-orbitals in each determinant, $|\Psi_I\rangle$, which we typically term configuration state functions (CSF). The MCSCF wavefunction can then be used as the starting point in a CI type expansion, where we then excite electrons from the occupied spin-orbitals into virtual orbitals, and then variationally optimize the expansion coefficients.

2.6 Coupled Cluster Theory

Coupled cluster (CC) theory[14,30] is an alternative approach to the linear expansion of the reference wavefunction in terms of excited Slater determinants. The coupled cluster expansion is:

$$|\Psi_{exact}\rangle = \exp(\hat{T})|\Psi_T\rangle. \tag{2.28}$$

The operator $\exp(\hat{T})$ is defined by its Taylor series expansion:

$$\exp(\hat{T}) = 1 + \hat{T} + \frac{\hat{T}^2}{2!} + \ldots = \sum_{k=0}^{N} \frac{\hat{T}_k}{k!} \tag{2.29}$$

where $\hat{T}$ is the cluster operator defined by:

$$\hat{T} \equiv \hat{T}_1 + \hat{T}_2 + \ldots + \hat{T}_N. \tag{2.30}$$

Here $\hat{T}_i$ is the i-electron excitation operator, which converts the reference Slater determinant into a linear combination of all Slater determinants with i electrons promoted to virtual orbitals. The $\hat{T}_1$ operator is defined as:

$$\hat{T}_1 \equiv \sum_{r=n+1}^{\infty} \sum_{i=1}^{n} t_i^r \Phi_i^r \tag{2.31}$$

where Φ_i^a is a singly excited Slater determinant with occupied spin-orbital χ_i replaced by χ_r, and t_i^r is referred to as the cluster amplitude. Similar operators are defined for $\hat{T}_2, \hat{T}_3$, and so on. The object of a CC calculation is then to determine the cluster amplitudes, and once they are known we have the exact wavefunction. As with CI theory, CC theory will also suffer from incompleteness in the one-electron basis set. It is also impractical to include all N excitations, so we typically truncate the cluster operator $\hat{T}$ at doubles (CCSD), or triples (CCSDT). Another method is to use the CCSD operator, and then include a fourth order perturbative treatment of triple excitations which leads to CCSD(T). CCSD(T), coupled with large basis sets, has been shown to recover a large amount of the correlation energy for most systems, as well as accurate results for molecular geometries, harmonic vibrational frequencies, infrared intensities, and electric dipole moments[14] when compared to experiment. The advantage of CC theory over CI theory is twofold. First, CC theory is size consistent. In addition, considering only single excitations ($\hat{T} \approx \hat{T}_1$) we see that in the Taylor expansion of $\exp(\hat{T}_1)$ that terms involving $\hat{T}_1^2$ and higher order powers of $\hat{T}_1$ occur. This has the effect of including certain double, triple, etc up to N-fold multiply-excited Slater determinants in the wavefunction. For this reason, CC theory recovers a larger amount of the correlation energy than its equivalent truncated CI form, albeit at the

expense of including more Slater determinants.

Chapter 3

Absorption Theory

3.1 Theory of Absorption Spectra

The absorption coefficient, $\alpha(\omega)$, as a function of frequency for monochromatic light is defined phenomenologically through Lambert's law[22]:

$$\alpha(\omega) = \frac{1}{L} \ln \frac{I_0(\omega)}{I(\omega)}, \tag{3.1}$$

where L is the path length and $I_0(\omega)$ and $I(\omega)$ are the incident and transmitted intensities respectively at circular frequency $\omega = 2\pi c\nu$. The absorption coefficient is a function not only of frequency, but also of temperature, density and the nature of the absorbing species as well. Theoretically, the absorption coefficient can be expressed in terms of the probability that a system will make a transition, induced by electromagnetic radiation, between two of its stationary states. The golden rule of quantum mechanics[17] gives the probability per unit time for such a transition as:

$$\mathcal{P}_{f \leftarrow i}(\omega) = \frac{\pi}{2\hbar^2} |\langle f | \mathbf{E}_0 \cdot \vec{\mu} | i \rangle|^2 \Delta(\omega). \tag{3.2}$$

In this expression, $\mathbf{E}_0 = E_0 \hat{\mathbf{E}}$ specifies the magnitude and direction of the oscillating electric field $\mathbf{E}(t) = \mathbf{E}_0 \cos(\omega t - \vec{k} \cdot \vec{r})$, $\vec{\mu}$ is the dipole moment operator for the system undergoing the transition, and $\Delta(\omega)$ is the Bohr frequency condition which requires that only states satisfying the following relation:

$$\omega_{fi} = \frac{|(E_f - E_i)|}{\hbar}, \tag{3.3}$$

can undergo a transition at angular frequency ω. Equation 3.2 holds for wavelengths that are much larger than the dimensions of the absorbing system (electric dipole approximation).

As stated in eqn 3.1 the absorption coefficient is defined phenomenologically in terms of the ratio of incident to transmitted intensity. In any given absorption event, one photon with energy $\hbar\omega$ is lost, and the rate of energy loss per unit time in a given frequency band is given by:

$$\begin{aligned}\frac{\delta E(\omega)}{\delta t} &= -\sum_{i,f} \hbar\omega_{fi}\mathcal{P}_{f\leftarrow i}\delta(\omega_{fi}-\omega) \\ &= -\frac{\pi}{2\hbar}\sum_{i,f}\omega_{fi}P_i|\langle f|\mathbf{E}_0\cdot\vec{\mu}|i\rangle|^2\{\delta(\omega_{fi}-\omega)+\delta(\omega_{fi}+\omega)\} \qquad (3.4)\end{aligned}$$

where P_i is the probability of finding the absorber in the ith state. The origin of the second delta function, $\delta(\omega_{fi}+\omega)$, is related to the possibility of stimulated emission, which occurs when the system, initially in state f, emits a photon in phase, in the same direction, and with the same frequency as the incident light, effectively adding energy to the beam. The sums are over all possible states, i and f, that are connected by the delta functions. Since we sum over both of these, we can interchange the indices in the second delta function (remembering that $\omega_{fi}=-\omega_{if}$), and simplify eqn 3.4 to:

$$\begin{aligned}\frac{\delta E(\omega)}{\delta t} &= -\frac{\pi}{2\hbar}\sum_{i,f}\omega_{fi}P_i|\langle f|\mathbf{E}_0\cdot\vec{\mu}|i\rangle|^2\{\delta(\omega_{fi}-\omega)+\delta(-\omega_{if}+\omega)\} \\ &= -\frac{\pi}{2\hbar}\sum_{i,f}\omega_{fi}P_i|\langle f|\mathbf{E}_0\cdot\vec{\mu}|i\rangle|^2\{\delta(\omega_{fi}-\omega)-\delta(\omega_{if}-\omega)\} \\ &= -\frac{\pi}{2\hbar}\sum_{i,f}\omega_{fi}|\langle f|\mathbf{E}_0\cdot\vec{\mu}|i\rangle|^2(P_i-P_f)\delta(\omega_{fi}-\omega) \qquad (3.5)\end{aligned}$$

where P_f is just the probability of finding the absorber in state f. We can further simplify eqn 3.5 by using the following relations. First, we replace the electric field vector with its magnitude and directions, $\mathbf{E}_0 = E_0\cdot\hat{\mathbf{E}}$. We also assume that the light is unpolarized, so we spherically average the transition dipole moment over all orientations of the polarization of $\hat{\mathbf{E}}$:

$$\overline{|\langle f|\hat{\mathbf{E}}\cdot\vec{\mu}|i\rangle|^2} = \frac{1}{3}\overline{|\langle f|\vec{\mu}|i\rangle|^2}, \qquad (3.6)$$

where the overbar indicates an average over the angular parts of $\hat{\mathbf{E}}$. Finally, we have that the probability of the absorber being in state f is (Boltzmann distribution):

$$P_f = P_i\exp(-\hbar\omega_{fi}/kT). \qquad (3.7)$$

Using these relations, and replacing ω_{fi} with ω because of the delta function, we have:

$$\frac{\delta E(\omega)}{\delta t} = -\frac{\pi E_0^2}{3 \cdot 2\hbar}\omega[1 - \exp(\hbar\omega/kT)] \sum_{i,f} P_i |\langle f|\vec{\mu}|i\rangle|^2 \delta(\omega_{fi} - \omega). \tag{3.8}$$

In order to determine the absorption coefficient, we need to determine an absorption cross section, σ_{abs}, and multiply by the number density of the absorbers. The absorption cross section is related to the rate of energy loss per unit time per unit frequency in the following manner. The rate of energy transport per unit area is related to the electromagnetic field through the Poynting vector (we assume the refractive index is one):

$$\mathbf{S} = \frac{1}{\mu_0}\mathbf{E} \times \mathbf{B}. \tag{3.9}$$

Since the magnetic and electric fields are orthogonal, the magnitude of the cross product $\mathbf{E} \times \mathbf{B}$ reduces to the product of the magnitudes of the two fields. Furthermore, the plane wave solution to the Maxwell equations requires that $|\mathbf{B}| = |\mathbf{E}|/c$, where c is the speed of light, and gives the magnitude of the electric field as:

$$|\mathbf{E}| = E_0 \sin(kx - \omega t). \tag{3.10}$$

Using these relations, and averaging the magnitude of the field over one period of oscillation, we find the average intensity of the Poynting vector as:

$$\begin{aligned} |\mathbf{S}| &= \frac{1}{\mu_0}|\mathbf{E}| \cdot |\mathbf{B}| \\ &= \frac{1}{c\mu_0} E_0^2 \overline{\sin^2(kx - \omega t)} \\ &= \frac{1}{c\mu_0}\frac{1}{2} E_0^2 \end{aligned} \tag{3.11}$$

where μ_0 is the permeability of vacuum and is related to the permittivity of vacuum through the equation $\mu_0 = 1/(\epsilon_0 c^2)$. The overbar means that we take the average value over one period of oscillation. The absorption cross section is then eqn 3.8 divided by eqn 3.11, and when multiplied by the number density of absorbers yields the absorption coefficient:

$$\alpha(\omega) = \frac{4\pi^2}{3\hbar c} n_1 n_2 V \omega[1 - \exp(-\hbar\omega/kT)] \sum_{i,f} P_i \frac{1}{4\pi\epsilon_0} |\langle f|\vec{\mu}|i\rangle|^2 \delta(\omega_{fi} - \omega). \tag{3.12}$$

Here n_i, is the number density of monomer i, and $n_1 n_2 V$ is the number of (1,2) pairs per unit volume; as we are interested in collision-induced absorption we assume that a pair of molecules constitutes the absorbing species.

Equation 3.12 will be the starting point for our calculations of the absorption coefficient. Further, it is useful to divide this equation into two parts:

$$\alpha(\omega) = \frac{4\pi^2}{3\hbar c} n_1 n_2 \omega [1 - \exp(-\hbar\omega/kT)] VG(\omega) \tag{3.13}$$

$$VG(\omega) = V \sum_{i,f} P_i \frac{1}{4\pi\epsilon_0} |\langle f|\vec{\mu}|i\rangle|^2 \delta(\omega_{fi} - \omega) \tag{3.14}$$

where $VG(\omega)$ is commonly termed the spectral density, and contains all terms directly related to states i and f. The units of $\alpha(\omega)$ are cm^{-1} while the units of $VG(\omega)$ are erg cm^6 s . The spectral density, eqn 3.14, is technically independent of volume, however for historical reasons it is written in this manner.

Since we are typically interested in calculating a density independent absorption coefficient in order to compare with experimental results, it is useful to normalize the absorption spectra with respect to the number densities of each species. To do this we express the number density in terms of amagat units, $\rho_i = n_i/N_i$, where n_i is the number density, and N_i is the number density of species i at 1 amagat. For ideal gases, N_i is given by Loschmidt's number, $N_L = 2.686736 \times 10^{19}$ cm^{-3} amagat^{-1}. The density independent absorption coefficient is then:

$$\frac{\alpha(\omega)}{\rho_1\rho_2} = \frac{4\pi^2}{3\hbar c} N_1 N_2 V \omega [1 - \exp(-\hbar\omega/kT)] VG(\omega), \tag{3.15}$$

and the units become cm^{-1} amagat^{-2}.

3.2 Evaluating $VG(\omega)$

3.2.1 Free-Free Absorption

We wish to evaluate the transition dipole moment integral for continuum-continuum matrix elements:

$$\langle f|\vec{\mu}|i\rangle. \tag{3.16}$$

In order to accomplish this we must first define the wavefunction for the final and initial states. Since both wavefunctions are continuum wavefunctions, we can focus on $|i\rangle$ without loss of generality. Using the Born-Oppenheimer approximation, we separate the wavefunction into a nuclear component and an electric component:

$$|i\rangle = |\Phi_n \Phi_e\rangle \tag{3.17}$$

where n and e correspond to nuclei and electrons, respectively. Before considering the nuclear wavefunctions, it is useful to simplify eqn 3.16 to separate the electronic and nuclear parts of the problem. Substituting eqn 3.17 into 3.16 we obtain:

$$\begin{aligned} \langle f|\vec{\mu}|i\rangle &= \langle \Phi_n^f \Phi_e^f |\vec{\mu}| \Phi_n^i \Phi_e^i \rangle \\ &= \langle \Phi_n^f | \langle \Phi_e^f |\vec{\mu}| \Phi_e^i \rangle | \Phi_n^i \rangle \\ &= \langle \Phi_n^f | \vec{\mu}_{elec}(R) | \Phi_n^i \rangle \end{aligned} \tag{3.18}$$

where we have defined $\vec{\mu}_{elec}(R)$ as the electronic expectation value of the dipole moment evaluated at the nuclear configuration R. We then wish to evaluate the nuclear wavefunction Φ_n, which is the wavefunction of relative motion of the components of the dimer. For a pair of atoms, we are looking for solutions to the nuclear Hamiltonian for a diatomic molecule:

$$H = -\frac{\hbar^2}{2m}\frac{d^2}{dR^2} + V^l(R) \tag{3.19}$$

where $V^l(R)$ is the isotropic potential for the dimer including the centrifugal potential:

$$V^l(R) = V(R) + \frac{\hbar^2 l(l+1)}{2mR^2} \tag{3.20}$$

and l is the angular momentum quantum number of the diatomic system. In Appendix A, we have given the wavefunction for an outgoing scattered state of a spherical potential, and shown how to normalize it. For the purposes of evaluating eqn 3.16 we wish to simplify equation A.1 by using the spherical harmonic addition theorem A.4. After substituting eqn A.4 into eqn A.1 we have a wave function that is a linear combination of spherical harmonics in $\hat{R}$. By then recognizing that each term of that expansion must be a solution to the Hamiltonian of relative motion for a specific angular momentum state, we can pick out a single term to continue our derivation. Finally we recognize that by suppressing terms not related to R (which are constant) our wave function will be of the form:

$$\Phi_n(E, l, m) = \frac{u_l(E, R)}{R} Y_l^m(\theta_R, \phi_R). \tag{3.21}$$

Here $u_l(E, R)$ is our energy normalized radial wavefunction (eqn A.25) which is a solution to the radial Schrödinger equation:

$$\left[-\frac{\hbar^2}{2m}\frac{d^2}{dR^2} + V(R) + \frac{\hbar^2 l(l+1)}{2mR^2} - E\right] u_l(E, R) = 0. \tag{3.22}$$

The dipole moment vector $\vec{\mu}$ in spherical coordinates can be expressed as:

$$\vec{\mu}_{elec}(R) = \mu_{elec}(R)\left(\frac{4\pi}{3}\right)^{1/2}\sum_{m=-1}^{m=1} Y_1^m(\theta_R, \phi_R) \tag{3.23}$$

where $\mu_{elec}(R)$ is the magnitude of the electronic dipole moment vector, and the spherical harmonics, Y_1^m, may be considered basis vectors spanning the spherical space. Substituting eqns 3.21 and 3.23 into 3.18 (ignoring normalization factors for convenience) we obtain:

$$\begin{aligned}&|\langle\Phi_n^f(E_f, l_f, m_f)|\mu_{elec}(R)|\Phi_n^i(E_i, l_i, m_i)\rangle|^2 = \\ &\left|\int_0^\infty dR\; u_{l_f}^*(E_f, R)\mu_{elec}(R)u_{l_i}(E_i, R)\sum_m \langle Y_{l_f}^{m_f}|Y_1^m|Y_{l_i}^{m_i}\rangle\right|^2\end{aligned} \tag{3.24}$$

where the transition dipole moment is reduced to an integral over R, involving the radial wavefunctions and the dipole moment, and an angular part that depends on the polar and azimuthal angles of the vector $\mathbf{R}$. The angular part can be evaluated using the Wigner-Eckart theorem[39]:

$$\begin{aligned}&\langle Y_{l_f}^{m_f}|Y_1^m|Y_{l_i}^{m_i}\rangle = \\ &\quad(-1)^{-m_f}[(2l_f+1)(2l_i+1)]^{1/2}\begin{pmatrix} l_f & 1 & l_i \\ -m_{l_f} & m & m_{l_i}\end{pmatrix}\begin{pmatrix} l_f & 1 & l_i \\ 0 & 0 & 0\end{pmatrix}.\end{aligned} \tag{3.25}$$

The symbols in parentheses are the Wigner 3-j symbols, and are equal to zero unless $l_f + l_i + 1 = 0$, and the triangle inequalities hold, $|l_i - 1| \leq l_f \leq l_i + 1$. The Wigner 3-$j$ symbols thus enforce the common spectroscopic selection rule, $l_f = l_i \pm 1$, which is attributed to a photon having one unit, $\hbar$, of angular momentum, and thus causing a transition from initial angular momentum state l to $l \pm 1$. We ultimately are interested in the square of eqn 3.25, so recalling that our summation is over orthogonal spherical components of the dipole vector:

$$\begin{aligned}\left|\sum_m \langle Y_{l_f}^{m_f}|Y_1^m|Y_{l_i}^{m_i}\rangle\right|^2 &= \left|\sum_m \langle Y_{l_f}^{m_f}|Y_1^m|Y_{l_i}^{m_i}\rangle\right|\left|\sum_{m'} \langle Y_{l_f}^{m_f}|Y_1^{m'}|Y_{l_i}^{m_i}\rangle\right| \\ &= \sum_{m,m'}\left|\langle Y_{l_f}^{m_f}|Y_1^m|Y_{l_i}^{m_i}\rangle\right|\left|\langle Y_{l_f}^{m_f}|Y_1^{m'}|Y_{l_i}^{m_i}\rangle\right|\end{aligned} \tag{3.26}$$

The terms in this sum with $m \neq m'$ can be shown to be zero, so we have:

$$\left|\sum_m \langle Y_{l_f}^{m_f}|Y_1^m|Y_{l_i}^{m_i}\rangle\right|^2 = \sum_m |\langle Y_{l_f}^{m_f}|Y_1^m|Y_{l_i}^{m_i}\rangle|^2$$
$$= (2l_f+1)(2l_i+1)\begin{pmatrix} l_f & 1 & l_i \\ 0 & 0 & 0 \end{pmatrix}^2 \sum_m \begin{pmatrix} l_f & 1 & l_i \\ -m_{l_f} & m & m_{l_i} \end{pmatrix}^2. \tag{3.27}$$

The sum over m is equal to 1 due to the orthogonality relations of the Wigner 3-j symbols [39], and the remaining terms can be shown to equal the larger of l_i and l_f subject to the selection rules mentioned above. Substituting eqn 3.26 back into eqn 3.24 we obtain:

$$|\langle \Phi_n^f(E_f, l_f, m_f)|\mu_{elec}(R)|\Phi_n^i(E_i, l_i, m_i)\rangle|^2 =$$
$$l_i \left|\int_0^\infty dR\, u_{l_i-1}^*(E_f, R)\mu_{elec}(R)u_{l_i}(E_i, R)\right|^2$$
$$+ (l_i+1)\left|\int_0^\infty dR\, u_{l_i+1}^*(E_f, R)\mu_{elec}(R)u_{l_i}(E_i, R)\right|^2 \tag{3.28}$$

or:

$$|\langle \Phi_n^f(E_f, l_f, m_f)|\mu_{elec}(R)|\Phi_n^i(E_i, l_i, m_i)\rangle|^2 =$$
$$l_i|\langle \Phi_n^f(E_f, l_i-1)|\mu_{elec}(R)|\Phi_n^i(E_i, l_i)\rangle|^2$$
$$+ (l_i+1)|\langle \Phi_n^f(E_f, l_i+1)|\mu_{elec}(R)|\Phi_n^i(E_i, l_i)\rangle|^2. \tag{3.29}$$

Once $\mu_{elec}(R)$ is known, eqn 3.29 can be evaluated using a suitable computational method for determining the radial wavefunctions.

The transition moment integral of eqn 3.29 appears in the spectral density, eqn 3.14, accompanied by the probability, P_i, that the colliding atoms are in initial state $|i\rangle$. This probability is given by the Boltzmann factor:

$$P_i = \frac{\exp(-E_i/kT)}{Z(T)} \tag{3.30}$$

where $Z(T)$ is the pair partition function for the system, and is given by a sum over the bound and free partition functions for dissimilar pairs:

$$Z(T) = Z_{bound}(T) + Z_{free}(T) \tag{3.31}$$

At low densities, the second term in $Z(T)$ is orders of magnitude larger than the first, and $Z(T)$ is given by:

$$Z(T) \approx Z_{free}(T) = V\lambda_0^{-3} \tag{3.32}$$

where:

$$\lambda_0 = \left(\frac{2\pi\hbar^2}{mkT}\right)^{1/2} \tag{3.33}$$

is the thermal de Broglie wavelength, with m being the reduced mass of the system. The volume, V, of the system cancels with the volume in eqn 3.13 and thus the absorption coefficient is independent of volume.

In order to complete our computation of $VG(\omega)$, we need to sum over the initial and final states of our system. However, in the continuum our distribution of energy eigenvalues is continuous, and we can convert our sums into integrals. Before doing this, we recognize that the delta function in eqn 3.14 allows us to fix the final energy, if the photon frequency, ω, and initial state are known. Thus, the integral over final and initial states reduces to an integral over the initial states, and we have:

$$VG(\omega) = \frac{\lambda_0^3 V\hbar}{4\pi\epsilon_0}\int_0^\infty \sum_{l=0}^{\infty} \exp(-E_i/kT)\left[l|\langle\Phi_n^f(E_f, l-1)|\mu_{elec}(R)|\Phi_n^i(E_i,l)\rangle|^2 \right.$$
$$\left. +(l+1)|\langle\Phi_n^f(E_f,l+1)|\mu_{elec}(R)|\Phi_n^i(E_i,l)\rangle|^2\right] dE_i. \tag{3.34}$$

3.2.2 Absorption due to Bound States

If the system of interest forms bound states, several other types of absorption must be taken into account. We must also account for bound-free absorption, bound-bound absorption, and free-bound absorption. When bound states are involved, there exist discrete eigenvalues for the energies, and thus the spectral density is reduced to a summation over initial states, where the final states are fixed due to the delta function. We can take the wavefunction for a bound state to be of the same form as eqn 3.21, which is square-integrable and is normalized in the conventional manner ($|\Phi_n|^2 = 1$)[20]. Thus the derivation of these spectral densities is similar to that for free-free absorption, with the integrals replaced by sums over the initial states. We then have for the bound-bound spectral density:

$$VG(\omega) = \frac{\lambda_0^3 V\hbar}{4\pi\epsilon_0}\sum_{v_i,v_f,l} \exp(-E_{v_i,l}/kT)\left[l|\langle\Phi_n^f(E_{v_f,l-1}, l-1)|\mu_{elec}(R)|\Phi_n^i(E_{v_i,l},l)\rangle|^2 \right.$$
$$\left. +(l+1)|\langle\Phi_n^f(E_{v_f,l+1},l+1)|\mu_{elec}(R)|\Phi_n^i(E_{v_i,l},l)\rangle|^2\right]\delta(E_{fi}-\hbar\omega) \tag{3.35}$$

the bound-free spectral density:

$$VG(\omega) = \frac{\lambda_0^3 V\hbar}{4\pi\epsilon_0}\sum_{v_i,l} \exp(-E_{v_i,l}/kT)\left[l|\langle\Phi_n^f(E_{v_i,l}+\hbar\omega, l-1)|\mu_{elec}(R)|\Phi_n^i(E_{v_i,l},l)\rangle|^2 \right.$$
$$\left. +(l+1)|\langle\Phi_n^f(E_{v_f,l+1}+\hbar\omega,l+1)|\mu_{elec}(R)|\Phi_n^i(E_{v_i,l},l)\rangle|^2\right] \tag{3.36}$$

and the free-bound spectral density:

$$
\begin{aligned}
VG(\omega) = \frac{\lambda_0^3 V\hbar}{4\pi\epsilon_0} \sum_{v_f,l} \Big[& \exp(-(E_{v_f,l-1} - \hbar\omega)/kT) \times \\
& l|\langle \Phi_n^f(E_{v_f,l-1}, l-1)|\mu_{elec}(R)|\Phi_n^i(E_{v_f,l-1} - \hbar\omega, l)\rangle|^2 \\
+ \quad & \exp(-(E_{v_f,l} - \hbar\omega)/kT) \times \\
& (l+1)|\langle \Phi_n^f(E_{v_f,l+1}, l+1)|\mu_{elec}(R)|\Phi_n^i(E_{v_f,l} - \hbar\omega, l)\rangle|^2 \Big] .
\end{aligned}
\tag{3.37}
$$

In cases where there is only one potential energy surface (no electronic transitions), free-bound transitions contribute only to emission and not absorption. The bound-bound contributions will only arise when the initial state and final state energies differ exactly by the photon energy $\hbar\omega$, and are the rotovibrational spectra of the dimer.

Chapter 4

Helium-Xenon

4.1 Ab Initio

4.1.1 Potential Energy Surface

We have calculated the ground-state potential energy surface of the He-Xe dimer using coupled cluster theory including single and double excitations and a perturbative treatment of triple excitations [abbreviated as CCSD(T)][14]. The xenon atom has been treated with a relativistic effective core potential (ECP)[35] that replaces the [Ar]$3d^{10}$ electrons with an effective pseudo-potential that includes relativistic and spin-orbit effects. The electronic structure calculations thus consider explicitly only the 26 outermost Xe electrons ($4s^2 4p^6 4d^{10} 5s^2 5p^6$) and the $1s^2$ electrons of the He atom. All of these electrons are correlated in the CCSD(T) calculations. Our interaction energies are obtained using a supermolecular approach that includes the standard counterpoise correction[9]. All our calculations are performed using the 2003 version of Gaussian[21].

We begin by using correlation-consistent basis sets[19], coupled with the ECP, to investigate the convergence of the He-Xe interaction energy to the basis set limit for this level of theory. We use the aug-cc-pVXZ basis sets on helium[49] (X=D,T,Q) and the aug-cc-pVXZ-PP basis sets on Xe[35], which have been optimized for use with the ECP[35]. In addition to these basis sets, we include a small set of 3s3p2d1f midbond functions at the midpoint of the van der Waals bond; their exponents are listed in Ref [47]. These functions have been shown to improve the basis set description of the van der Waals interaction, and their effect is nearly independent of location along the van der Waals bond[46]. We have also investigated the effect of adding extra uncontracted diffuse functions to these basis sets, with the exponents being determined in an even-tempered manner. These functions consist of one primitive Gaussian of each symmetry with an exponent one third as large as the smallest exponent of the same symmetry in the standard basis set. We designate

Table 4.1: Basis set convergence for the He-Xe dimer

atomic basis set	midbond set	R_e (a_0)	D_e (cm^{-1})
aug-cc-pVTZ	3s3p2d	7.606	19.111
aug-cc-pVTZ	3s3p2d1f	7.584	19.503
D-aug-cc-pVTZ	3s3p2d	7.601	19.230
D-aug-cc-pVTZ	3s3p2d1f	7.580	19.606
aug-cc-pVQZ	3s3p2d	7.555	19.867
aug-cc-pVQZ	3s3p2d1f	7.545	20.013
D-aug-cc-pVQZ	3s3p2d	7.548	19.976
D-aug-cc-pVQZ	3s3p2d1f	7.556	20.141

these basis sets as D-aug-cc-pVXZ (X=D,T,Q). Inclusion of these diffuse functions changes the He-Xe binding energy by less than 0.15 cm^{-1} near the equilibrium bond length, R_e. Our results for the different basis sets are presented in table 4.1. These values have been computed by fitting a cubic polynomial to the energies calculated at 7.4, 7.5, 7.6, and 7.7 bohr, and calculating the corresponding minimum of the cubic.

Upon examination of the results we find that a combination of the aug-cc-pVQZ basis on helium, the aug-cc-pVQZ-PP basis on xenon, and the 3s3p2d1f set of midbond functions provides reasonably accurate results at an affordable level of calculation. We present our calculated potential energy surface in Fig. 4.1 and Table 4.2.

We compare our results with other potentials in the literature[3,16,45] in Table 4.3. We note that our potential is in excellent agreement with the other potentials listed; however, the current work is the only ab initio potential that has been determined for the He-Xe dimer. We also compute the bound state energy levels of our potential. We find six $v = 0$ bound states ($J = 0 - 5$), as well as a single $v = 1$ bound state ($J = 0$). In comparison, we calculate the bound state energy levels of both the Aziz[3] and Tang-Toennies[45] potentials, and find that they support the same number of bound states as our potential. We calculate the bound states using the Numerov-Cooley method[13], integrating the potentials from R=4 bohr to 100 bohr, using a step size of 0.00192 bohr. Our results are presented in Table 4.4.

4.1.2 Dipole Moment

We calculate the interaction-induced dipole moment, μ, of the He-Xe dimer as the first derivative of the interaction potential with respect to an externally applied electric field, $\mu = -(\partial V/\partial F)_{F=0}$, aligned with the He-Xe bond, with the He atom at the origin and the Xe atom on the z axis. The derivative is calculated using a finite difference analysis of the interaction potential perturbed by electric fields with strength $F = \pm 0.001$ au. This analysis is accurate when the interaction energies depend quadratically on F, for small field

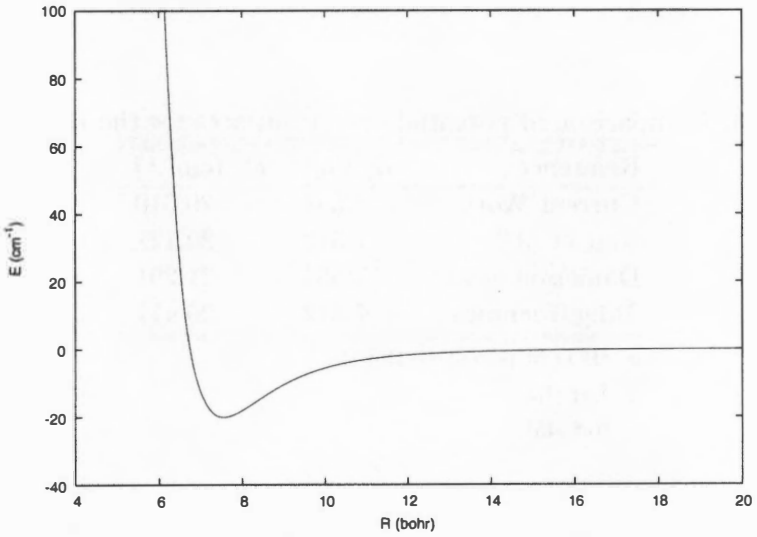

Figure 4.1: Potential energy surface of the He-Xe dimer calculated in current work.

Table 4.2: Potential energy surface of He-Xe dimer[a]

R (a_0)	E (cm^{-1})	R (a_0)	E (cm^{-1})
2.0	227089.539	7.56	-20.0089532
2.5	103761.824	7.6	-19.9753738
3.0	48078.1187	7.7	-19.7273228
3.5	21362.1791	8.0	-18.0282387
4.0	9058.08384	8.5	-14.0913683
4.5	3666.33604	9.0	-10.4523909
5.0	1403.94965	9.5	-7.61697644
5.5	494.680613	10.0	-5.54697954
6.0	147.743599	10.5	-4.06660162
6.5	25.0003542	11.0	-3.01713956
7.0	-12.5652295	11.5	-2.26344172
7.4	-19.6294815	12.0	-1.7213615
7.5	-19.9698422	13.0	-1.03047726
7.54	-20.0078338	14.0	-0.644948109
7.55	-20.0095233	15.0	-0.419306278

a) see text for basis set details.

Table 4.3: Comparison of potential energy surfaces for the He-Xe dimer

Reference	R_e (a_0)	D_e (cm^{-1})
Current Work	7.554	20.010
Aziz et al.[a]	7.512	20.121
Danielson et al.[b]	7.553	21.291
Tang-Toennies[c]	7.512	20.411

a. HFD-fit potential, Ref [3]

b. Ref [16]

c. Ref [45]

Table 4.4: He-Xe bound state energy levels. Energies are measured with respect to the potential minimum.

Potential		Current Work	Aziz et al.[a]	Tang-Toennies[b]
v	J		$E(cm^{-1})$	
0	0	11.955	11.838	12.087
0	1	12.396	12.284	12.533
0	2	13.274	13.170	13.420
0	3	14.577	14.486	14.737
0	4	16.287	16.214	16.465
0	5	18.372	18.320	18.575
1	0	19.959	20.023	20.313

a. HFD-fit potential, Ref [3]

b. Ref [45]

Table 4.5: Dipole moment surface of He-Xe dimer.

$R(a_0)$	μ (a.u.)	$R(a_0)$	μ (a.u.)
2.0	-0.760878563	6.5	-0.0109204995
2.2	-1.11384749	7.0	-0.00499594957
2.4	-1.08353281	7.5	-0.00211699982
2.5	-1.01088381	8.0	-0.000791549974
2.6	-0.929340243	8.5	-0.000225949945
2.8	-0.771184802	9.0	-3.90000332E-06
3.0	-0.635610938	9.5	7.44999707E-05
3.5	-0.392594427	10.0	8.3650033E-05
4.0	-0.240467295	10.5	7.2899973E-05
4.5	-0.142772943	11.0	6.13000229E-05
5.0	-0.0810810477	11.5	4.32000088E-05
5.5	-0.0438130982	12.0	2.87000021E-05
6.0	-0.022483848	13.0	1.50999704E-05

strengths. In order to confirm that this is the case for the He-Xe dimer, we compute the interaction energy of the dimer at R=2.0, 5.0, and 10.0 bohr for field strengths ranging from $F = -0.003$ au to $F = +0.003$ au, confirming that our interaction energy does indeed depend quadratically on F, for field strengths below 0.003 au. Therefore our finite difference analysis estimate of the derivative $(\partial V/\partial F)_{F=0}$ should be accurate. We present results for $R = 5.0$ bohr in Fig. 4.2. We present our results for the dipole moment in Fig. 4.3 and Table 4.5.

For comparison with our results, we show an empirical form for the dipole moment, the "exp-7" dipole of Frommhold et al.[24]. This form of the dipole moment is a three parameter model that includes an exponential term that models short range overlap interactions as well as a term that attempts to account for the long range dispersion-induced dipole. This model may be expressed as

$$\mu(R) = \mu_0 \exp\left[\frac{-(R-\sigma)}{\rho}\right] - D_7/R^7 \tag{4.1}$$

where μ_0 is the dipole strength at the root σ of the potential ($\sigma = 6.703a_0$), ρ determines the range of the overlap-induced dipole, and D_7 determines the strength of the dispersion term. The three parameters were optimized by Frommhold et al.[24] using the HFD-fit potential of Aziz et al.[3], and finding the best set of parameters to reproduce the experimental spectra measured by Dore et al.[18]. As noted by Frommhold et al., this is a crude model, which attempts to model all of the higher order dispersion terms using a single coefficient, D_7. We were unable to find a satisfactory fit of our finite difference dipole moments to this

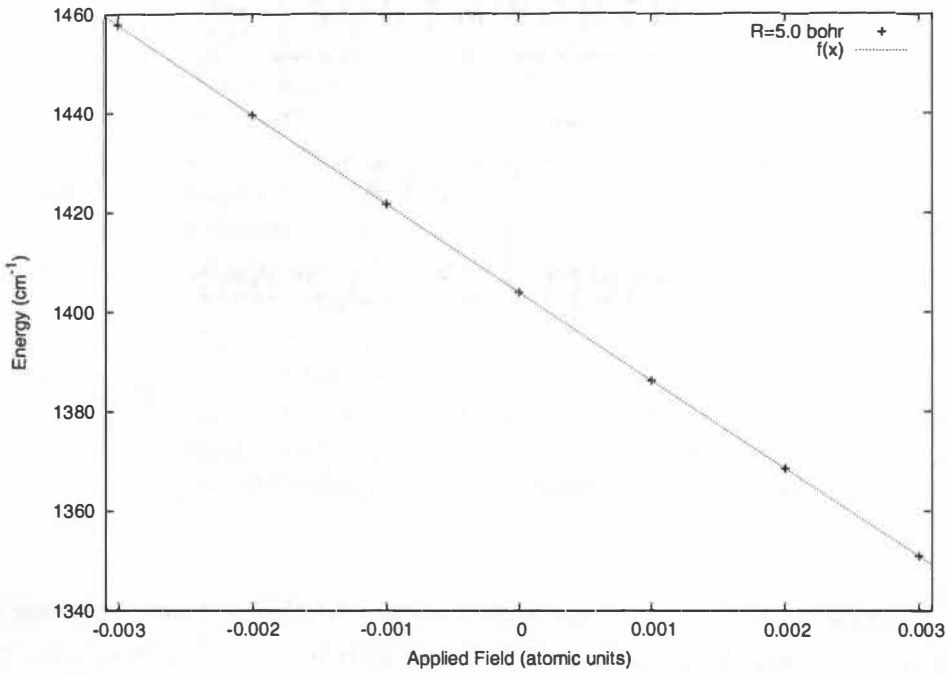

Figure 4.2: Figure that shows validity of finite-field method for $R = 5.0$ bohr. Solid line is a quadratic fit to the data, the residuals are smaller than the respective points.

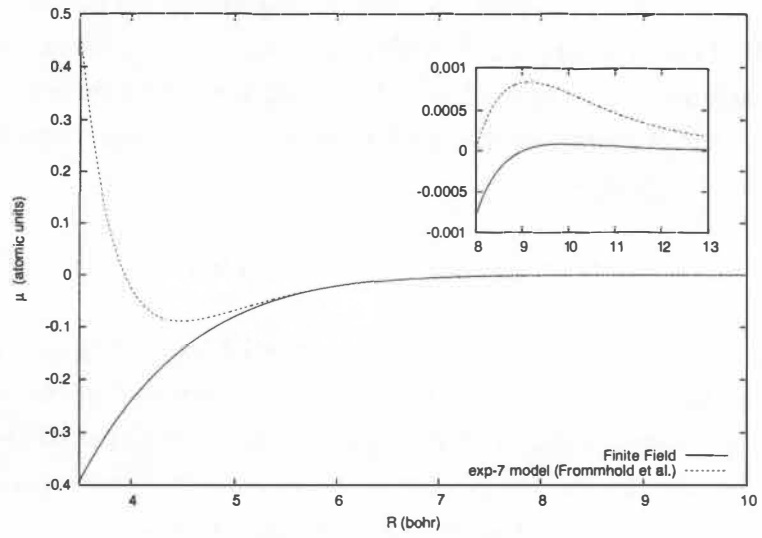

Figure 4.3: Dipole moment of the He-Xe dimer. Shown for comparison is the exp-7 model of Frommhold et al[24].

functional form, even upon adding higher order terms to the exponential term. We find that the major difference between our model and that of Frommhold et al. is in the repulsive region. At short bond lengths the $1/R^7$ term begins to dominate eqn 4.1, and the model becomes unphysical. Also, at longer bond lengths the model tends to overestimate the dipole moment.

4.2 Absorption Profile

In order to calculate the absorption profile of the He-Xe dimer, we must first determine which types of absorption contribute to the spectrum. We first calculate the mass action constant[22], $K(T)$, which is a ratio of the number of bound dimers to the number of pairs in volume v, and is given by:

$$K(T) = \frac{n_{2b}}{n_1 n_2} \approx Z_{2b}(T)\frac{\lambda_1^3 \lambda_2^3}{v}, \tag{4.2}$$

where n_{2b} is the number density of bound dimers, n_i is the number density of monomer i, Z_{2b} is the bound state partition function, v is the volume, and λ_i is the de Broglie wavelength of monomer i. We present our calculation of the mass action constant in figure 4.4, and note that for temperatures above 100 K the bound dimers make up less than a tenth of a percent of the overall constituents of the gas. Hence, we shall neglect the bound-free contributions to the absorption spectrum, and focus on the free-free absorption elements.

We use eqn 3.15 and eqn 3.34 to calculate the free-free absorption coefficient for the He-Xe dimer. We numerically integrate the transition dipole matrix elements, eqn 3.28, for the individual states. We compute the final and initial state wavefunctions for each energy point using the Numerov method[48], with 30 integration points per thermal de Broglie wavelength of the final energy state. The wavefunctions are integrated to a distance of 350 bohr, where we energy normalize them (cf Appendix A.3). The integration of the matrix element is carried out using trapezoid integration, using the same number of points as the wavefunction integrations.

In order to calculate the energy integral, we first interchange the integral over energy and the sum over l in eqn 3.34, and we use 12 point Gauss-Laguerre integration[36] to evaluate the integral. We then sum over l values up to $l = 350$. We find that the majority of absorption occurs for $l \gg 1$, and make the approximation that $l - 1 \approx l \approx l + 1$, which means that we can replace the two terms of the summation in eqn 3.34 and write a simplified

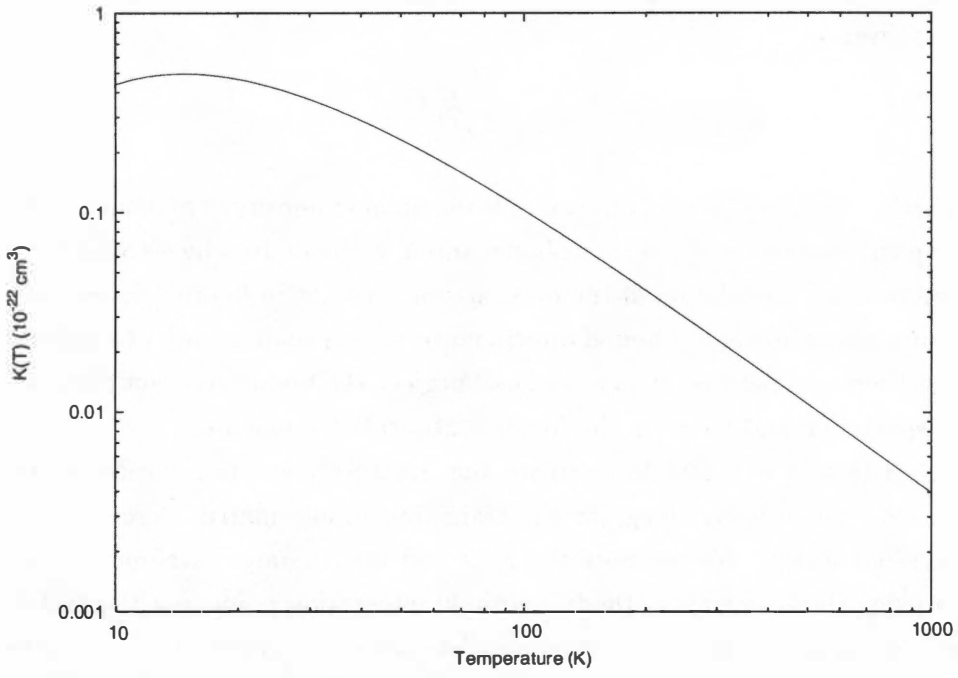

Figure 4.4: Calculated mass action constant

version of $VG(\omega)$ as:

$$VG(\omega) = \lambda_0^3 V\hbar \int_0^\infty \sum_{l=0}^{\infty} \exp(-E_i/kT) \left[(2l+1) \frac{1}{4\pi\epsilon_0} |\langle \Phi_n^f(E_f, l) | \mu_{elec}(R) | \Phi_n^i(E_i, l) \rangle|^2 \right] dE_i. \tag{4.3}$$

Sample calculations using the rigorous selection rules show that this approximation makes virtually no difference in the calculated absorption coefficient. A convergence analysis of our results, which was performed by expanding the parameters of the calculation (number of de Broglie points, summation over l, and number of Gauss-Laguerre points) show that our results are converged to well within $\pm 1\%$.

4.3 Results

We present in Figure 4.5 the results for the binary absorption coefficient of He-Xe at 298 K. The experimental absorption coefficient was measured at 298 $\pm$ 1 K by Dore et al[18]. We find that our results reproduce both the experimental lineshape and the absolute intensity of the He-Xe absorption feature fairly well; our binary absorption coefficient generally falls within the experimental uncertainty[18] of $\pm 10\%$. Our results tend to underestimate the absorption coefficient at frequencies below 300 cm^{-1}; above this, they begin to overestimate the coefficient. However, at large frequencies, the scatter in the data is more pronounced, indicating that the results may be less accurate than the error quoted by Dore et al[18].

As a test of our computational methods, we also present a calculation (cf figure 4.5) using the dipole moment of eqn 4.1, with the parameters given by Frommhold et al [24], and the potential energy surface of Aziz et al.[3]. We find our results in agreement with the calculated absorption coefficient of Frommhold et al.[24] The absorption coefficient of Frommhold et al. matches the overall intensity of the experimental coefficient better than our calculations; however, the peak is shifted to lower frequency values and the overall lineshape of the feature does not agree as well with experiment.

In order to better understand the dependence of the absorption spectrum on the dipole moment, we also evaluate the functional derivative of the absorption coefficient with respect to dipole moment. This allows us to determine the regions most affected by variations in the dipole moment. The functional derivative is defined as

$$\frac{\delta F[f(x)]}{\delta f(y)} = \lim_{\epsilon \to 0} \frac{F[f(x) - \epsilon\delta(x-y)] - F[f(x)]}{\epsilon}. \tag{4.4}$$

Since it is the spectral density, $VG(\omega)$, that depends on the dipole moment, we first calculate the functional derivative of the spectral density with respect to the dipole moment by

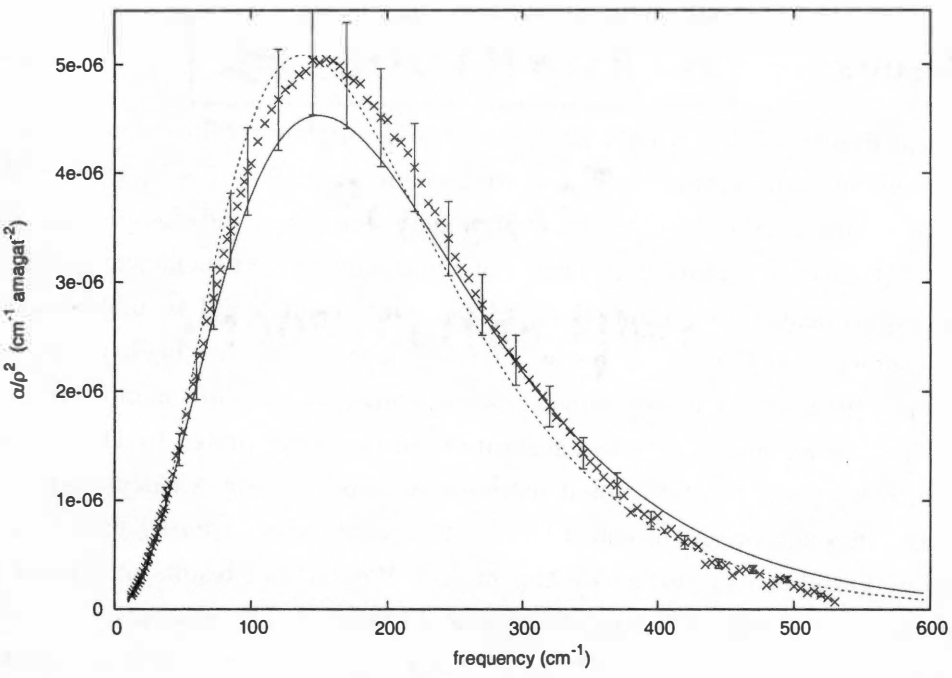

Figure 4.5: He-Xe absorption coefficient at 298 K. Solid line is current work, dashed line is calculation using Aziz potential and Frommhold dipole. Crosses are experimental points of Dore et al.[18,23], with error bars indicating ±10%.

substituting $VG(\omega)$ and $\mu_{elec}(R)$ into eqn 4.4 and obtain

$$\frac{\delta VG[\mu_{elec}(R)]}{\delta\mu_{elec}(R^*)} = -2\lambda_0^3\hbar\sum_{J=0}^{\infty}\int_0 dE_i VP_i \times \left\{(2J+1)\frac{1}{4\pi\epsilon_0}\langle\Phi_f^J|\mu_{elec}(R)|\Phi_i^J\rangle\Phi_f^J(R^*)\Phi_i^J(R^*)\right\}. \tag{4.5}$$

Substituting eqn 4.5 into eqn 3.15 we can in turn obtain the functional derivative of the absorption coefficient with respect to the dipole moment:

$$\frac{1}{\rho_{Xe}\rho_{He}}\frac{\delta\alpha(\omega)}{\delta\mu_{elec}(R^*)} = \frac{4\pi^2}{3\hbar c}N_{Xe}N_{He}V\omega[1-\exp(-\hbar\omega/kT)]\frac{\delta VG[\mu_{elec}(R)]}{\delta\mu_{elec}(R^*)}. \tag{4.6}$$

The functional derivative of $VG(\omega)$ with respect to dipole moment, eqn 4.5, has units of erg cm^6 s C^{-1} m^{-2}. The functional derivative of the absorption coefficient with respect to dipole moment, eqn 4.6, has units of cm^{-1} amagat^{-2} C^{-1} m^{-2}. Our results for the functional derivative of $\alpha(\omega)$ at 298 K are shown in figure 4.6. We have calculated the functional derivative of $\alpha(\omega)$ at every 0.05 bohr from 4 to 10 bohr, and at frequencies every 10 cm^{-1} from 10 cm^{-1} to 490 cm^{-1}.

The functional derivative shows us which regions of the dipole moment function make important contributions to the various regions of the spectrum. Referring to figure 4.6, we see that the low frequency regions of the spectrum depend most strongly on the small R region of the dipole moment. As the frequency increases, the dipole at larger R values begins to play a more important role. This helps to explain the difference between our spectrum and that calculated by Frommhold et al. Our dipole moment is both qualitatively and quantitatively similar to that of Frommhold et al. in the region of 5 to 8 bohr. From figure 4.6 we see that this is the only region of the dipole that plays a large role in the absorption at 50 cm^{-1} or less. As the frequency begins to increase above 50 cm^{-1}, however, we see that the values of the dipole moment at larger R begin to play a larger role in the absorption. At these bond lengths we find that small discrepancies between Frommhold's dipole and ours (see the inset of figure 4.3) give rise to the increased intensity in the calculated spectra of Frommhold et al.

At higher temperatures, He-Xe collisions will probe higher energy regions of the repulsive branch of the potential; this suggests that high temperature collision-induced absorption spectra will be increasingly sensitive to the behavior of the He-Xe dipole moment function at small R values. To demonstrate this, and to stimulate further experimental investigations of this system, we have computed the absorption coefficient and its functional derivative with respect to the dipole moment at T=1000 K. We present our results for the absorption coefficient in figure 4.7, and its functional derivative with respect to the dipole moment in figure 4.8.

The absorption coefficient calculated using the Frommhold dipole and Aziz potential

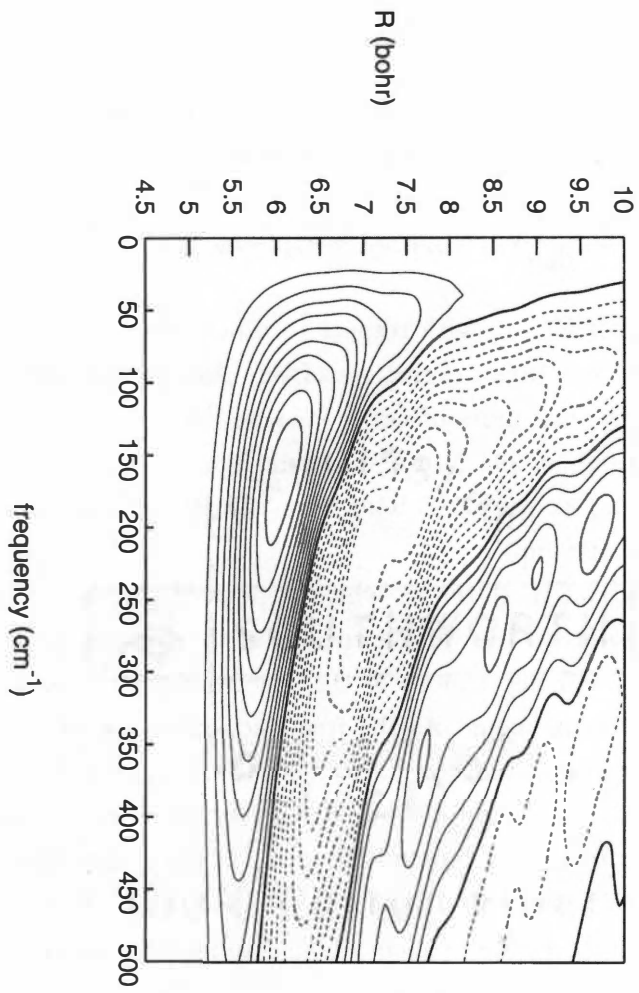

Figure 4.6: 298 K Functional derivative of the He-Xe binary absorption coefficient, $\alpha(\omega)/\rho^2$, with respect to the He-Xe dipole moment. Solid lines indicate positive values of the functional derivative, dashed lines are negative values, and the bold line is where the functional derivative is zero. Contours drawn on the base are in increments of 1×10^{35} units of the functional derivative (see text for details).

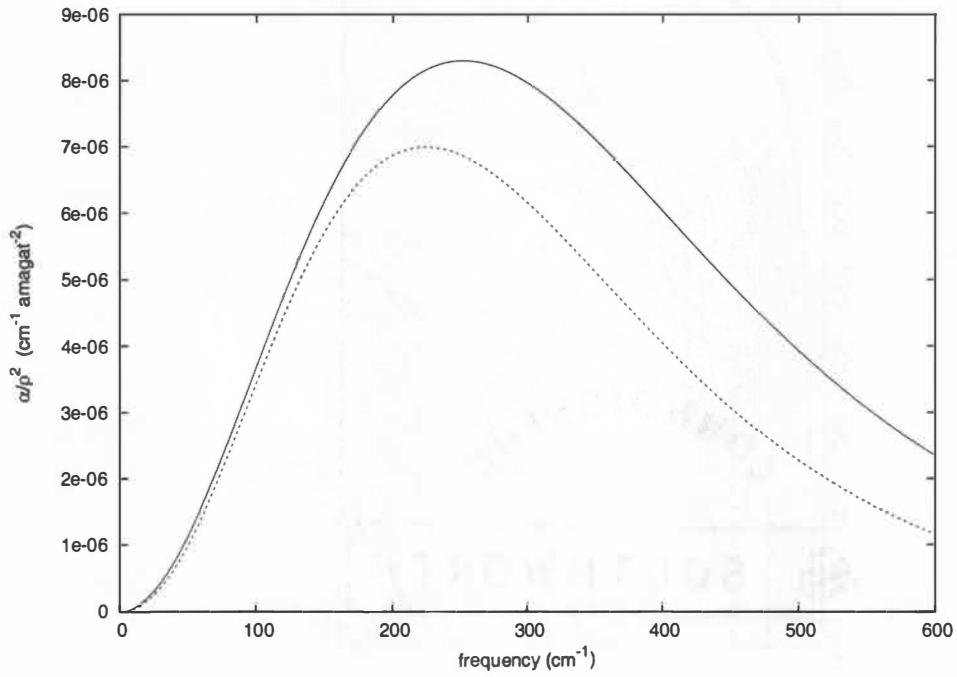

Figure 4.7: He-Xe spectrum at 1000 K. Solid line is present work; dashed line is calculation using Aziz potential and Frommhold dipole.

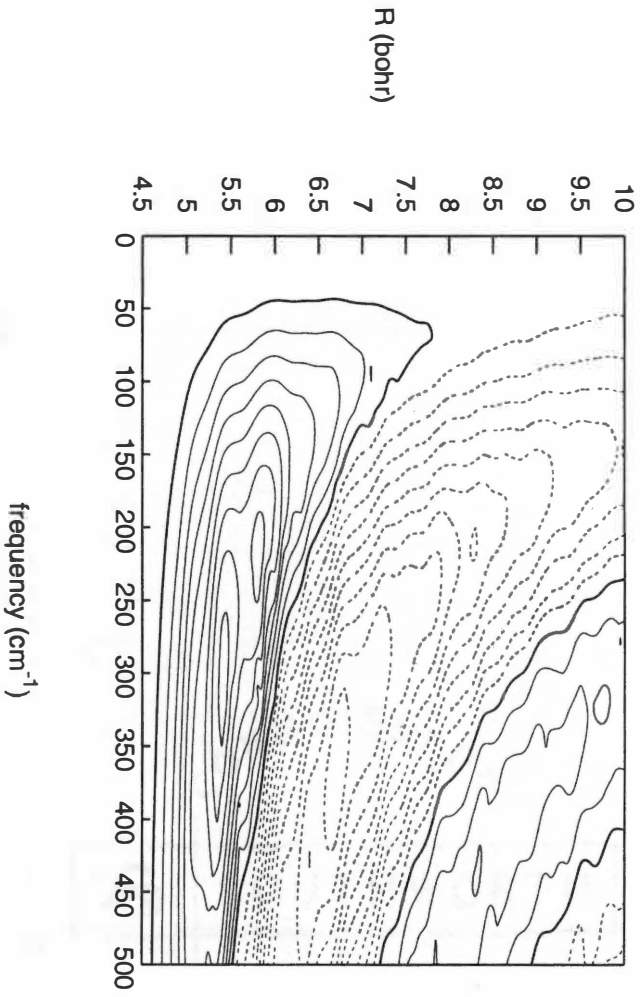

Figure 4.8: 1000 K Functional derivative of the He-Xe binary absorption coefficient, $\alpha(\omega)/\rho^2$, with respect to the He-Xe dipole moment. Solid lines indicate positive values of the functional derivative, dashed lines are negative values, and the bold line is where the functional derivative is zero. Contours drawn on the base are in increments of 1×10^{35} units of the functional derivative (see text for details).

Table 4.6: Microwave transition dipoles and energies

Initial State	Final State	ΔE (cm^{-1})	$\lvert\langle\Phi_{v_f,J_f}\lvert\mu_{elec}\rvert\Phi_{v_i,J_i}\rangle\rvert^2$
$v=0, J=0$	$v=0, J=1$	0.440	1.0383×10^{-8}
$v=0, J=1$	$v=0, J=2$	0.876	9.6034×10^{-9}
$v=0, J=2$	$v=0, J=3$	1.301	8.3670×10^{-9}
$v=0, J=3$	$v=0, J=3$	1.707	6.7670×10^{-9}
$v=0, J=4$	$v=0, J=3$	2.083	4.9238×10^{-9}
$v=0, J=0$	$v=1, J=1$	8.004	2.1732×10^{-11}

now differs substantially from the ab initio results, and lies below the ab initio results at all frequencies. This is consistent with our expectation that smaller R values of the dipole play a larger role in the high temperature spectrum. Referring to the functional derivative at 1000 K (figure 4.8), we see that the region between 4.5 and 6 bohr plays a much larger role in the absorption coefficient than it did at 298 K (figure 4.6).

4.4 Microwave Spectrum

Finally, we present our results for the transition dipole matrix elements and transition energies for the microwave spectrum of He-Xe in table 4.6. This should allow for comparison between experiment and theory, by substituting the matrix elements and transition energies into eqn 3.35, in order to calculate values of the absorption coefficients for those transitions at the temperature of interest.

4.5 Conclusion

In conclusion, we have presented fully ab initio computations of the He-Xe potential energy surface and the dipole moment using large correlation consistent basis sets and a relativistic effective core potential on Xe. Using these surfaces, we have performed a fully quantum mechanical calculation of the translational absorption coefficient at 298 K, which is in good agreement with experiment. We also present results for the absorption coefficient at 1000 K. We have performed an analysis of the functional derivative of the absorption coefficient with respect to the dipole moment at both of these temperatures, and used these derivatives to analyze differences in spectra calculated using our ab initio potentials, and those of others in the literature. Finally, we have presented results for the transition dipole moment integrals of the microwave transitions, in order to compare with future theoretical and experimental results.

Chapter 5

Sodium-Helium

5.1 Introduction

The purpose of this study is to determine the broadening of the Na D-line due to atomic Helium under conditions relative to brown dwarf atmospheres. Brown dwarf atmospheres typically have temperatures between 800 and 2000 K, with high concentrations of H_2 and He surrounding neutral sodium atoms[12]. The Na D-line is an electronic transition between the $^2S_{1/2}$ ground state and the $^2P_{1/2}$ (D_1 line) and $^2P_{3/2}$ (D_2 line) excited states of the atom. The D-line appears in the visible region of the electromagnetic spectrum, at 589.158 nm ($^2S_{1/2} \rightarrow {}^2P_{3/2}$) and at 589.757 nm ($^2S_{1/2} \rightarrow {}^2P_{1/2}$)[42]. Under the conditions of interest, the two components of the D-line cannot be resolved, so we neglect spin-orbit coupling and take the value of the transition wavelength to be 589.358 nm (there is a 2:1 degeneracy ratio of the D_2 and D_1 states).

In order to calculate the broadening, we must have accurate potential energy surfaces for both the ground and excited electronic states of Na-He, as well as transition dipole moments between these states. Computation of these potential energy surfaces and transition moments reduces to a one dimensional problem with axial symmetry, where it is only necessary to calculate these quantities as functions of bond length (chosen to lie on the z-axis). We choose the overall symmetry of the problem to be C_{2v}, which is the highest symmetry subgroup of $C_{\infty v}$ that is possible to use with the electronic structure program Dalton[27]. The ground state is then a ^2S Sodium atom interacting with a ^1S Helium atom, with an overall molecular symmetry of $^2\Sigma$ which has A_1 symmetry. The excited states consist of a ^2P Sodium atom interacting with a ^1S Helium atom; however the Helium atom breaks the degeneracy of the Sodium P orbitals, and we have three excited states. The $^2\Sigma$ molecular state, with degeneracy 1, consists of the excited electron in the P_z atomic orbital of Sodium and has A_1 symmetry. The $^2\Pi$ molecular state, which is doubly degenerate, consists of the excited electron in the $P_{x,y}$ atomic orbitals of Sodium, and has B_1 (x) and

B_2 (y) symmetries respectively.

5.2 Potential Energy Surface

Due to the low-lying excited states in the Na atom it is necessary to use a multi-reference method for the calculation. The repulsive wall is very important for the determination of the absorption spectra, and it is here that the multi-reference character will be most pronounced. We choose to treat the electronic structure problem using the multi-reference complete active space SCF method (CASSCF)[44], with the ROHF method for individual determinants. Because we are calculating a doublet state, it is necessary to have an open shell formalism, however, UHF was judged to be insufficient due to spin contamination. In the CASSCF method, the orbitals are divided into three subspaces. The first subspace is an occupied core, consisting of spatial orbitals that are doubly occupied in each Slater determinant. This is called the frozen core approximation. The second subspace is the active space, which consists of the remaining occupied orbitals, as well as the subset of virtual orbitals that are chosen to be significant to the calculation. The active space is the set of orbitals from which we form all of our Slater determinants in the MCSCF calculation. The final subset are the remaining virtual orbitals, that are not allowed to be occupied in any Slater determinant. In the limit of zero electrons in the frozen core, we have a full CI calculation in the active space, and in the limit that every electron is in the frozen core we have a HF calculation. The advantage of this formalism is that it allows us to treat the more important electrons for our physical problem at a high level of theory, while still providing a reasonably accurate description of the core electrons. The MCSCF treatment also allows us to optimize the core orbitals with every excited Slater determinant, which is important as the two atoms collide. In the case of Na-He, we have a 13 electron problem. We choose to keep the 10 core electrons ($1s^2 2s^2 2p^6$) of the Na atom in the frozen core, and put the three valence electrons (Na $3s$, He $1s^2$) in the active space. We choose the active space to be composed of the full set of virtual orbitals contained in the basis set, thus reducing the number of subspaces in the problem to two. The calculations were performed using the MCSCF module of the quantum chemical program Dalton v1.2.1[27]. In order to calculate the excited states, we use the same CASSCF method, but calculate the energies for the first excited state of appropriate symmetry. We only perform the calculations for the $^2\Pi$ state using B_1 symmetry, as the B_2 symmetry state is degenerate with the B_1 state. Our energies are obtained using a supermolecular approach that includes the standard counterpoise correction[9].

We have calculated the energies using correlation consistent basis sets on Na and He, using cc-pCVXZ (X=D,T,Q) basis sets on Na[50], and aug-cc-pVXZ on Helium[49]. The cc-pCVXZ basis sets for Na are core-valence (CV) basis sets that include extra s, p, and

d orbitals on the core to improve the description of the core orbitals. The aug-cc-pVXZ basis sets for He include extra diffuse functions that allow for a better description of van der Waals bonding. Unfortunately, a drawback to the MCSCF method is that it scales factorially with the number of active electrons and basis set functions. We were only able to perform test calculations at the ROHF level for the QZ basis sets, as the number of determinants needed for this calculation at the MCSCF level is intractable. At the DZ level, approximately 4000 determinants are needed, while at the TZ level approximately 60,000 determinants are used. We also attempted to use a small set of mid-bond functions [47], however the DZ+midbond calculations were higher in energy than the TZ calculations, and we were unable to perform the calculation using the TZ+midbond set.

In order to assess the accuracy of our potential, we first compare our ground state potential with that of Partridge et al.[33], who have performed calculations on the ground state using a single reference CCSD(T) method with large correlation consistent basis sets augmented by mid-bond functions. The valence electrons, as well as the outer core electrons are included in the correlation treatment, with only the innermost $1s^2$ electrons on Na frozen. Our calculations compare reasonably well, we find a van der Waals minimum at R_e=12.70 a_0 with D_e=0.958 cm^{-1} compared to Partridge et al values of R_e=11.85 a_0 and D_e=1.528 cm^{-1}. We find that our potential is more repulsive than the results of Partridge et al., (see table 5.1), which is a result of the increased core-valence correlation included in the coupled cluster calculations. Our excited state potentials compare favorably with results in the literature[6,29,34] in terms of the overall shape and range of the potentials. The excited $^2\Sigma$ potential has a small well with R_e=12.70 a_0, and D_e=0.958 cm^{-1}. Our excited $^2\Pi$ potential has a relatively deep well with R_e=4.42 a_0 and D_e=390.06 cm^{-1}. This should be compared with the experimentally determined well depth of Havey et al.[26] of D_e=480 $\pm$ 50 cm^{-1} and R_e=4.4 $\pm$ 0.2 a_0. Calculations by Bililign et al.[6], using an MCSCF method with an active space composed of the He 1s orbitals and the Na 3s and 3p orbitals, found a well depth of D_e=513 cm^{-1} and R_e=4.44 a_0.

Our results for the potential energy surfaces of the ground and excited states are presented in Fig. 5.1 and Table 5.2. Finally, we can calculate the asymptotic energy difference between the excited states, and calculate the deviation from the spin-orbit averaged Na D-line. We find that our asymptotic energy difference, obtained from an energy calculation of the dimer at 50 bohr, corresponds to a transition wavelength of 628.316 nm, which is 6.5 % lower than the spin-orbit averaged transition energy for Na.

We present the bound state energy levels in table 5.3. These levels were calculated using the Numerov-Cooley method[13] and are well-converged with respect to integration step and integration interval.

Table 5.1: Difference between current $^2\Sigma$ ground state potential and Partridge et al.[a]

R (a_0)	ΔV (cm^{-1})
2.5	728.187594
3.0	308.178587
3.5	123.309316
4.0	62.6897881
4.5	50.2019563
5.0	47.97766
5.5	45.1777322
6.0	39.8116918
6.5	32.9964077
7.0	26.107534
7.5	19.9305745
8.0	14.7474289
8.5	10.6120443
9.0	7.45817266
9.5	5.14405789
10.0	3.49994868
10.5	2.35780734
11.0	1.57705883
11.5	1.05010905
12.0	0.695854616
12.5	0.461463179
14.0	0.134358193
15.0	0.0606614629

a. Ref [33]

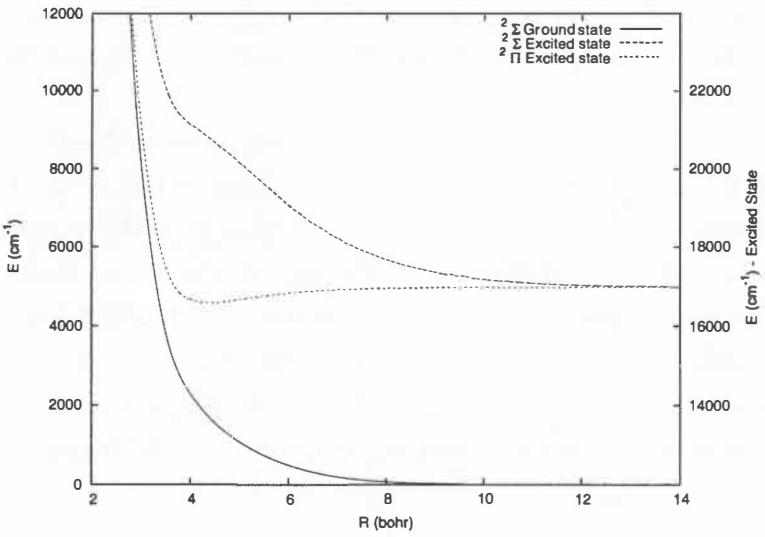

Figure 5.1: Calculated potential energy surfaces of Na-He dimer.

Table 5.2: Potential energy surfaces of the ground and excited states of the Na-He dimer

R (a_0)	$^2\Sigma$ Ground State (E_h)	$^2\Sigma$ (E_h)	$^2\Pi$ (E_h)
1.0	2.73381516	2.76562535	2.69733875
1.5	0.956943145	0.958372398	0.938287967
2.0	0.30227557	0.298986506	0.281909966
2.5	0.0990011669	0.0971379567	0.0787754358
3.0	0.037009445	0.0388018176	0.0188314227
3.5	0.0174928486	0.0231732823	0.00235770895
4.0	0.0104524857	0.0189425895	-0.00140222895
4.5	0.00706001695	0.0167587903	-0.00176604597
5.0	0.00489042231	0.0144307489	-0.00141039446
5.5	0.0033342449	0.0119077898	-0.00101036173
6.0	0.00221179542	0.00949276165	-0.000700604907
6.5	0.0014263527	0.00738218455	-0.000482501151
7.0	0.000895824681	0.00563860177	-0.000332961451
7.5	0.000548530382	0.00424734193	-0.000230892864
8.0	0.000327124232	0.00316217365	-0.000161133233
8.5	0.000189282033	0.00232972877	-0.00011330754
9.0	0.000105441936	0.00169984611	-8.0356503E-05
9.5	5.5688053E-05	0.00122897403	-5.7503293E-05
10.0	2.696694E-05	0.000880823937	-4.1537022E-05
10.5	1.0932961E-05	0.000626005131	-3.0300905E-05
11.0	2.37560897E-06	0.000441244452	-2.2336951E-05
11.5	-1.885351E-06	0.000308455903	-1.6650014E-05
12.0	-3.74945299E-06	0.000213810724	-1.2555143E-05
12.5	-4.32741899E-06	0.000146886998	-9.57862702E-06
14.0	-3.40781901E-06	4.4667457E-05	-4.548482E-06
15.0	-2.47360603E-06	1.8727141E-05	-2.91088199E-06
16.0	-1.74246E-06	7.02568298E-06	-1.92794803E-06
17.0	-1.22421201E-06	2.020648E-06	-1.31564502E-06
19.0	-6.23933005E-07	-6.12960008E-07	-6.59883E-07
20.0	-4.55267013E-07	-7.45365014E-07	-4.81863992E-07

Table 5.3: Bound state energy levels in E_h of the $^2\Pi$ state

J	v=0	v=1	v=2	v=3	v=4
0	0.0003500806	0.0009315673	0.0013376767	0.0016026403	0.0017382841
1	0.0003579335	0.0009383266	0.0013432101	0.001610948	0.0017435268
2	0.000373625	0.0009518251	0.0013542509	0.00162331	0.0017511953
3	0.0003971244	0.0009720209	0.0013707445	0.0016396023	0.0017610217
4	0.0004283884	0.0009988525	0.0013926088	0.0016596492	0.0017725562
5	0.0004673584	0.0010322361	0.0014197306	0.0016832126	
6	0.0005139607	0.0010720651	0.0014519624	0.0017099726	
7	0.0005681062	0.0011182079	0.0014891177	0.0017394922	
8	0.0006296889	0.0011705065	0.0015309631	0.0017711442	
9	0.000698587	0.0012287736	0.0015772104		
10	0.000774657	0.001292787	0.0016274976		
11	0.0008577378	0.0013622862	0.0016813681		
12	0.0009476453	0.0014369669	0.0017382286		
13	0.0010441689	0.0015164673			
14	0.0011470705	0.0016003535			
15	0.0012560775	0.0016880981			
16	0.0013708727				
17	0.0014910917				
18	0.0016162994				
19	0.0017459678				

Table 5.4: Dipole moment surface of Na-He $^2\Sigma$ ground state

R (a_0)	μ (a.u.)	R (a_0)	μ (a.u.)
1.5	1.01176043	8.0	0.07978292
2.0	1.15104425	8.5	0.05291711
2.5	1.25172714	9.0	0.03455124
3.0	1.24686198	9.5	0.02221700
3.5	1.14636423	10.0	0.01406915
4.0	0.98631350	10.5	0.00877205
4.5	0.80381127	11.0	0.00537498
5.0	0.62709058	11.5	0.00322965
5.5	0.47221563	12.0	0.00189505
6.0	0.34543861	12.5	0.00108311
6.5	0.24664936	13.0	0.00059580
7.0	0.17245739	13.5	0.00030445
7.5	0.11832678	14.0	0.00014183

5.3 Dipole Moments

5.3.1 Ground State Dipole Moment

In order to calculate the collision induced absorption (CIA) spectrum for the ground state of the Na-He dimer, we need to have the dipole moment as a function of bond length. The evaluation of MCSCF dipole moments is straightforward; they are calculated as an expectation value of the electronic dipole operator evaluated over the MCSCF wavefunction obtained at a given internuclear distance. The dipole moment of the ground state is presented in table 5.4.

5.3.2 Electronic Transition Dipole Moments

In order to calculate the electronic transition dipole moment, we use linear response theory. Response theory measures the response of a molecule to a time-dependent external field, and is implemented in Dalton using time-dependent multi-reference Hartree Fock theory [15]. For the dipole moment operator, the response function is calculated as a function of frequency; using time-dependent perturbation theory this response function can be shown to be equivalent to[43]:

$$\langle\langle \mu_\alpha ; \mu_\beta \rangle\rangle_\omega = \sum_k{}' \left[\frac{\langle 0|\mu_\alpha|k\rangle\langle k|\mu_\beta|0\rangle}{\hbar\omega - \hbar\omega_{k0}} - \frac{\langle 0|\mu_\alpha|k\rangle\langle k|\mu_\beta|0\rangle}{\hbar\omega + \hbar\omega_{k0}} \right] \tag{5.1}$$

where the left hand side of the equation is the frequency dependent dipole-dipole polarizability. In this equation α, β correspond to the cartesian components of the dipole moment

operator, the prime on the sum omits the ground state, $|0\rangle$, from the summation and the sum is over all of the excited states, $|k\rangle$. The energies in the denominator $\hbar\omega_{k0}$ correspond to the excitation energy of state $|k\rangle$. The bra-ket pairs in the numerators correspond to the oscillator strengths for a given transition, and can be determined using the linear response function. For positive frequencies, ω, the linear response function will have poles corresponding to the excitation energy $\hbar\omega_{k0}$. To determine the oscillator strengths for the transitions we must find the poles of this function and then calculate the residues at each pole.

We perform this single residue analysis at each internuclear separation using Dalton; this yields the transition dipole moments for the Na-He system as a function of bond length. We have calculated the transition dipoles using the same MCSCF formalism as for the potential energy surfaces, at the DZ and TZ levels of theory. The TZ calculations were used to check the accuracy of the DZ calculations, and the two were found to be in reasonable agreement. Because of the expense of the TZ calculations, we therefore used the DZ basis sets to compute the transition moments as a function of bond length; our results are shown in table 5.5. To assess the accuracy of our transition dipole moments, we can compare our asymptotic transition moments with those of the unperturbed Na atom. We calculate the spin-orbit averaged oscillator strength[20] for the isolated Na atom from the experimental oscillator strengths[42], and use those values to calculate an average transition moment for the unperturbed atom[20]. We obtain a value of 2.492 e a_0 for the average, which compares fairly well to our asymptotic value of 2.60 e a_0.

5.4 Translational Spectra of Ground State

As the ground state potential does not support any bound states, the only contributions to the spectrum are from free-free continuum states. We perform calculations of the CIA spectrum of the ground state using eqn 3.15 and eqn 3.34. We numerically integrate the transition dipole matrix elements, eqn 3.28, for the individual states. We integrate the final and initial state wavefunctions for each energy point using the Numerov method[48], with 30 integration points per thermal de Broglie wavelength of the final energy state. The wavefunctions are integrated to a distance of 350 bohr, where we energy normalize them (cf Appendix A.3). The integration of the matrix element is carried out using trapezoid integration,using the same number of points as the wavefunction integrations.

In order to calculate the energy integral, we first interchange the integral over energy and the sum over l in eqn 3.34, and we use 12 point Gauss-Laguerre integration[36] to evaluate the integral. We then sum over l values up to $l = 350$. We find that the majority of absorption occurs for $l \gg 1$, and make the approximation that $l - 1 \approx l \approx l + 1$, which means that we can replace the two terms of the summation in eqn 3.34 and write a

Table 5.5: Transition dipole moments of the Na-He dimer. DZ corresponds to the cc-pCVDZ basis on Na and the aug-cc-pVDZ basis on He. TZ corresponds to the cc-pCVTZ basis on Na and the aug-cc-pVTZ basis on He.

A_1 state			B_1 state		
R (a_0)	DZ (ea_0)	TZ (ea_0)	R(a_0)	DZ (ea_0)	TZ (ea_0)
3.0	2.1516167		3.0	2.6996479	
3.25	2.1553012		3.25	2.6898742	
3.5	2.1721222		3.5	2.6798396	
3.75	2.1995741		3.75	2.6700980	
4.0	2.2338385		4.0	2.6609330	
4.25	2.2706806		4.25	2.6525204	
4.5	2.3069016	2.2830238	4.5	2.6444580	2.6417007
4.75	2.3403384		4.75	2.6370604	
5.0	2.3704835	2.3484068	5.0	2.6301830	2.6272649
5.5	2.4205249		5.5	2.6183212	
6.0	2.4601838		6.0	2.6095147	
6.5	2.4925631		6.5	2.6036004	
7.0	2.5193888		7.0	2.5996892	
7.5	2.5414987		7.5	2.5980310	
8.0	2.5593342		8.0	2.5971339	
9.0	2.5838154		9.0	2.5970195	
10.0	2.5968623		10.0	2.5978637	
11.0	2.6027320		11.0	2.5987230	
12.0	2.6047979		12.0	2.5994771	
13.0	2.6050807		13.0	2.6000474	
14.0	2.6045106		14.0	2.6004311	

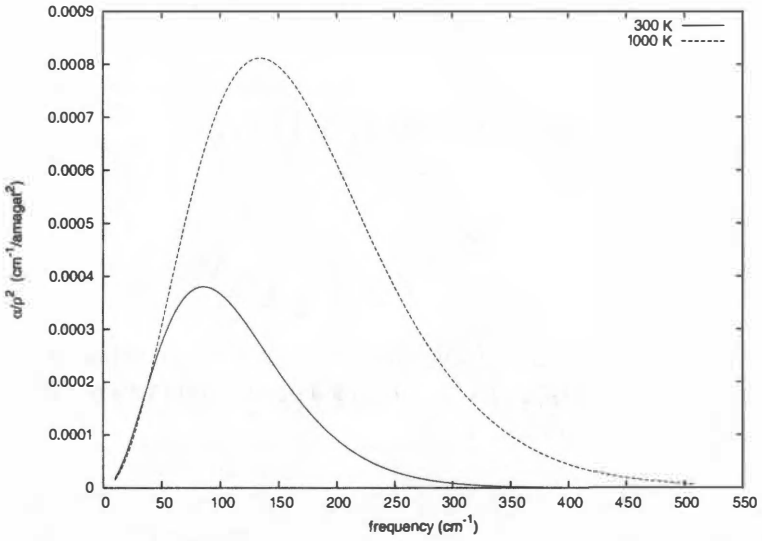

Figure 5.2: Absorption coefficient of the $^2\Sigma$ ground state of the Na-He dimer.

simplified version of $VG(\omega)$ as in eqn 4.3. Sample calculations using the rigorous selection rules show that this approximation makes virtually no difference in the calculated absorption coefficient. A convergence analysis of our results, which was performed by expanding the parameters of the calculation (number of de Broglie points, summation over l, and number of Gauss-Laguerre points) show that our results are converged to well within $\pm 1\%$.

We present our results for 300 K and 1000 K in figure 5.2. We find that our results compare favorably with those of Bottcher et al.[7]. They performed a quantum calculation for the 300 K coefficient, and used a classical method for the 1000 K coefficient. Our calculations do indicate that the dimer absorbs more strongly at higher frequencies in the case of 1000 K, however the overall intensity at the strongest absorption frequency of Bottcher et al. is stronger than ours.

5.5 Broadening of the Na-D line

The calculation for the broadening of Na-D line by Na-He collisions is a bit more complicated due to the form of the transition dipole moment integral, eqn 3.29. The electronic transition dipole moment does not asymptotically go to zero at large Na-He distances, due to the fact that the transition is allowed in the unperturbed Na atom, and hence the integral is non-convergent in its present form. We thus describe a method for transforming the integral into a convergent form that is suitable for calculation[28]. Our nuclear wavefunctions, $\Phi_n(E, l, m)$, are eigenfunctions of the nuclear Hamiltonian with eigenvalues:

$$\hat{H}_n|\Phi_n(E, l, m)\rangle = K^2|\Phi_n(E, l, m)\rangle \tag{5.2}$$

where $K = (2\mu E/\hbar^2)^{1/2}$. Taking advantage of the hermiticity of the Hamiltonian, we can insert the commutator of the dipole moment operator and the Hamiltonian operator into a bra-ket pair and obtain:

$$\begin{aligned}
&\left\langle \Phi_n(E_f, l_f, m_f)\right| \left[\hat{H}_n, \mu_{elec}\right] \left|\Phi_n(E_i, l_i, m_i)\right\rangle = \\
&= \langle \Phi_n(E_f, l_f, m_f)|(\hat{H}_n^f \mu_{elec} - \mu_{elec}\hat{H}_n^i)|\Phi_n(E_i, l_i, m_i)\rangle \\
&= \langle \Phi_n(E_f, l_f, m_f)|(K_f^2 \mu_{elec} - \mu_{elec}K_i^2)|\Phi_n(E_i, l_i, m_i)\rangle \\
&= (K_f^2 - K_i^2)\langle \Phi_n(E_f, l_f, m_f)|\mu_{elec}|\Phi_n(E_i, l_i, m_i)\rangle
\end{aligned} \tag{5.3}$$

where $\hat{H}_n^f$ is the nuclear Hamiltonian for the final state, which depends on the interaction potential and angular momentum of that state. We can also expand the Hamiltonian into its kinetic and potential parts, and evaluate $\hat{H}_n^f \mu_{elec} - \mu_{elec}\hat{H}_n^i$ as:

$$\hat{H}_n^f \mu_{elec} - \mu_{elec}\hat{H}_n^i = \left[\hat{T}, \mu_{elec}\right] + \frac{2\mu \Delta V^{eff} \mu_{elec}}{\hbar^2}. \tag{5.4}$$

where ΔV^{eff} is the difference potential (including the centrifugal barrier term) between the initial and final states. If we assume that the difference between the l and $l \pm 1$ centrifugal barriers is minimal, this term reduces to:

$$\Delta V^{eff} \approx \Delta V \tag{5.5}$$

where ΔV is the difference potential $V_f(R) - V_i(R)$ of the interaction energies, which goes to zero as $R \to \infty$. The magnitude of the commutator between the dipole function and the kinetic energy operator is on the order of the Born-Oppenheimer correction terms[28], and can be neglected. It is also noted that as the relative separation of the atoms increases, the dipole moment becomes constant and the commutator is rigorously zero. Substituting eqn 5.4 into eqn 5.3 and solving for the transition dipole matrix we obtain:

$$\langle \Phi_n(E_f, l_f, m_f)|\mu_{elec}|\Phi_n(E_i, l_i, m_i)\rangle = \frac{2\mu\langle \Phi_n(E_f, l_f, m_f)|\Delta V \mu_{elec}|\Phi_n(E_i, l_i, m_i)\rangle}{\hbar^2(K_f^2 - K_i^2)} \tag{5.6}$$

This reduces our transition dipole matrix integral into an integral that is convergent and easily evaluated using numerical techniques.

Using this form of the transition dipole moment integral, eqn 5.6, we evaluate the broadening of the Na D-line using eqns 3.15 and 3.34. We adjust our excited state potentials so that the difference in excited and ground states corresponds to the experimental value of the Na D-line, putting the experimental Na D-line at the line-center by construction. As the $^2\Pi$ state has several bound states, we also need to evaluate the continuum-bound

contributions, using eqn 3.37.

We integrate the continuum wavefunctions using the Numerov method[48], with 30 points per de Broglie wavelength of the higher energy state, to a distance of $R = 350\, a_0$, where we energy normalize the wavefunctions. The dipole moment integral is evaluated using trapezoid integration, with the same number of points as the wavefunction integration. The contributions from the different electronic states are calculated separately, then we sum over the electronic states taking into account their degeneracies. The energy integrals are performed using Gauss-Laguerre integration[36], summing over the l quantum number up to $l = 350$. We find that the majority of absorption occurs for $l \gg 1$, and make the approximation that $l - 1 \approx l \approx l + 1$, which means that we can replace the two terms of the summation in eqn 3.34 and write a simplified version of $VG(\omega)$ as in eqn 4.3. with the transition dipole moment evaluated using eqn 5.6. An analogous formula holds for the free-bound absorption eqn 3.37. Sample calculations using the rigorous selection rules show that this approximation makes virtually no difference in the calculated absorption coefficient of either the free-free absorption or the free-bound absorption.

5.6 Results

5.6.1 Blue Wing

We present results for the blue wing of the Na D-line calculated using 100 Gauss Laguerre points at 1000 K in figures 5.3 and 5.4. We have calculated the spectra for wavelengths between 475 nm and 585 nm, at intervals of 2 nm. Figure 5.3 shows the contributions of each state to the blue wing. As expected[1,12] from the shapes of the potentials, the contribution is mostly due to the $^2\Sigma$ state. The shape of the absorption coefficient is very sensitive to the difference potential, ΔV, which is shown in figure 5.5. Maxima in the difference potentials will give rise to line satellites, which we find at $\sim$ 19,000 cm^{-1}. This corresponds to a wavelength of $\sim$ 530 nm, which corresponds well to the satellite found by Allard et al[1] at 520 nm.

5.6.2 Red Wing

Unfortunately, we were unable to obtain sufficient convergence of the absorption coefficient for the red wing of the Na D-line broadening, due to convergence of the $^2\Pi$ contribution. For photon energies less than the atomic line, the integrand of the energy integral in eqn 4.3 is zero for initial state energies satisfying $E_i > E_{\text{D-line}} - \hbar\omega$. We have attempted to translate the integral, setting the zero of energy to be $E_0 = E_i + (E_{\text{D-line}} - \hbar\omega)$, however, we have still experienced convergence problems. We present results for 100 Gauss-Laguerre points of the $^2\Pi$ state in figure 5.6, as well as the convergence behavior as we increase

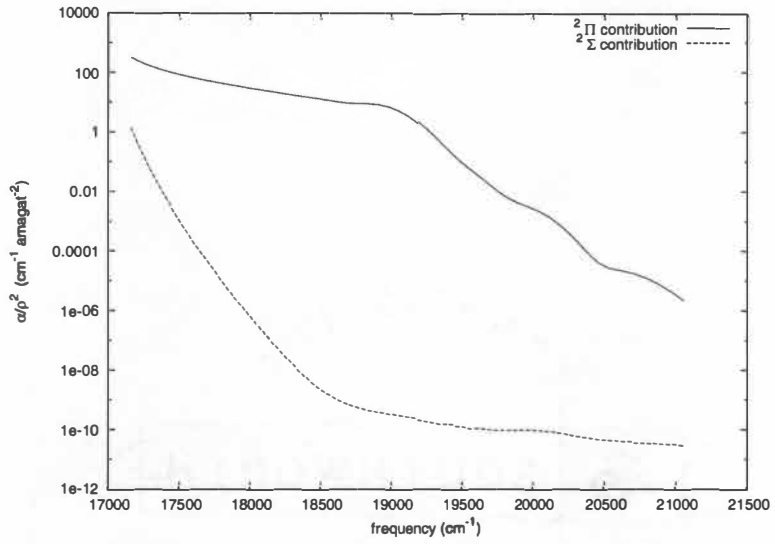

Figure 5.3: Figure showing contribution of each excited state to the blue wing free-free absorption coefficient at 1000 K for the Na-He dimer

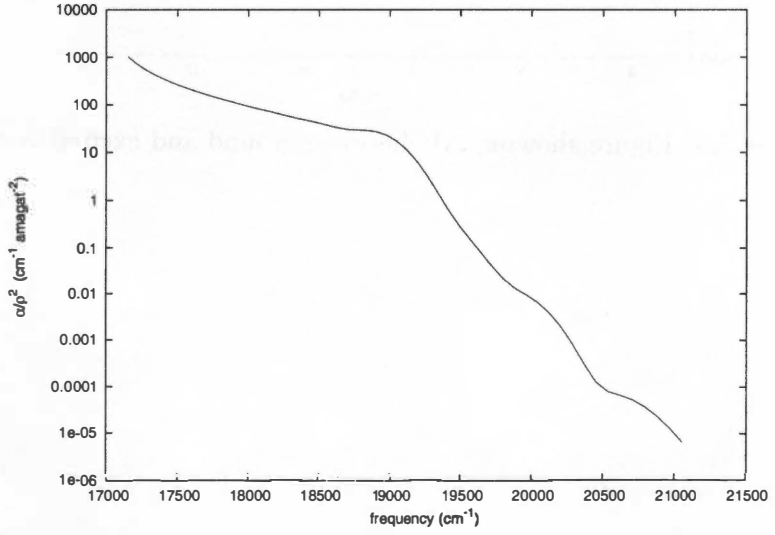

Figure 5.4: Free-free absorption coefficient of the blue wing at 1000 K for the Na-He dimer.

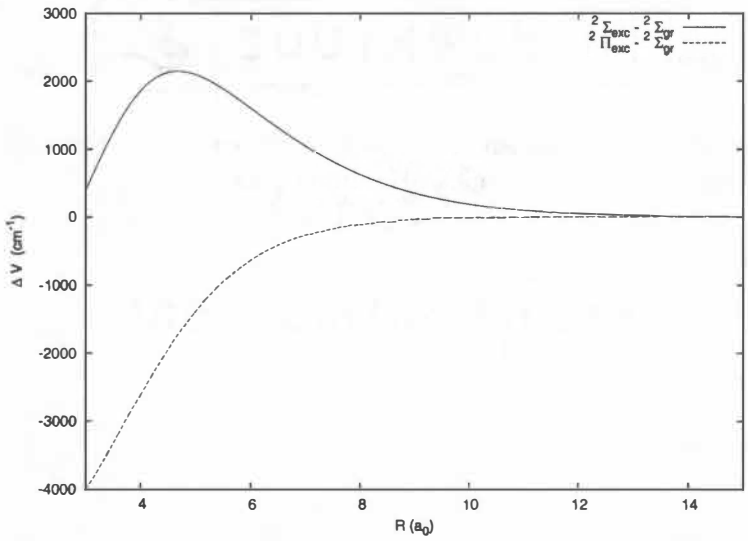

Figure 5.5: Figure showing ΔV between ground and excited states.

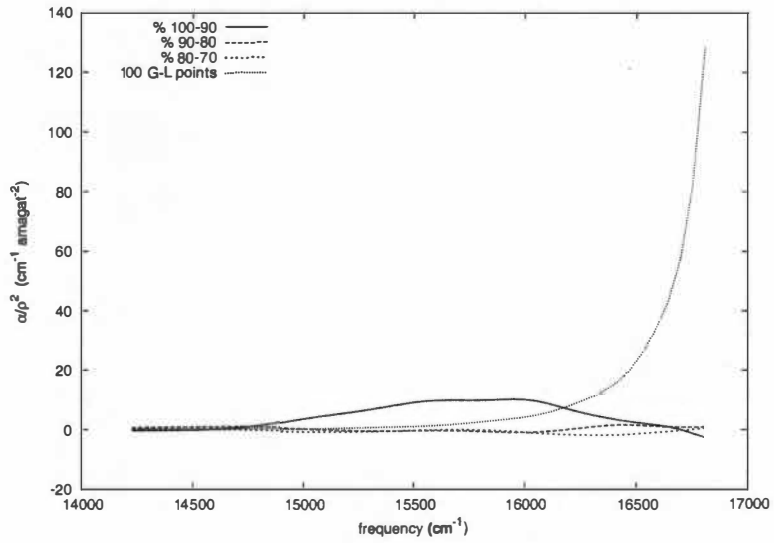

Figure 5.6: Gauss-Laguerre convergence of the $^2\Pi$ contribution to the Na D-line red wing.

in increments of 10 Gauss-Laguerre points from 70 to 100. As is evident from the plot, the result for 100 Gauss-Laguerre points is not well converged. The results do indicate, however, that we are converged to within $\sim$ 10 %, especially close to the D-line. There is the possibility that quasi-bound resonance states are contributing to the absorption[40]. These states occur when the molecule becomes temporarily trapped in a centrifugal barrier well that is coupled to a continuum state. This could cause an anomalous increase in the value at a given Gauss-Laguerre energy point, which could lead to convergence difficulties due to the method by which Gauss-Laguerre energy points are chosen[36].

The double degeneracy of the $^2\Pi$ state increases the amount of error in our final calculated absorption coefficient for the red wing. We estimate that our results are converged within $\sim$ 20 % of the converged value, however, the line-shape overall should not change appreciably, as the majority of error occurs in regions where the absorption is weak. We present our results for the red wing of the Na D-line calculated using 100 Gauss Laguerre points at 1000 K in figures 5.7 and 5.8. The spectra have been calculated from 595 to 703 nm in increments of 2 nm. Figure 5.7 shows the contributions of each state to the red wing. As expected, the majority of the contribution to the red wing occurs due to the $^2\Pi$ state.

5.6.3 Free-Bound

We have also calculated the free-bound contribution to the red wing of the Na D-line. As the bound states of the excited state $^2\Pi$ dimer all lie at negative energies with respect to the asymptotic energy, they can only contribute to the red-wing of the spectrum. The results for the free-bound absorption at 1000 K are presented in figure 5.9.

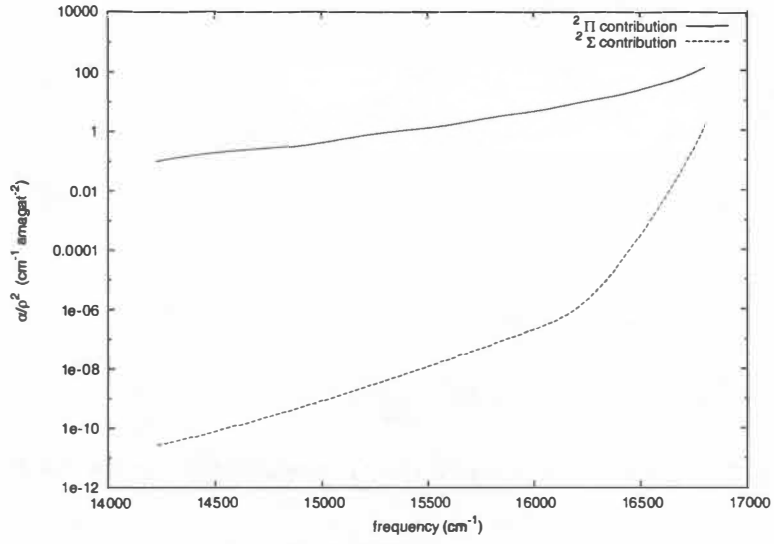

Figure 5.7: Figure showing contribution of each excited state to the red wing free-free absorption coefficient at 1000 K for the Na-He dimer

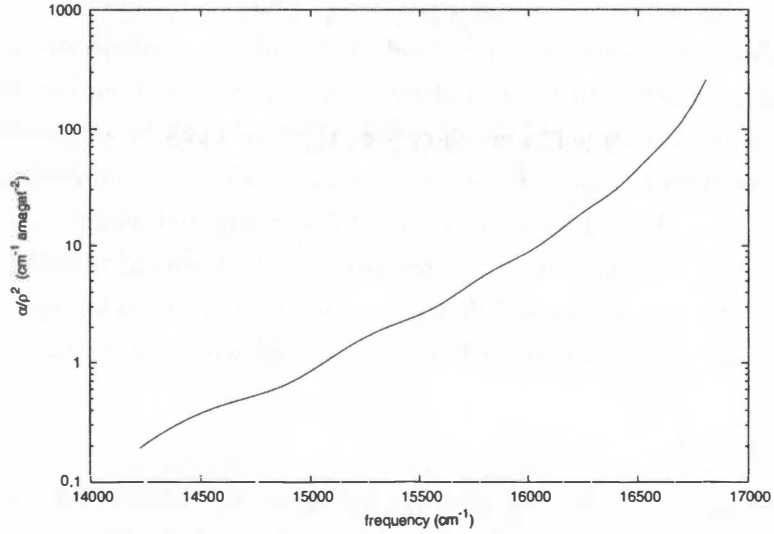

Figure 5.8: Free-free absorption coefficient of the red wing at 1000 K for the Na-He dimer.

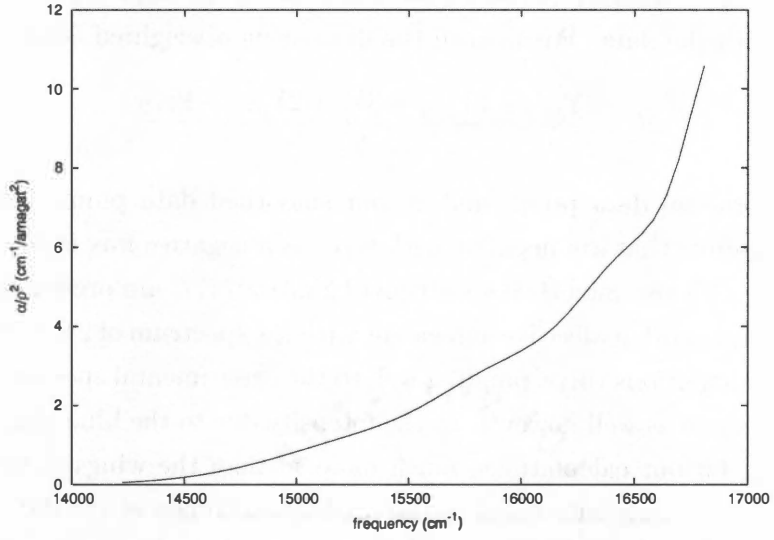

Figure 5.9: Free-bound absorption coefficient at 1000 K for the Na-He dimer

5.7 Comparison to Brown Dwarf Spectra

We present the final results for the broadening of the Na D-line due to atomic Helium at 1000 K in figure 5.10. We find that the blue wing of the D-line shows significantly more absorption than the red wing, in accordance with other theoretical results[1,12]. The slopes of the wings are also markedly different, with the slope of the red wing remaining relatively steep, while the slope of the blue wing is more shallow until it passes the satellite. In order to validate our theory and results, we can compare our line shapes with those of the brown dwarf 2MJ1507477[37,38]. This data was collected between 380 and 865 nm using the Low Resolution Imaging Spectrograph (LRIS) on the Keck II telescope. The experimental data is measured as the flux emitted by the brown dwarf, which is inversely proportional to the absorption coefficient. Due to experimental conditions, as well as the strength of the absorption in the proximity of the D-line, the noise in the data is pronounced and it is beneficial to smooth the data. We smooth the data using a weighted 5-point formula:

$$S_j = \frac{Y_{j-2} + 2Y_{j-1} + 3Y_j + 2Y_{j+1} + Y_{j+2}}{9} \tag{5.7}$$

where Y_j is our original data point, and S_j our smoothed data point. Furthermore, we replace any data points that are negative with zero, as a negative flux is clearly unphysical. Our results, along with the smoothed spectrum of 2MJ1507477, are presented in figure 5.11. We find that we have good qualitative agreement with the spectrum of 2MJ1507477, with the lineshape of our calculations corresponding well to the experimental spectrum. The relative intensities do not agree as well however, as the intensity due to the blue wing is much larger than the red wing for our calculations, much more so than the wings of the experimental data. We are however, only interested in the qualitative trends of the data, as the Na-He absorption alone is unlikely to fully explain the experimental spectrum. It is expected that the Na-H_2 absorption would show the same trends as the Na-He absorption[1,12], and we find it encouraging that our line shape agrees qualitatively with the astrophysical observations.

5.8 Conclusion

In conclusion, we have presented fully ab initio computations of the Na-He potential energy ground and excited state surfaces, using large correlation consistent basis sets. Further, we have calculated the ground state dipole moment, as well as the transition dipole moments between the ground and excited states. Using these surfaces, we have performed fully quantum mechanical calculations of the collision induced absorption spectrum of the ground state, as well as the wings of the broadened Na D-line due to atomic helium. Work is currently underway to resolve the convergence issues with respect to the red wing of the

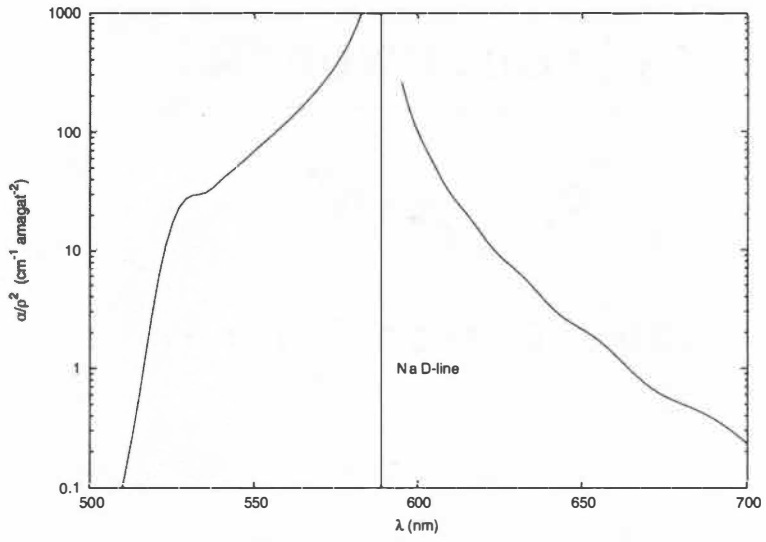

Figure 5.10: Broadening of the Na D-line due to atomic Helium at 1000 K.

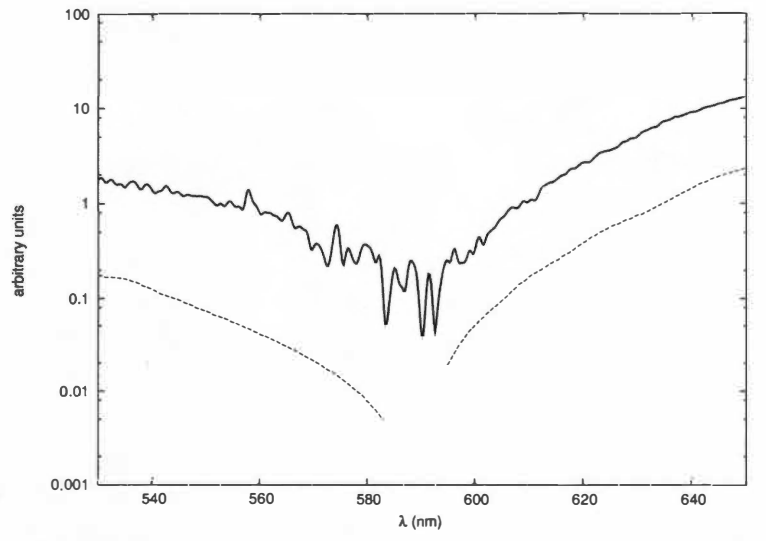

Figure 5.11: Comparison of current work with experimental spectrum of 2MJ1507477. Solid line is smoothed experimental data, dashed lines are current work.

broadened D-line.

Bibliography

Bibliography

[1] Allard, N., Allard, F., Hauschildt, P., Kielkopf, J., and Machin, L. (2003). A new model for brown dwarf spectra including accurate unified line shape theory for the Na I and K I resonance profiles. *Astronomy & Astrophysics*, 411:L473–L476.

[2] Arfken, G. B. and Weber, H. J. (2001). *Mathematical Methods for Physicists*. Harcourt/Academic Press, 5th edition.

[3] Aziz, R., Buck, U., Jónsson, H., Ruiz-Suárez, J., Schmidt, B., Scoles, G., Slaman, M., and Xu, J. (1989). Two- and three-body forces in the interaction of He atoms with Xe overlayers adsorbed on (0001) graphite. *Journal of Chemical Physics*, 91:6477–6493.

[4] Basri, G. (2000). Observations of brown dwarfs. *Annual Reviews in Astronomy and Astrophysics*, 38:485–519.

[5] Bernstein, R. B. (1960). Quantum mechanical (phase shift) analysis of differential elastic scattering of molecular beams. *Journal of Chemical Physics*, 33:795–804.

[6] Bililign, S., Gutowski, M., Simons, J., and Breckenridge, W. H. (1994). Potential energy curves of M(np ^2P)· RG($^2\Pi$) excited states and M^+· RG ground states (M=Li, Na; RG= He,Ne). *Journal of Chemical Physics*, 100:8212–8218.

[7] Bottcher, C., Dalgarno, A., and Wright, E. (1973). Collision-induced absorption in alkali-metal-atom-inert-gas mixtures. *Physical Review A*, 7:1606–1609.

[8] Boys, S. (1950). Electronic wave functions I. A general method of calculation for stationary states of any molecular system. *Proc. R. Soc. London A*, 200:542.

[9] Boys, S. and Bernardi, F. (1970). The calculation of small molecular interactions by the differences of separate total energies. Some procedures with reduced errors. *Molecular Physics*, 19:553–566.

[10] Burrows, A., Hubbard, W., Lunine, J., and Liebert, J. (2001). The theory of brown dwarfs and extrasolar giant planets. *Reviews in Modern Physics*, 73:719–765.

[11] Burrows, A., Marley, M., and Sharp, C. (2000). The near-infrared and optical spectra of methane dwarfs and brown dwarfs. *The Astrophysical Journal*, 531:438–446.

[12] Burrows, A. and Volobuyev, M. (2003). Calculations of the far-wing line profiles of sodium and potassium in the atmospheres of substellar-mass objects. *Astrophysical Journal*, 583:985–995.

[13] Cooley, J. (1961). An improved eigenvalue corrector formula for solving the Schrödinger equation for central fields. *Mathematics of Computation*, 15:363–374.

[14] Crawford, T. and Schaefer, H. (2000). An introduction to coupled cluster theory for computational chemists. *Rev. Comp. Chem*, 14:33–136.

[15] Dalgaard, E. (1979). Time-dependent multiconfigurational Hartree-Fock theory. *Journal of Chemical Physics*, 72:816–823.

[16] Danielson, L. J. and Keil, M. (1988). Interatomic potentials for HeAr, HeKr, and HeXe from multiproperty fits. *Journal of Chemical Physics*, 88:851–870.

[17] Dirac, P. (2001). *The Principles of Quantum Mechanics.* Clarendon Press, 4th edition.

[18] Dore, P., Finzi, L., Nucara, A., Postorino, P., and Rovere, M. (1995). Translational absorption band in low density mixtures of noble gases: the He-Xe case. *Molecular Physics*, 84:1065–1075.

[19] Dunning, Jr., T. H. (1989). Gaussian basis sets for use in correlated molecular calculations. I. The atoms boron through neon and hydrogen. *Journal of Chemical Physics*, 90:1007–1023.

[20] Friedrich, H. (1990). *Theoretical Atomic Physics.* Springer-Verlag.

[21] Frisch, M. J., Trucks, G. W., Schlegel, H. B., Scuseria, G. E., Robb, M. A., Cheeseman, J. R., Montgomery, Jr., J. A., Vreven, T., Kudin, K. N., Burant, J. C., Millam, J. M., Iyengar, S. S., Tomasi, J., Barone, V., Mennucci, B., Cossi, M., Scalmani, G., Rega, N., Petersson, G. A., Nakatsuji, H., Hada, M., Ehara, M., Toyota, K., Fukuda, R., Hasegawa, J., Ishida, M., Nakajima, T., Honda, Y., Kitao, O., Nakai, H., Klene, M., Li, X., Knox, J. E., Hratchian, H. P., Cross, J. B., Bakken, V., Adamo, C., Jaramillo, J., Gomperts, R., Stratmann, R. E., Yazyev, O., Austin, A. J., Cammi, R., Pomelli, C., Ochterski, J. W., Ayala, P. Y., Morokuma, K., Voth, G. A., Salvador, P., Dannenberg, J. J., Zakrzewski, V. G., Dapprich, S., Daniels, A. D., Strain, M. C., Farkas, O., Malick, D. K., Rabuck, A. D., Raghavachari, K., Foresman, J. B., Ortiz, J. V., Cui, Q., Baboul, A. G., Clifford, S., Cioslowski, J., Stefanov, B. B., Liu, G., Liashenko, A., Piskorz, P., Komaromi, I.,

Martin, R. L., Fox, D. J., Keith, T., Al-Laham, M. A., Peng, C. Y., Nanayakkara, A., Challacombe, M., Gill, P. M. W., Johnson, B., Chen, W., Wong, M. W., Gonzalez, C., and Pople, J. A. (2004). Gaussian 03, Revision C.02. Gaussian, Inc., Wallingford, CT.

[22] Frommhold, L. (1993). *Collision-Induced Absorption in Gases.* Cambridge University Press.

[23] Frommhold, L. (2005). Private communication.

[24] Frommhold, L. and Dore, P. (1996). Analysis of the He-Xe absorption spectrum in the far infrared. *Physical Review A*, 54:1717–1719.

[25] Geltman, S. (1969). *Topics in Atomic Collision Theory.* Academic Press.

[26] Havey, M., Frolking, S., and Wright, J. (1980). Experimental potentials for the $X^2\Sigma^+$ and the $A^2\Pi$ states of NaHe. *Physical Review Letters*, 45:1783–1786.

[27] Helgaker, T., Jensen, H. J. A., Joergensen, P., Olsen, J., Ruud, K., Aagren, H., Auer, A., Bak, K., Bakken, V., Christiansen, O., Coriani, S., Dahle, P., Dalskov, E. K., Enevoldsen, T., Fernandez, B., Haettig, C., Hald, K., Halkier, A., Heiberg, H., Hettema, H., Jonsson, D., Kirpekar, S., Kobayashi, R., Koch, H., Mikkelsen, K. V., Norman, P., Packer, M. J., Pedersen, T. B., Ruden, T. A., Sanchez, A., Saue, T., Sauer, S. P. A., Schimmelpfennig, B., Sylvester-Hvid, K. O., Taylor, P. R., , and Vahtras, O. (2001). Dalton, a molecular electronic structure program, release 1.2. See http://www.kjemi.uio.no/software/dalton/dalton.html.

[28] Herman, P. and Sando, K. (1978). Theoretical study of wings of resonance lines of lithium and sodium perturbed by rare gases. *Journal of Chemical Physics*, 68:1153–1160.

[29] Leo, P., Peach, G., and Whittingham, I. (2000). Investigation of sodium-helium interaction potentials. *Journal of Physics B: Atomic, Molecular and Optical Physics*, 33:4779–4797.

[30] Levine, I. (1991). *Quantum Chemistry.* Prentice-Hall, 4th edition.

[31] Lodders, K. (1999). Alkali element chemistry in cool dwarf atmospheres. *The Astrophysical Journal*, 519:793–801.

[32] Nakajima, T., Oppenheimer, B., Kulkarni, S., Golimowski, D., Matthews, K., and Durrance, S. (1995). Discovery of a cool brown dwarf. *Nature*, 378:463–65.

[33] Partridge, H., Stallcop, J. R., and Levin, E. (2001). Potential energy curves and transport properties for the interaction of He with other ground-state atoms. *Journal of Chemical Physics*, 115:6471–6488.

[34] Pascale, J. (1983). Use of l-dependent pseudopotentials in the study of alkali-metal-atom-He systems. the adiabatic molecular potentials. *Physical Review A*, 28:632–644.

[35] Peterson, K. A., Figgen, D., Goll, E., Stoll, H., and Dolg, M. (2003). Systematically convergent basis sets with relativistic pseudopotentials. II. Small-core pseudopotentials and correlation consistent basis sets for the post-d 16-18 elements. *Journal of Chemical Physics*, 119:1113–11123.

[36] Press, W. H., Flannery, B. P., Teukolsky, S. A., and Vetterling, W. T. (1992). *Numerical Recipes: The Art of Scientific Computing.* Cambridge University Press, 2nd edition.

[37] Reid, I. N. (2000). Data was obtained from http://www-int.stsci.edu/~inr/ultracool.html.

[38] Reid, I. N., Kirkpatrick, J. D., Geis, J., Dahn, C., Monet, D., Williams, R. J., Liebert, J., and Burgasser, A. (2000). Four nearby L dwarfs. *The Astronomical Journal*, 119:369–377.

[39] Rose, M. E. (1995). *Elementary Theory of Angular Momentum.* Dover Publications.

[40] Sando, K. and Dalgarno, A. (1971). The absorption of radiation near 600 A by helium. *Molecular Physics*, 20:103–112.

[41] Schmidt, M. W. and Gordon, M. S. (1998). The construction and interpretation of MCSCF wavefunctions. *Annual Review of Physical Chemistry*, 49:233–266.

[42] Steck, D. A. (2003). Sodium d line data. revision 1.6, available from http://steck.us/alkalidata.

[43] Stone, A. (1997). *The Theory of Intermolecular Forces.* Clarendon Press.

[44] Szabo, A. and Ostlund, N. S. (1989). *Modern Quantum Chemistry.* Dover Publications.

[45] Tang, K. and Toennies, J. (2003). The van der Waals potentials between all the rare gas atoms from He to Rn. *Journal of Chemical Physics*, 118:4976–4983.

[46] Tao, F. (1992). The use of midbond functions for ab initio calculations of the asymmetric potentials of He-Ne and He-Ar. *Journal of Chemical Physics*, 98:3049–3059.

[47] Tao, F. and Pan, Y. (1992). Møller-Plesset perturbation investigation of the He_2 potential and the role of midbond basis functions. *Journal of Chemical Physics*, 97:4989–4995.

[48] Thijssen, J. M. (2000). *Computational Physics.* Cambridge University Press.

[49] Woon, D. and Dunning, Jr., T. (1994). Gaussian basis sets for use in correlated molecular calculations. iv. calculation of static electrical response properties. *Journal of Chemical Physics*, 100:2975.

[50] Woon, D. and Dunning, Jr., T. (2005). To be published.

Appendix

Appendix A

Normalization of Continuum Wavefunctions

A.1 Continuum Wavefunctions

We consider a structureless particle scattering from a stationary, spherically symmetric potential center located at the origin of our coordinate system. If the potential goes to zero more quickly than $1/r^2$, the outgoing wavefunction for the scattered particle can be expanded using Legendre polynomials in the following form[25]:

$$\Psi^{+}_{\vec{k}} = (2\pi)^{-3/2} \sum_{l=0}^{\infty} i^l (2l+1) e^{i\eta_l} \frac{u_l(k,r)}{kr} P_l(\cos\theta) \tag{A.1}$$

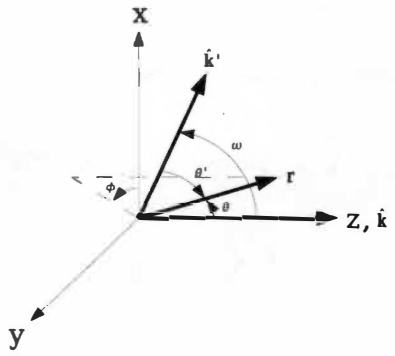

Figure A.1: Relevant coordinate system for normalization of continuum wavefunctions.

where $\cos\theta = \hat{k} \cdot \hat{r}$, and the vectors k,r are depicted in fig A.1. The function $u_l(k,r)$ is a solution to the radial Schrödinger equation (in atomic units):

$$[\nabla^2 - \frac{l(l+1)}{r^2} - \frac{2\mu}{\hbar^2}V(r) + k^2]u_l(k,r) = 0 \tag{A.2}$$

with asymptotic form ($r \to \infty$):

$$u_l(k,r) \sim \sin(kr - \frac{l\pi}{2} + \eta_l) \tag{A.3}$$

where η_l is the scattering phase shift. The Legendre polynomial may also be expanded in terms of the spherical harmonic addition theorem[2]:

$$P_l(\cos\theta) = \frac{4\pi}{2l+1}\sum_{m=-l}^{m=1} Y_l^{m*}(\theta_k,\phi_k)\, Y_l^m(\theta_r,\phi_r)\,. \tag{A.4}$$

We wish to show that the continuum wavefunctions are orthonormal, i.e.:

$$\int_{-\infty}^{\infty} d\vec{r}\Psi_{\vec{k'}}^{+*}\Psi_{\vec{k}}^{+} = \delta(\vec{k'} - \vec{k}). \tag{A.5}$$

We first introduce:

$$F_l(k,r) = \left(\frac{2}{\pi}\right)^{1/2}\frac{u_l(k,r)}{r} \tag{A.6}$$

then:

$$\Psi_{\vec{k}}^{+} = \frac{1}{4\pi}\sum_{l=0}^{\infty} i^l(2l+1)e^{i\eta_l}\frac{F_l(k,r)}{k}P_l(\cos\theta). \tag{A.7}$$

Upon substitution of eqn A.7 into eqn A.5 we obtain:

$$\begin{aligned}\int_{-\infty}^{\infty} d\vec{r}\Psi_{\vec{k'}}^{+*}\Psi_{\vec{k}}^{+} = \int_{-\infty}^{\infty} d\vec{r}\frac{1}{4\pi}\sum_{l'=0}^{\infty}(-i)^{l'}(2l'+1)e^{-i\eta_{l'}}\frac{F_{l'}(k',r)}{k'}P_{l'}^*(\cos\theta') \times \\ \frac{1}{4\pi}\sum_{l=0}^{\infty} -i^l(2l+1)e^{-i\eta_l}\frac{F_l(k,r)}{k}P_l^*(\cos\theta) \\ = \frac{1}{(4\pi)^2}\int_0^{\infty} r^2dr\int_0^{\pi}\sin\theta d\theta\int_0^{2\pi} d\phi\sum_{l'=0}^{\infty}\sum_{l=0}^{\infty} i^{l-l'}(2l'+1)(2l+1)e^{i(\eta_l-\eta_{l'})} \times \\ P_{l'}^*(\cos\theta')P_l(\cos\theta)\frac{F_{l'}(k',r)F_l(k,r)}{k'k}.\end{aligned} \tag{A.8}$$

Upon interchanging the order of integration and summation, and grouping variables with their respective integrals we have:

$$\int_{-\infty}^{\infty} d\vec{r}\Psi_{\vec{k}'}^{+*}\Psi_{\vec{k}}^{+} = \frac{1}{(4\pi)^2 k'k}\sum_{l'=0}^{\infty}\sum_{l=0}^{\infty} i^{l-l'}e^{i(\eta_l-\eta_{l'})}(2l'+1)(2l+1)\times$$
$$\int_0^{\infty} r^2 dr F_{l'}(k',r)F_l(k,r)\int_0^{\pi}\sin\theta d\theta\int_0^{2\pi} d\phi P_{l'}^{*}(\cos\theta')P_l(\cos\theta). \tag{A.9}$$

In section A.2 of this appendix we demonstrate:

$$\int_0^{\infty} r^2 F_{l'}(k',r)F_l(k,r)dr = \delta(k'-k) \tag{A.10}$$

reducing eqn A.9 to integrals over the solid angle. Using the addition theorem for Legendre polynomials[2]:

$$P_{l'}(\cos\theta') = P_{l'}(\cos\theta)P_{l'}(\cos\omega)$$
$$+2\sum_{m'=1}^{l'}\frac{(l'-m')!}{(l'+m')!}P_{l'}^{m'}(\cos\theta)P_{l'}^{m'}(\cos\omega)\cos(m'\phi) \tag{A.11}$$

where ω is the angle between $\vec{k}$ and $\vec{k'}$ we obtain:

$$\int_0^{\pi}\sin\theta d\theta\int_0^{2\pi} d\phi P_{l'}^{*}(\cos\theta')P_l(\cos\theta) = \int_0^{2\pi} d\phi\int_0^{\pi}\sin\theta d\theta P_{l'}(\cos\theta')P_{l'}(\cos\omega)P_{l'}(\cos\theta)$$
$$+2\sum_{m'=1}^{l'}\frac{(l'-m')!}{(l'+m')!}P_{l'}^{m'}(\cos\omega)\int_0^{\pi}\sin\theta d\theta P_{l'}^{m'}(\cos\theta)P_l(\cos\theta)\int_0^{2\pi} d\phi\cos m'\phi. \tag{A.12}$$

The integration over ϕ in the second term is zero for any nonzero integer m', so only the first term contributes to the integral. Using the orthogonality of the Legendre polynomials we simplify eqn A.12 and get:

$$\int_0^{2\pi} d\phi\int_0^{\pi}\sin\theta d\theta P_{l'}(\cos\theta')P_{l'}(\cos\omega)P_{l'}(\cos\theta) = \frac{4\pi}{2l+1}P_{l'}(\cos\omega)\delta_{ll'}. \tag{A.13}$$

Substituting eqns A.10 and A.13 back into eqn A.9 we obtain:

$$\int_{-\infty}^{\infty} d\vec{r}\Psi_{\vec{k'}}^{+*}\Psi_{\vec{k}}^{+} = \frac{1}{(4\pi)^2 k'k}\sum_{l'=0}^{\infty}\sum_{l=0}^{\infty} e^{i(\eta_l-\eta_{l'})}(2l'+1)(2l+1)\times$$
$$\delta(k'-k)P_{l'}(\cos\omega)\frac{4\pi}{(2l+1)}\delta_{ll'}$$
$$= \frac{1}{4\pi k'k}\sum_{l=0}^{\infty}(2l+1)\delta(k'-k)P_l(\cos\omega). \tag{A.14}$$

Furthermore, we can use the identity:

$$\sum_{0}^{\infty}(2l+1)P_l(\cos\omega) = 2\delta(1-\cos\omega) \tag{A.15}$$

to obtain:

$$\int_{-\infty}^{\infty} d\vec{r}\Psi_{\vec{k'}}^{+*}\Psi_{\vec{k}}^{+} = \frac{1}{2\pi kk'}\delta(1-\cos\omega)\delta(k'-k). \tag{A.16}$$

Upon integrating eqn A.16 over all momentum space $(\vec{k})$ we obtain:

$$\int_0^{\infty} k^2dk\int_0^{\pi}\sin\theta d\theta\int_0^{2\pi} d\phi\frac{1}{2\pi kk'}\delta(1-\cos\omega)\delta(k'-k) = 1. \tag{A.17}$$

thus completing our proof.

A.2 Normalization of Radial Wavefunctions

We wish to show that the radial part of our wavefunctions are normalized:

$$\int_0^{\infty} drr^2F_l(k',r)F_l(k,r) = \delta(k'-k) \tag{A.18}$$

or equivalently:

$$\lim_{\Delta k\to 0}\int_{k-\Delta k}^{k+\Delta k} dk'\int_0^{\infty} drr^2F_l(k',r)F_l(k,r) = 1. \tag{A.19}$$

In order to accomplish this we first set $F_l = F_l^a + y_l$, where F_l^a is the asymptotic form of the radial wavefunction, $(2/\pi)^{1/2}(1/r)\sin(kr - l\pi/2 + \eta_l)$, and y_l goes to zero as r approaches

infinity. Then:

$$\lim_{\Delta k\to 0}\int_{k-\Delta k}^{k+\Delta k} dk' F_l(k',r) = \lim_{\Delta k\to 0}(2\Delta k y_l(k,r)$$
$$-(2/\pi)^{1/2} r^{-2}\cos[k'r - l\pi/2 + \eta_l(k')])|_{\Delta k-k}^{\Delta k+k}$$
$$= \lim_{\Delta k\to 0} 2(2/\pi)^{1/2} r^{-2}\sin(kr - l\pi/2 + \eta_l)\sin(r\Delta k) \qquad \text{(A.20)}$$

where $\lim_{\Delta k\to 0} 2\Delta k y_l(k,r)$ goes to zero since y_l is bounded for all r by definition. The term $\sin(r\Delta k)$ does not vanish because r is not bounded. Substituting the previous expression into our integral:

$$\lim_{\Delta k\to 0}\int_{k-\Delta k}^{k+\Delta k} dk' \int_0^\infty dr r^2 F_l(k',r)F_l(k,r)$$
$$= 2(2/\pi)^{1/2}\lim_{\Delta k\to 0}\int_0^\infty [F_l^a(k,r) + y_l(k,r)]\sin(kr - l\pi/2 + \eta_l)\sin(r\Delta k)$$
$$= (4/\pi)\lim_{\Delta k\to 0}\int_0^\infty dr\frac{\sin(r\Delta k)}{r}\sin^2(kr - l\pi/2 + \eta_l) \qquad \text{(A.21)}$$

where the term containing $y_l(k,r)$ vanishes as $\Delta k \to 0$ because it provides an effective upper bound to the value that r can take in the integral. Finally as $\Delta k \to 0$ the period of oscillation for $\sin(r\Delta k)/r$ will be much larger than that of $\sin^2(kr - l\pi/2 + \eta_l)$ so that we may replace the $\sin^2$ term inside the integral with its average value of $1/2$. We then obtain:

$$\lim_{\Delta k\to 0}\int_{k-\Delta k}^{k+\Delta k} dk' \int_0^\infty dr r^2 F_l(k',r)F_l(k,r) =$$
$$\frac{2}{\pi}\lim_{\Delta k\to 0}\int_0^\infty d(r\Delta k)\frac{\sin(r\Delta k)}{r\Delta k} = 1. \qquad \text{(A.22)}$$

A.3 Energy Normalization of Radial Wavefunctions

We now show how to energy normalize the radial wave functions. Using eqn A.18 and remembering that $F_l(k,r) = (2/\pi)^{1/2}u_l(k,r)/r$ we substitute into our integral and get:

$$\int_0^\infty dr u_l(k',r)u_l(k,r) = \frac{\pi}{2}\delta(k' - k) \qquad \text{(A.23)}$$

$u_l(k,r)$ is the wavefunction that we obtain upon numerical integration of the radial Schrödinger equation, eqn A.2. To energy normalize this we use the following relations:

$$\begin{aligned} E &= \frac{\hbar^2 k^2}{2\mu} \\ \frac{\partial E}{\partial k} &= \frac{\hbar^2 k}{\mu} \\ \delta(k'-k) &= \frac{\partial E}{\partial k}\delta(E'-E). \end{aligned} \tag{A.24}$$

Upon substitution of the expressions in eqn A.24 into eqn A.23, we obtain the energy normalized wavefunction $u_l(E,r)$:

$$u_l(E,r) = \left(\frac{2}{\pi}\right)^{1/2}\left(\frac{\mu}{\hbar^2 k}\right)^{1/2} u_l(k,r). \tag{A.25}$$

Appendix B

Fortran Programs

This appendix includes Fortran 77 code that was written by the author to perform the calculations presented in this dissertation. Several of these programs require subroutines that can be obtained from *Numerical Recipes*[36], and will be indicated as needed.

B.1 He-Xe Programs

B.1.1 Collision Induced Absorption

This is the main program, gabsorb.f, for the calculation of the collision induced absorption spectrum of He-Xe. It requires several subroutines: gliff.f, which is the Gauss-Laguerre integrator of the energy integral and returns the spectral density $VG(\omega)$; matrix.f, which evaluates the transition dipole matrix element; and gammln.f, gaulag.f, spline.f, and splint.f which are available from *Numerical Recipes*. The program is compiled via:
g77 gabsorb.f gliff.f matrix.f gammln.f gaulag.f spline.f splint.f -o GABSORB

gabsorb.f

```
Implicit Real *8 (a-h,o-z)
Real *8 interval,convert,kT,loschmidt
integer pts,epts
Dimension pho(10000)
Character *20 filename
Write (6,*) 'What output file?'
Read (5,*) filename
Write (6,*) 'How many energy points?'
Read (5,*) epts
Write (6,*) 'What temperature?'
```

```
      Read (5,*) Temp
      Write (6,*) 'How many energies?'
      Read (5,*) Ntot
      Write (6,*) 'Starting Energy (cm-1)?'
      Read (5,*) start
      Write (6,*) 'What interval?'
      Read (5,*) interval
c  constants ( I will use ergs for energy)
c                1e-7 J = 1 erg
      Pi = 4*atan(1.)
      h=6.626068d-34 / 1d-7  ! erg*s
      hbar=h/2./Pi
      loschmidt=2.68673d19 ! cm^-3 amagat^-1
      sol=299792458. * 100. ! cm/s
      boltz=1.3806503d-23 / 1d-7  ! erg/K
      kT=boltz*Temp  ! erg
      front= 4*Pi**2 * loschmidt**2 / 3 / hbar / sol
c  conversion from hartree * bohr**6 * a.u.(time) to erg * cm**6 * s
c  just multiply convert with quantity in atomic units to get other units
      convert=4.359748d-11*(5.291772d-09)**6 * 2.418884326505d-17
      open (37,file=filename)
      Write (37,*) '# Gauss-Laguerre integration of HeXe absorption'
      Write (37,*) '# Temp= ',Temp,' Number of GL points= ',epts
      do i=1,Ntot
           pho(i)=start+(i-1)*interval
      end do
      do i=1,Ntot
c  convert pho(i) from wavenumber(cm-1) to hartree
          photon=pho(i)/219474.63068
c  frequency of photon
          freq=2*Pi*sol*pho(i) ! radians / s
          call gliff(photon,Temp,epts,output)
c output is in atomic units see above
c gomega is in erg * cm**6 * s
          gomega=output*convert
          alpha = front * freq * (1.-exp(-1.*hbar*freq/kT)) * gomega
      Write (37,*) pho(i),output,gomega,alpha
      end do
```

```
close (37)
stop
end
```

gliff.f

```
subroutine gliff (photon,Temp,epts,output)
Implicit Real *8 (a-h,o-z)
real *8 otwo,output,output3,sumout,output2,en,kT
integer Jval,sele,epts,pts,ppts,zcount
Dimension Eint(200),x(200),w(200)
hbar=1.
fourpiepsn=1.
Pi=4*atan(1.)
atomboltz=3.16681520371153e-6 ! hartree/K
kT=atomboltz*Temp
atomone=131.2936
atomtwo=4.0026
redmass=(atomone*atomtwo)/(atomone+atomtwo)/5.4857990e-4
thermDB=sqrt(2*Pi*hbar**2/redmass/kT)
n=epts
alpha=0.
call gaulag(x,w,n,alpha)
intcounter=0
output3=0.
do i=1,epts
   en=kT*x(i)
   otwo=0.
   mval=0
   tollpercent=0.1
   turn=2.
   do k=1,501
      Jval=k-1
      call matrix(en,photon,Jval,turn,outturn,output2)
      turn=outturn
      sumout=(2.*Jval+1.)*output2
      otwo=otwo + sumout
      converge=sumout/otwo*100.
```

```
            if (converge.le.tollpercent) mval = mval +1
            if (mval.eq.20) goto 335
          end do
335       Eint(i)=kT*otwo/fourpiepsn
336       output3old=output3
          output3=output3 + w(i)*Eint(i)
          if (i.gt.40) then
                  diff=abs(output3-output3old)
            if (diff.lt.1e-8) then
                  intcounter=intcounter+1
          end if
          end if
          if (intcounter.ge.8) goto 337
        end do
337     output=hbar*thermDB**3*output3
        return
        END
```

The subroutine that calculates the transition dipole moment matrix elements has the potential energy and dipole moment surfaces included as data arrays. Also included is the potential energy and dipole moment surfaces used by Frommhold et al.[24], and the program can be easily converted to calculate the spectrum using either set of surfaces.

matrix.f

```
      Subroutine matrix (energy,photon,J,turnin,outturn,output)
      Implicit Real *8 (a-h,o-z)
      Integer J,points,lolow,lohigh,intstart,sel,ppot,pdip
      Real *8 Lowcheck,Hicheck
      Dimension plo(1050000),phi(1050000)
      Dimension Vhigh(1050000),Vlow(1050000),Vdiff(1050000)
      Dimension trandip(1050000),x(1050000),y2(1050000)
      Dimension Ghigh(1050000),Glow(1050000)
      Dimension xnodelow(100000),xnodehigh(100000)
c change these if number of points in potential or dipole change
      Parameter (ppot=31,pdip=29)
      Dimension Rpot(ppot),Vpot(ppot),Rdip(pdip),Dip(pdip)
c  Here I have hardwired in my Potential Surface and Transition
c  Dipole surface for use with spline later
```

```
      Data Rpot/ 2.,2.5,3.,3.5,4.,4.5,5.,5.5,6.,6.5,7.,7.4,7.5,
     +   7.54,7.55,7.56,7.6,
     +   7.7,8.,8.5,9.,9.5,
     +   10.,10.5,11.,11.5,12.,13.,14.,15.,20. /
      Data Vpot/ 1.03469613,0.472773668,0.219060029,0.0973332561,
     +   0.0412716671,0.0167050558,0.0063968655,
     +   0.0022539308,0.0006731694,0.00011391,-5.72514E-05,
     +   -8.94385E-05,-9.09893E-05,
     +   -9.11624E-05,-9.11701E-05,-9.11675E-05,
     +   -9.10145E-05,-8.98843E-05,
     +   -8.21427E-05,-6.4205E-05,-4.76246E-05,-3.47055E-05,
     +   -2.52739E-05, -1.85288E-05, -1.37471E-05, -1.0313E-05,
     +   -7.8431E-06, -4.69519996E-06, -2.93859996E-06,
     +   -1.91050003E-06, 0. /
      Data Rdip/ 2.,2.2,2.4,2.5,2.6,2.8,3.,3.5,
     +     4.,4.5,5.,5.5,6.,6.5,7.,
     +     7.5,8.,8.5,9.,9.5,10.,10.5,
     +     11.,11.5,12.,13.,14.,15.,20.  /
      Data Dip/ -0.760878564,-1.1138475,-1.0835328,-1.01088375,
     + -0.929340256,
     + -0.771184813,-0.63561092,-0.392594431,-0.240467289,
     + -0.142772943,-0.0810810461,-0.0438130979, -0.0224838489,
     + -0.0109204995,-0.00499594973,-0.00211699988,
     + -0.000791549971,-0.000225949944,-3.90000325E-06,
     + 7.44999713E-05,8.36500356E-05,7.28999715E-05,6.13000208E-05,
     + 4.320001E-05,2.87000028E-05,1.50999708E-05, 0.,0.,0. /
        hbar=1.
        atomone=131.2936 !NIST
        atomtwo=4.0026
        Pi= 4*atan(1.0)
        redmass=1/5.4857990e-4*(atomone*atomtwo)/(atomone+atomtwo)
        s=timestep
        Enlow=energy
        Enhigh=energy+photon
c  this is tolerance for exponential increase of wave function
c  and other parameters for integration
        tolpsi=1.0D250
        DBnum=30.
```

```
       final=300.
       cutoff=20.
c  this determines selection rules for J-J transitions
c  J to J is selection=0.
c  J to J+1 is selection=1.
c  J to J is selection=-1.
       selection=0.
c  define an initial starting point
       turninterval=0.
3457   turn=turnin + turninterval
c   Determine step size want DBnum points per DeBroglie wavelength
c   We use higher energy wave function to determine step size
      debroglie=hbar/(2.*redmass*Enhigh)**(1/2.)
      s=debroglie/DBnum
      rational=(final-turn)/debroglie*DBnum
      points=int(rational)
      if (points.gt.1000000) then
        Write (6,*) 'ERRORERRORERRORERRORERRORERRORERRORERRORERROR'
        write (6,*) ''
        Write (6,*) 'Enhigh= ',Enhigh
        Write (6,*) 'DeBroglie= ',debroglie
        Write (6,*) 'Turn= ',turn
        Write (6,*) 'Outer= ',final
        Write (6,*) 'stepsize= ',s
        Write (6,*) 'points= ',points
        Write (6,*) ''
        Write (6,*) 'ERRORERRORERRORERRORERRORERRORERRORERRORERROR'
        output=0.
        outturn=turn
        goto 1292
      end if
      do i=0,points
        x(i+1)=turn+i*s
      end do
C Initialize Potential energy surface
      gr1=(Vpot(2)-Vpot(1))/(Rpot(2)-Rpot(1))
      grn=(Vpot(ppot)-Vpot(ppot-1))/(Rpot(ppot)-Rpot(ppot-1))
      call spline (Rpot,Vpot,ppot,gr1,grn,y2)
```

```
      do i=1,points+1
      rad=x(i)
      if (rad.gt.cutoff) then
         Vlow(i)=0.
         Vhigh(i)=0.
      else
         call splint(Rpot,Vpot,y2,ppot,rad,en)
         Vlow(i)=en
         Vhigh(i)=en
      end if
      end do
C Initialize Dipole moment surface
      td1=(Dip(2)-Dip(1))/(Rdip(2)-Rdip(1))
      tdn=(Dip(pdip)-Dip(pdip-1))/(Rdip(pdip)-Rdip(pdip-1))
      call spline(Rdip,Dip,pdip,td1,tdn,y2)
      do i=1,points+1
      rad=x(i)
      if (rad.gt.cutoff) then
         trandip(i)=0.
      else
         call splint(Rdip,Dip,y2,pdip,rad,td)
         trandip(i)=td
      end if
      end do
ccccccccccccccccccccccccccccccccccccccccccccccccccccccccc
c
c     Following is potential and dipole
c     used in Frommhold PRA 54,1717,1996
c
ccccccccccccccccccccccccccccccccccccccccccccccccccccccccc
c      do i=1,points+1
c      if (x(i).gt.cutoff) then
c         Vlow(i)=0.
c         Vhigh(i)=0.
c      else
c      xval=x(i)*0.529177249
c       hf=5.3864e6*(xval**(-3.))*exp(-2.56779*xval)
c       six=1.168e4*xval**-6.
```

```
c       eight=8.54255e4*xval**-8.
c       ten=7.65364e5*xval**-10.
c       twelve=8.635317e6*xval**-12.
c       fteen=1.19625036e8*xval**-14.
c       disp=six+eight+ten+twelve+fteen
c       if (xval.ge.5.12) then
c          fr=1.
c       else
c          fr=exp(-(5.12/xval -1)**2)
c       end if
c       azizenergy=hf-fr*disp
c       hartree=azizenergy/1000/27.2113961
c
c       Vlow(i)=hartree
c       Vhigh(i)=hartree
c      end if
c      end do
c
c      convert=1.d18*.393456
c      rconv=1/.529177249
c      do i=1,points+1
c      if (x(i).gt.cutoff) then
c         trandip(i)=0.
c      else
c      dip=7.068e-20*convert*exp(-(x(i)-3.547*rconv)/(.432812*rconv))
c     + -12000/x(i)**7
c      trandip(i)=dip
c      end if
c      end do
ccccccccccccccccccccccccccccccccccccccccccccccccc
      do i=1,points+1
           al=J
           Glow(i)=2*redmass/(hbar*hbar)*(Vlow(i)-Enlow)
     ++ al*(al+1)/(x(i)**2)
           alhigh=J+selection
           Ghigh(i)=2*redmass/(hbar*hbar)*(Vhigh(i)-Enhigh)
     ++ alhigh*(alhigh+1)/(x(i)**2)
      end do
```

```
      plo(1)=0.
      plo(2)=0.0001
      phi(1)=0.
      phi(2)=0.0001
      nodelow=1
      xnodelow(1)=0.
      nodehigh=1
      xnodehigh(1)=0.
      do i=2,points
      plo(i+1)=(2*plo(i)-plo(i-1)+5*Glow(i)*plo(i)*s**2/6
     ++Glow(i-1)*plo(i-1)*s**2/12)/(1-Glow(i+1)*s**2/12)
      phi(i+1)=(2*phi(i)-phi(i-1)+5*Ghigh(i)*phi(i)*s**2/6
     ++Ghigh(i-1)*phi(i-1)*s**2/12)/(1-Ghigh(i+1)*s**2/12)
      if (plo(i+1).gt.tolpsi) then
         turninterval=turninterval+.1
         goto 3457
      end if
      if (phi(i+1).gt.tolpsi) then
         turninterval=turninterval+.1
         goto 3457
      end if
      testlow=plo(i)*plo(i+1)
      if (testlow.le.0.) then
         nodelow=nodelow+1
         xnodelow(nodelow)=x(i)-plo(i)*((x(i+1)-x(i))
     +/(plo(i+1)-plo(i)))
         nodelowmax=nodelow
      end if
      testhigh=phi(i)*phi(i+1)
      if (testhigh.le.0.) then
         nodehigh=nodehigh+1
         xnodehigh(nodehigh)=x(i)-phi(i)*((x(i+1)-x(i))
     +/(phi(i+1)-phi(i)))
         nodehighmax=nodehigh
      end if
      end do
c  first we find maximum of last peak in wavefunctions
c  ground state
```

```
      do i=2,points
      if (plo(i).le.0) then
         goto 456
      end if
      if (plo(i).gt.plo(i+1).and.plo(i).gt.plo(i-1)) then
      if (xnodelow(nodelowmax).gt.x(i)) then
         amaxlow=plo(i)
         rmaxlow=x(i)
         goto 456
      end if
      end if
456   end do
c  excited state
      do i=2,points
      if (phi(i).le.0) then
         goto 457
      end if
      if (phi(i).gt.phi(i+1).and.phi(i).gt.phi(i-1))
     +then
      if (xnodehigh(nodehighmax).gt.x(i)) then
         amaxhigh=phi(i)
         rmaxhigh=x(i)
         goto 457
      end if
      end if
457   end do
      checklo=sqrt(2*redmass*Enlow/hbar**2)
      checkhi=sqrt(2*redmass*Enhigh/hbar**2)
c changed normalization to use input values of energies
      Enormlow=sqrt(2*redmass/Pi/hbar**2/checklo)
      scalefactorlow=1/amaxlow * Enormlow
      Enormhigh=sqrt(2*redmass/Pi/hbar**2/checkhi)
      scalefactorhigh=1/amaxhigh * Enormhigh
      wavelengthlow=2.*(xnodelow(nodelowmax)-xnodelow(nodelowmax-1))
      wavevectorlow=2.0 * Pi / wavelengthlow
      wavelengthhigh=2*(xnodehigh(nodehighmax)-xnodehigh(nodehighmax-1))
      wavevectorhigh=2.0 * Pi / wavelengthhigh
      Hicheck=abs(checkhi-wavevectorhigh)
```

```
      Lowcheck=abs(checklo-wavevectorlow)
      tolerance=0.1
      Tolen=tolerance**2*hbar**2/2./redmass
      if (Hicheck.gt.tolerance.or.Lowcheck.gt.tolerance) then
         Write (6,*) 'ErrorErrorErrorErrorErrorError'
         Write (6,*)  'Energy= ',energy
         Write (6,*)  'photon= ',photon
         Write (6,*)  'J= ',J
         Write (6,*)  'Hicheck= ',Hicheck**2*hbar**2/2./redmass
         Write (6,*)  'Lowcheck= ',Lowcheck**2*hbar**2/2./redmass
         Write (6,*)  'tolerance= ',Tolen
         Write (6,*) '#ErrorErrorErrorErrorErrorError'
         output=0.
         outturn=0.
         goto 1292
      end if
      do i=1,points+1
         plo(i)=plo(i)*scalefactorlow
         phi(i)=phi(i)*scalefactorhigh
      end do
c now we do the radial part of the transition dipole moment integral
      value=0.0
      do i=1,points
         if (x(i).gt.cutoff) goto 45
         v=plo(i)*phi(i)*trandip(i)
         vplusone=plo(i+1)*phi(i+1)*trandip(i+1)
         value=value + .5*(x(i+1)-x(i))*(v+vplusone)
      end do
45    continue
      output=value**2
      outturn=turn
1292  return
      END
```

B.1.2 Functional Derivative

This is the main program, fdgabsorb.f, for the evaluation of the functional derivative of the absorption coefficient with respect to the dipole moment of the collision induced absorption

spectrum of He-Xe. It requires several subroutines: fdgliff.f, which is the Gauss-Laguerre integrator of the energy integral and returns the functional derivative of the spectral density, $VG(\omega)$, with respect to the dipole; fdmatrix.f, which evaluates the transition dipole matrix element of the functional derivative; and gammln.f, gaulag.f, spline.f, and splint.f which are available from *Numerical Recipes*. The program is compiled via:
g77 fdgabsorb.f fdgliff.f fdmatrix.f gammln.f gaulag.f spline.f splint.f -o FDGABSORB

fdgabsorb.f

```
      Implicit Real *8 (a-h,o-z)
      Real *8 interval,convert,kT,loschmidt
      integer pts,epts
      Dimension pho(10000)
      Character *20 filename
      Write (6,*) 'What output file?'
      Read (5,*) filename
      Write (6,*) 'How many energy points?'
      Read (5,*) epts
      Write (6,*) 'What temperature?'
      Read (5,*) Temp
      Write (6,*) 'How many energies?'
      Read (5,*) Ntot
      Write (6,*) 'Starting Energy (cm-1)?'
      Read (5,*) start
      Write (6,*) 'What interval?'
      Read (5,*) interval
      Write (6,*) 'What point to evaluate the Functional Derivative?'
      read (5,*) eval
c  constants ( I will use ergs for energy)
c                 1e-7 J = 1 erg
      Pi = 4*atan(1.)
      h=6.626068d-34 / 1d-7  ! erg*s
      hbar=h/2./Pi
      loschmidt=2.68673d19 ! cm^-3 amagat^-1
      sol=299792458. * 100. ! cm/s
      boltz=1.3806503d-23 / 1d-7  ! erg/K
      kT=boltz*Temp  ! erg
      front= 4*Pi**2 * loschmidt**2 / 3 / hbar / sol
```

```
c  conversion from hartree * bohr**6 * a.u.(time) to erg * cm**6 * s
c  just multiply convert with quantity in atomic units to get other units
      convert=4.359748d-11*(5.291772d-09)**6 * 2.418884326505d-17
c converts factor of 1/(e(electron charge)*a_0^2) to 1/(C(coulombs) * cm^2)
c one debye is 0.39456 atomic units of dipole (e*a_0) is 3.338*10^-30 C*m
c we have atomic units of dipole times bohr (inverse)
c so we multiply to get normal units
      dconvert= .39456/3.338d-30/100/(5.291772d-9)
      open (37,file=filename)
      Write (37,*) '# Gauss-Laguerre integration of HeXe absorption'
      Write (37,*) '# Temp= ',Temp,' Number of GL points= ',epts
      do i=1,Ntot
           pho(i)=start+(i-1)*interval
      end do
      do i=1,Ntot
c  convert pho(i) from wavenumber(cm-1) to hartree
          photon=pho(i)/219474.63068
c  frequency of photon
          freq=2*Pi*sol*pho(i) ! radians / s
          call fdgliff(photon,Temp,epts,eval,output)
c output is in atomic units see above
c gomega is in erg * cm**6 * s / (C * cm^2)
          gomega=output*convert * dconvert
          alpha = front * freq * (1.-exp(-1.*hbar*freq/kT)) * gomega
      Write (37,*) pho(i),eval,gomega,alpha
      end do
      close (37)
      stop
      end
```

fdgliff.f

```
      subroutine fdgliff (photon,Temp,epts,eval,output)
      Implicit Real *8 (a-h,o-z)
      real *8 otwo,output,output3,sumout,output2,en,kT
      integer Jval,sele,epts,pts,ppts,zcount
      Dimension Eint(200),x(200),w(200)
      hbar=1.
```

```
      fourpiepsn=1.
      Pi=4*atan(1.)
      atomboltz=3.16681520371153e-6 ! hartree/K
      kT=atomboltz*Temp
      atomone=131.2936
      atomtwo=4.0026
      redmass=(atomone*atomtwo)/(atomone+atomtwo)/5.4857990e-4
      thermDB=sqrt(2*Pi*hbar**2/redmass/kT)
c units of derivative have extra factor of 1/(e (electron charge) * a_0^2)
      n=epts
      alpha=0.
      call gaulag(x,w,n,alpha)
      intcounter=0
      output3=0.
      do i=1,epts
         en=kT*x(i)
         otwo=0.
         mval=0
         tollpercent=0.1
         turn=2.
         do k=1,501
            Jval=k-1
            call fdmatrix(en,photon,Jval,turn,eval,outturn,output2)
            turn=outturn
c inserted minus 2 from derivative formula into sumout
            sumout=-2. * (2.*Jval+1.)*output2
            otwo=otwo + sumout
            converge=sumout/otwo*100.
            if (converge.le.tollpercent) mval = mval +1
            if (mval.eq.20) goto 335
         end do
335      Eint(i)=kT*otwo/fourpiepsn
336      output3old=output3
         output3=output3 + w(i)*Eint(i)
         if (i.gt.40) then
                diff=abs(output3-output3old)
            if (diff.lt.1e-8) then
                intcounter=intcounter+1
```

```
          end if
          end if
          if (intcounter.ge.8) goto 337
        end do
337     output=hbar*thermDB**3*output3
        return
        END
```

fdmatrix.f

```
      Subroutine fdmatrix (energy,photon,J,turnin,eval,outturn,output)
      Implicit Real *8 (a-h,o-z)
      Integer J,points,lolow,lohigh,intstart,sel,ppot,pdip
      Real *8 Lowcheck,Hicheck,prodpsi
      Dimension plo(1050000),phi(1050000)
      Dimension Vhigh(1050000),Vlow(1050000),Vdiff(1050000)
      Dimension trandip(1050000),x(1050000),y2(1050000)
      Dimension Ghigh(1050000),Glow(1050000)
      Dimension xnodelow(100000),xnodehigh(100000)
c change these if number of points in potential or dipole change
      Parameter (ppot=31,pdip=29)
      Dimension Rpot(ppot),Vpot(ppot),Rdip(pdip),Dip(pdip)
c  Here I have hardwired in my Potential Surface and
c  Transition Dipole surface for use with spline later
      Data Rpot/ 2.,2.5,3.,3.5,4.,4.5,5.,5.5,6.,6.5,7.,7.4,7.5,
     +   7.54,7.55,7.56,7.6,
     +   7.7,8.,8.5,9.,9.5,
     +   10.,10.5,11.,11.5,12.,13.,14.,15.,20. /
      Data Vpot/ 1.03469613,0.472773668,0.219060029,0.0973332561,
     +   0.0412716671,0.0167050558,0.0063968655,
     +   0.0022539308,0.0006731694,0.00011391,-5.72514E-05,
     +   -8.94385E-05,-9.09893E-05,
     +   -9.11624E-05,-9.11701E-05,-9.11675E-05,
     +   -9.10145E-05,-8.98843E-05,
     +   -8.21427E-05,-6.4205E-05,-4.76246E-05,-3.47055E-05,
     +   -2.52739E-05, -1.85288E-05, -1.37471E-05, -1.0313E-05,
     +   -7.8431E-06, -4.69519996E-06, -2.93859996E-06,
     +   -1.91050003E-06, 0. /
```

```
      Data Rdip/ 2.,2.2,2.4,2.5,2.6,2.8,3.,3.5,
     +     4.,4.5,5.,5.5,6.,6.5,7.,
     +     7.5,8.,8.5,9.,9.5,10.,10.5,
     +     11.,11.5,12.,13.,14.,15.,20.  /
      Data Dip/ -0.760878564,-1.1138475,-1.0835328,-1.01088375,
     + -0.929340256,
     + -0.771184813,-0.63561092,-0.392594431,-0.240467289,
     + -0.142772943,-0.0810810461,-0.0438130979, -0.0224838489,
     + -0.0109204995,-0.00499594973,-0.00211699988,
     + -0.000791549971,-0.000225949944,-3.90000325E-06,
     + 7.44999713E-05,8.36500356E-05,7.28999715E-05,6.13000208E-05,
     + 4.320001E-05,2.87000028E-05,1.50999708E-05, 0.,0.,0. /
        hbar=1.
        atomone=131.2936 !NIST
        atomtwo=4.0026
        Pi= 4*atan(1.0)
        redmass=1/5.4857990e-4*(atomone*atomtwo)/(atomone+atomtwo)
        s=timestep
        Enlow=energy
        Enhigh=energy+photon
c  this is tolerance for exponential increase of wave function
c  and other parameters for integration
        tolpsi=1.0D250
        DBnum=30.
        final=300.
        cutoff=20.
c  this determines selection rules for J-J transitions
c  J to J is selection=0.
c  J to J+1 is selection=1.
c  J to J is selection=-1.
        selection=0.
c  define an initial starting point
        turninterval=0.
3457    turn=turnin + turninterval
c    Determine step size want DBnum points per DeBroglie wavelength
c    We use higher energy wave function to determine step size
       debroglie=hbar/(2.*redmass*Enhigh)**(1/2.)
       s=debroglie/DBnum
```

```
      rational=(final-turn)/debroglie*DBnum
      points=int(rational)
      if (points.gt.1000000) then
        Write (6,*) 'ERRORERRORERRORERRORERRORERRORERRORERRORERROR'
        write (6,*) ''
        Write (6,*) 'Enhigh= ',Enhigh
        Write (6,*) 'DeBroglie= ',debroglie
        Write (6,*) 'Turn= ',turn
        Write (6,*) 'Outer= ',final
        Write (6,*) 'stepsize= ',s
        Write (6,*) 'points= ',points
        Write (6,*) ''
        Write (6,*) 'ERRORERRORERRORERRORERRORERRORERRORERRORERROR'
        output=0.
        outturn=turn
        goto 1292
      end if
      do i=0,points
        x(i+1)=turn+i*s
      end do
C Initialize Potential energy surface
      gr1=(Vpot(2)-Vpot(1))/(Rpot(2)-Rpot(1))
      grn=(Vpot(ppot)-Vpot(ppot-1))/(Rpot(ppot)-Rpot(ppot-1))
      call spline (Rpot,Vpot,ppot,gr1,grn,y2)
      do i=1,points+1
      rad=x(i)
      if (rad.gt.cutoff) then
         Vlow(i)=0.
         Vhigh(i)=0.
      else
         call splint(Rpot,Vpot,y2,ppot,rad,en)
         Vlow(i)=en
         Vhigh(i)=en
      end if
      end do
C Initialize Dipole moment surface
      td1=(Dip(2)-Dip(1))/(Rdip(2)-Rdip(1))
      tdn=(Dip(pdip)-Dip(pdip-1))/(Rdip(pdip)-Rdip(pdip-1))
```

```
 call spline(Rdip,Dip,pdip,td1,tdn,y2)
 do i=1,points+1
 rad=x(i)
 if (rad.gt.cutoff) then
    trandip(i)=0.
 else
    call splint(Rdip,Dip,y2,pdip,rad,td)
    trandip(i)=td
 end if
 end do
 do i=1,points+1
      al=J
      Glow(i)=2*redmass/(hbar*hbar)*(Vlow(i)-Enlow)
++ al*(al+1)/(x(i)**2)
      alhigh=J+selection
      Ghigh(i)=2*redmass/(hbar*hbar)*(Vhigh(i)-Enhigh)
++ alhigh*(alhigh+1)/(x(i)**2)
 end do
 plo(1)=0.
 plo(2)=0.0001
 phi(1)=0.
 phi(2)=0.0001
 nodelow=1
 xnodelow(1)=0.
 nodehigh=1
 xnodehigh(1)=0.
 do i=2,points
 plo(i+1)=(2*plo(i)-plo(i-1)+5*Glow(i)*plo(i)*s**2/6
++Glow(i-1)*plo(i-1)*s**2/12)/(1-Glow(i+1)*s**2/12)
 phi(i+1)=(2*phi(i)-phi(i-1)+5*Ghigh(i)*phi(i)*s**2/6
++Ghigh(i-1)*phi(i-1)*s**2/12)/(1-Ghigh(i+1)*s**2/12)
 if (plo(i+1).gt.tolpsi) then
    turninterval=turninterval+.1
    goto 3457
 end if
 if (phi(i+1).gt.tolpsi) then
    turninterval=turninterval+.1
    goto 3457
```

```
      end if
      testlow=plo(i)*plo(i+1)
      if (testlow.le.0.) then
         nodelow=nodelow+1
         xnodelow(nodelow)=x(i)-plo(i)*((x(i+1)-x(i))
     +/(plo(i+1)-plo(i)))
         nodelowmax=nodelow
      end if
      testhigh=phi(i)*phi(i+1)
      if (testhigh.le.0.) then
         nodehigh=nodehigh+1
         xnodehigh(nodehigh)=x(i)-phi(i)*((x(i+1)-x(i))
     +/(phi(i+1)-phi(i)))
         nodehighmax=nodehigh
      end if
      end do
c  first we find maximum of last peak in wavefunctions
c  ground state
      do i=2,points
      if (plo(i).le.0) then
         goto 456
      end if
      if (plo(i).gt.plo(i+1).and.plo(i).gt.plo(i-1)) then
      if (xnodelow(nodelowmax).gt.x(i)) then
         amaxlow=plo(i)
         rmaxlow=x(i)
         goto 456
      end if
      end if
456   end do
c  excited state
      do i=2,points
      if (phi(i).le.0) then
         goto 457
      end if
      if (phi(i).gt.phi(i+1).and.phi(i).gt.phi(i-1))
     +then
      if (xnodehigh(nodehighmax).gt.x(i)) then
```

```
         amaxhigh=phi(i)
         rmaxhigh=x(i)
         goto 457
      end if
      end if
457   end do
      checklo=sqrt(2*redmass*Enlow/hbar**2)
      checkhi=sqrt(2*redmass*Enhigh/hbar**2)
c changed normalization to use input values of energies
      Enormlow=sqrt(2*redmass/Pi/hbar**2/checklo)
      scalefactorlow=1/amaxlow * Enormlow
      Enormhigh=sqrt(2*redmass/Pi/hbar**2/checkhi)
      scalefactorhigh=1/amaxhigh * Enormhigh
      wavelengthlow=2.*(xnodelow(nodelowmax)-xnodelow(nodelowmax-1))
      wavevectorlow=2.0 * Pi / wavelengthlow
      wavelengthhigh=2*(xnodehigh(nodehighmax)-xnodehigh(nodehighmax-1))
      wavevectorhigh=2.0 * Pi / wavelengthhigh
      Hicheck=abs(checkhi-wavevectorhigh)
      Lowcheck=abs(checklo-wavevectorlow)
      tolerance=0.1
      Tolen=tolerance**2*hbar**2/2./redmass
      if (Hicheck.gt.tolerance.or.Lowcheck.gt.tolerance) then
         Write (6,*) 'ErrorErrorErrorErrorErrorError'
         Write (6,*)  'Energy= ',energy
         Write (6,*)  'photon= ',photon
         Write (6,*)  'J= ',J
         Write (6,*)  'Hicheck= ',Hicheck**2*hbar**2/2./redmass
         Write (6,*)  'Lowcheck= ',Lowcheck**2*hbar**2/2./redmass
         Write (6,*)  'tolerance= ',Tolen
         Write (6,*) '#ErrorErrorErrorErrorErrorError'
         output=0.
         outturn=0.
         goto 1292
      end if
      do i=1,points+1
         plo(i)=plo(i)*scalefactorlow
         phi(i)=phi(i)*scalefactorhigh
      end do
```

```
c   now we do an analysis of the wavefunction
c   product at the evaluation R value
      do i=1,points+1
         if (x(i).le.eval.and.x(i+1).ge.eval) then
            slope= (plo(i+1)-plo(i))/(x(i+1)-x(i))
            yint= plo(i+1) - slope * x(i+1)
            ploval= slope * eval + yint
            slope= (phi(i+1)-phi(i))/(x(i+1)-x(i))
            yint= phi(i+1) - slope * x(i+1)
            phival= slope * eval + yint
            prodpsi= ploval * phival
            goto 2876
         end if
      end do
2876  continue
c now we do the radial part of the transition dipole moment integral
      value=0.0
      do i=1,points
         if (x(i).gt.cutoff) goto 45
         v=plo(i)*phi(i)*trandip(i)
         vplusone=plo(i+1)*phi(i+1)*trandip(i+1)
         value=value + .5*(x(i+1)-x(i))*(v+vplusone)
      end do
45    continue
      output=value * prodpsi
      outturn=turn
1292  return
      END
```

B.2 Na-He Programs

B.2.1 Collision Induced Absorption

This is the main program, gabsorb_nahe.f, for the calculation of the collision induced absorption spectrum of Na-He. It requires several subroutines: gliff_nahe.f, which is the Gauss-Laguerre integrator of the energy integral and returns the spectral density $VG(\omega)$; matrix_cia_nahe.f, which evaluates the transition dipole matrix element; and gammln.f, gaulag.f, spline.f, and splint.f which are available from *Numerical Recipes*. The program is

compiled via:
g77 gabsorb_nahe.f gliff_nahe.f matrix_cia_nahe.f gammln.f gaulag.f spline.f splint.f -o GABSORB

gabsorb_nahe.f

```
c MAIN PROGRAM
      Implicit Real *8 (a-h,o-z)
      Real *8 interval,convert,kT,loschmidt
      integer pts,epts
      Dimension pho(10000)
      Dimension phonm(10000)
      Character *20 filename
      Write (6,*) 'What output file?'
      Read (5,*) filename
      Write (6,*) 'How many energy points?'
      Read (5,*) epts
      Write (6,*) 'What temperature?'
      Read (5,*) Temp
      Write (6,*) 'How many energies?'
      Read (5,*) Ntot
      Write (6,*) 'Starting Energy (cm-1)?'
      Read (5,*) start
      Write (6,*) 'What interval? (cm-1)'
      Read (5,*) interval
c  constants ( I will use ergs for energy)
c                1e-7 J = 1 erg
      Pi = 4*atan(1.)
      h=6.626068d-34 / 1d-7  ! erg*s
      hbar=h/2./Pi
      loschmidt=2.68673d19 ! cm^-3 amagat^-1
      sol=299792458. * 100. ! cm/s
      boltz=1.3806503d-23 / 1d-7  ! erg/K
      kT=boltz*Temp  ! erg
      front= 4*Pi**2 * loschmidt**2 / 3 / hbar / sol
c  conversion from hartree * bohr**6 * a.u.(time) to erg * cm**6 * s
c  just multiply convert with quantity in atomic units to get other units
      convert=4.359748d-11*(5.291772d-09)**6 * 2.418884326505d-17
```

```
      open (37,file=filename)
      Write (37,*) '# Gauss-Laguerre integration of NaHe absorption'
      Write (37,*) '# Temp= ',Temp,' Number of GL points= ',epts
      do i=1,Ntot
           pho(i)=start + (i-1)*interval
      end do
      do i=1,Ntot
c  convert pho(i) from wavenumber(cm-1) to hartree
          photon=pho(i)/219474.63068
c  frequency of photon
          freq=2*Pi*sol*pho(i) ! radians / s
          call gliff_nahe(photon,Temp,epts,output)
c output is in atomic units see above
c gomega is in erg * cm**6 * s
999       gomega=output*convert
          alpha = front * freq * (1.-exp(-1.*hbar*freq/kT)) * gomega
      Write (37,1000) pho(i),output,gomega,alpha
1000  Format (1x,4(E15.8,1x))
      end do
      close (37)
      stop
      end
```

gliff_nahe.f

```
      subroutine gliff_nahe (photon,Temp,epts,output)
      Implicit Real *8 (a-h,o-z)
      real *8 otwo,output,output3,sumout,output2,en,kT
      integer Jval,sele,epts,pts,ppts,zcount,nsurf
      Dimension Eint(200),x(200),w(200)
      hbar=1.
      fourpiepsn=1.
      Pi=4*atan(1.)
      atomboltz=3.16681520371153e-6 ! hartree/K
      kT=atomboltz*Temp
      atomone=22.989770
      atomtwo=4.0026
      redmass=(atomone*atomtwo)/(atomone+atomtwo)/5.4857990e-4
```

```
      thermDB=sqrt(2*Pi*hbar**2/redmass/kT)
      n=epts
      alpha=0.
      call gaulag(x,w,n,alpha)
      intcounter=0
      output3=0.
      do i=1,epts
         en=kT*x(i)
         otwo=0.
         mval=0
         tollpercent=0.1
         turn=1.
         do k=1,351   ! changed from 501
            Jval=k-1
            call matrix_cia_nahe(en,photon,Jval,turn,outturn,output2)
            turn=outturn
            sumout=(2.*Jval+1.)*output2
            otwo=otwo + sumout
            converge=sumout/otwo*100.
            if (converge.le.tollpercent) mval = mval +1
            if (mval.eq.20) goto 335
         end do
335      Eint(i)=kT*otwo/fourpiepsn
336      output3old=output3
         output3=output3 + w(i)*Eint(i)
         if (i.gt.40) then
                  diff=abs(output3-output3old)
            if (diff.lt.1e-8) then
                  intcounter=intcounter+1
         end if
         end if
         if (intcounter.ge.8) goto 337
       end do
337    output=hbar*thermDB**3*output3
       return
       END
```

matrix_cia_nahe.f

```
      Subroutine matrix_cia_nahe (energy,photon,J,turnin,outturn,
     + output)
      Implicit Real *8 (a-h,o-z)
      Integer J,points,lolow,lohigh,intstart,sel,ppot,pdip,nsurf
      Real *8 Lowcheck,Hicheck
      Dimension plo(1050000),phi(1050000)
      Dimension Vhigh(1050000),Vlow(1050000)
      Dimension trandip(1050000),x(1050000),y2(1050000)
      Dimension Ghigh(1050000),Glow(1050000)
      Dimension xnodelow(100000),xnodehigh(100000)
c change these if number of points in potential or dipole change
      Parameter (ppot=30,pdip=28)
      Dimension Rpot(ppot),Apot(ppot),Bpot(ppot),Grpot(ppot)
      Dimension Expot(ppot),Dip(pdip)
      Dimension Rdip(pdip),Adip(pdip),Bdip(pdip)
c  Here I have hardwired in my Potential Surface's
c  and Transition Dipole surface's
c  for use with spline later
      Data Rpot/   1.,1.5,2.,2.5,3.,3.5,4.,4.5,5.,5.5,6.,6.5,7.,7.5,8.,
     +   8.5,9.,9.5,10.,10.5,11.,11.5,12.,12.5,14.,15.,16.,17.,19.,20. /
      Data Grpot/ 2.73381516,0.956943145,0.30227557,0.0990011669,
     + 0.037009445,0.0174928486,0.0104524857,0.00706001695,
     + 0.00489042231,0.0033342449,0.00221179542,0.0014263527,
     + 0.000895824681,0.000548530382,0.000327124232,
     + 0.000189282033,0.000105441936,5.5688053E-05,2.696694E-05,
     + 1.0932961E-05,2.37560897E-06,-1.885351E-06,-3.74945299E-06,
     + -4.32741899E-06,-3.40781901E-06,-2.47360603E-06,-1.74246E-06,
     + -1.22421201E-06,-6.23933005E-07,-4.55267013E-07/
      Data Rdip/ 1.0,1.5,2.0,2.5,3.0,3.5,4.0,4.5,5.0,5.5,6.0,6.5,7.0,
     +           7.5,8.0,8.5,9.0,9.5,10.0,10.5,11.0,11.5,12.0,12.5,
     +           13.0,13.5,14.0,20.0 /
      Data Dip/  0.44814370,1.01176043,1.15104425,1.25172714,1.24686198,
     +  1.14636423,0.98631350,0.80381127,0.62709058,0.47221563,
     +  0.34543861,0.24664936,0.17245739,0.11832678,0.07978292,
     +  0.05291711,0.03455124,0.02221700,0.01406915,0.00877205,
     +  0.00537498,0.00322965,0.00189505,0.00108311,0.00059580,
     +  0.00030445,0.00014183,0. /
       hbar=1.
```

```
c Na,He specific data
       atomone=22.989770
       atomtwo=4.0026
       phottolerance=1e-5
       Pi= 4*atan(1.0)
       redmass=1/5.4857990e-4*(atomone*atomtwo)/(atomone+atomtwo)
       Enlow=energy
       Enhigh=energy+photon      !-atomictransition
       if (Enhigh.le.phottolerance) then
c         write (6,*) J,Enlow,Enhigh,photon,atomictransition
          output=0.
          outturn=turnin
          goto 1292
       end if
c  this is tolerance for exponential increase of wave function
c  and other parameters for integration
       tolpsi=1.0D250
       DBnum=30.
       final=300.
       cutoff=20.
c  this determines selection rules for J-J transitions
c  J to J is selection=0.
c  J to J+1 is selection=1.
c  J to J is selection=-1.
       selection=0.
c  define an initial starting point
       turninterval=0.
3457   turn=turnin + turninterval
c   Determine step size want DBnum points per DeBroglie wavelength
c   We use higher energy wave function to determine step size
      if (Enhigh.gt.Enlow) then
        Encheck=Enhigh
       else
        Encheck=Enlow
      end if
      debroglie=hbar/(2.*redmass*Encheck)**(1/2.)
      s=debroglie/DBnum
      rational=(final-turn)/debroglie*DBnum
```

```
      points=int(rational)
      if (points.gt.1000000) then
        Write (6,*) 'ERRORERRORERRORERRORERRORERRORERRORERROR'
        write (6,*) ''
        Write (6,*) 'Enhigh= ',Enhigh
        Write (6,*) 'DeBroglie= ',debroglie
        Write (6,*) 'Turn= ',turn
        Write (6,*) 'Outer= ',final
        Write (6,*) 'stepsize= ',s
        Write (6,*) 'points= ',points
        Write (6,*) ''
        Write (6,*) 'ERRORERRORERRORERRORERRORERRORERRORERROR'
        output=0.
        outturn=turn
        goto 1292
      end if
      do i=0,points
        x(i+1)=turn+i*s
      end do
C Initialize Ground state Potential energy surface
      gr1=(Grpot(2)-Grpot(1))/(Rpot(2)-Rpot(1))
      grn=(Grpot(ppot)-Grpot(ppot-1))/(Rpot(ppot)-Rpot(ppot-1))
      call spline (Rpot,Grpot,ppot,gr1,grn,y2)
      do i=1,points+1
      rad=x(i)
      if (rad.gt.cutoff) then
         Vlow(i)=0.
         Vhigh(i)=0.
      else
         call splint(Rpot,Grpot,y2,ppot,rad,en)
         Vlow(i)=en
         Vhigh(i)=en
      end if
      end do
C Initialize Dipole moment surface
      td1=(Dip(2)-Dip(1))/(Rdip(2)-Rdip(1))
      tdn=(Dip(pdip)-Dip(pdip-1))/(Rdip(pdip)-Rdip(pdip-1))
      call spline(Rdip,Dip,pdip,td1,tdn,y2)
```

```
 done=Dip(pdip-1)
 dtwo=Dip(pdip)
 rone=Rdip(pdip-1)
 rtwo=Rdip(pdip)
 do i=1,points+1
 rad=x(i)
 if (rad.gt.Rdip(pdip)) then
     trandip(i)=0.
 else
    call splint(Rdip,Dip,y2,pdip,rad,td)
    trandip(i)=td
 end if
 end do
 do i=1,points+1
      al=J
      Glow(i)=2*redmass/(hbar*hbar)*(Vlow(i)-Enlow)
++ al*(al+1)/(x(i)**2)
      alhigh=J+selection
      Ghigh(i)=2*redmass/(hbar*hbar)*(Vhigh(i)-Enhigh)
++ alhigh*(alhigh+1)/(x(i)**2)
 end do
 plo(1)=0.
 plo(2)=0.0001
 phi(1)=0.
 phi(2)=0.0001
 nodelow=1
 xnodelow(1)=0.
 nodehigh=1
 xnodehigh(1)=0.
 do i=2,points
 plo(i+1)=(2*plo(i)-plo(i-1)+5*Glow(i)*plo(i)*s**2/6
++Glow(i-1)*plo(i-1)*s**2/12)/(1-Glow(i+1)*s**2/12)
 phi(i+1)=(2*phi(i)-phi(i-1)+5*Ghigh(i)*phi(i)*s**2/6
++Ghigh(i-1)*phi(i-1)*s**2/12)/(1-Ghigh(i+1)*s**2/12)
 if (plo(i+1).gt.tolpsi) then
    turninterval=turninterval+.1
    goto 3457
 end if
```

```
      if (phi(i+1).gt.tolpsi) then
         turninterval=turninterval+.1
         goto 3457
      end if
      testlow=plo(i)*plo(i+1)
      if (testlow.le.0.) then
         nodelow=nodelow+1
         xnodelow(nodelow)=x(i)-plo(i)*((x(i+1)-x(i))
     +/(plo(i+1)-plo(i)))
         nodelowmax=nodelow
      end if
      testhigh=phi(i)*phi(i+1)
      if (testhigh.le.0.) then
         nodehigh=nodehigh+1
         xnodehigh(nodehigh)=x(i)-phi(i)*((x(i+1)-x(i))
     +/(phi(i+1)-phi(i)))
         nodehighmax=nodehigh
      end if
      end do
c  first we find maximum of last peak in wavefunctions
c  ground state
      do i=2,points
      if (plo(i).le.0) then
         goto 456
      end if
      if (plo(i).gt.plo(i+1).and.plo(i).gt.plo(i-1)) then
      if (xnodelow(nodelowmax).gt.x(i)) then
         amaxlow=plo(i)
         rmaxlow=x(i)
         goto 456
      end if
      end if
456   end do
c  excited state
      do i=2,points
      if (phi(i).le.0) then
         goto 457
      end if
```

```
      if (phi(i).gt.phi(i+1).and.phi(i).gt.phi(i-1))
     +then
      if (xnodehigh(nodehighmax).gt.x(i)) then
         amaxhigh=phi(i)
         rmaxhigh=x(i)
         goto 457
      end if
      end if
457   end do
      checklo=sqrt(2*redmass*Enlow/hbar**2)
      checkhi=sqrt(2*redmass*Enhigh/hbar**2)
c changed normalization to use input values of energies
      Enormlow=sqrt(2*redmass/Pi/hbar**2/checklo)
      scalefactorlow=1/amaxlow * Enormlow
      Enormhigh=sqrt(2*redmass/Pi/hbar**2/checkhi)
      scalefactorhigh=1/amaxhigh * Enormhigh
      wavelengthlow=2.*(xnodelow(nodelowmax)-xnodelow(nodelowmax-1))
      wavevectorlow=2.0 * Pi / wavelengthlow
      wavelengthhigh=2*(xnodehigh(nodehighmax)-xnodehigh(nodehighmax-1))
      wavevectorhigh=2.0 * Pi / wavelengthhigh
      Hicheck=abs(checkhi-wavevectorhigh)
      Lowcheck=abs(checklo-wavevectorlow)
      tolerance=0.1
      Tolen=tolerance**2*hbar**2/2./redmass
      if (Hicheck.gt.tolerance.or.Lowcheck.gt.tolerance) then
         Write (6,*) 'ErrorErrorErrorErrorErrorError'
         Write (6,*)  'Energy= ',energy
         Write (6,*)  'photon= ',photon
         Write (6,*)  'J= ',J
         Write (6,*)  'Hicheck= ',Hicheck**2*hbar**2/2./redmass
         Write (6,*)  'Lowcheck= ',Lowcheck**2*hbar**2/2./redmass
         Write (6,*)  'tolerance= ',Tolen
         Write (6,*) '#ErrorErrorErrorErrorErrorError'
         output=0.
         outturn=0.
         goto 1292
      end if
      do i=1,points+1
```

```
         plo(i)=plo(i)*scalefactorlow
         phi(i)=phi(i)*scalefactorhigh
      end do
c now we do the radial part of the transition dipole moment integral
      value=0.0
      do i=1,points
         if (x(i).gt.cutoff) goto 45
         v=plo(i)*phi(i)*trandip(i)
         vplusone=plo(i+1)*phi(i+1)*trandip(i+1)
         value=value + .5*(x(i+1)-x(i))*(v+vplusone)
      end do
45    continue
      output=value**2
      outturn=turn
1292  return
      END
```

B.2.2 Free-Free Broadening of the Na D-line

This is the main program, gabsorb_nahe.f, for the calculation of the broadening of the Na D-line due to helium, from free-free matrix contributions. It requires several subroutines: gliff_nahe.f, which is the Gauss-Laguerre integrator of the energy integral and returns the spectral density $VG(\omega)$; matrix_nahe.f, which evaluates the transition dipole matrix element; and gammln.f, gaulag.f, spline.f, and splint.f which are available from *Numerical Recipes*. The program is compiled via:
g77 gabsorb_nahe.f gliff_nahe.f matrix_cia_nahe.f gammln.f gaulag.f spline.f splint.f -o GABSORB_NAHE

gabsorb_nahe.f

```
      Implicit Real *8 (a-h,o-z)
      Real *8 interval,convert,kT,loschmidt
      integer pts,epts
      Dimension pho(10000)
      Dimension phonm(10000)
      Character *20 filename
      Write (6,*) 'What output file?'
      Read (5,*) filename
      Write (6,*) 'How many energy points?'
```

```
      Read (5,*) epts
      Write (6,*) 'What temperature?'
      Read (5,*) Temp
      Write (6,*) 'How many energies?'
      Read (5,*) Ntot
      Write (6,*) 'Starting Energy (nm)?'
      Read (5,*) start
      Write (6,*) 'What interval? (nm)'
      Read (5,*) interval
      Write (6,*) 'Which Potential Surface (A=0, B=1)?'
      read (5,*) nsurf
c  constants ( I will use ergs for energy)
c                1e-7 J = 1 erg
      Pi = 4*atan(1.)
      h=6.626068d-34 / 1d-7  ! erg*s
      hbar=h/2./Pi
      loschmidt=2.68673d19 ! cm^-3 amagat^-1
      sol=299792458. * 100. ! cm/s
      boltz=1.3806503d-23 / 1d-7  ! erg/K
      kT=boltz*Temp  ! erg
      front= 4*Pi**2 * loschmidt**2 / 3 / hbar / sol
c  conversion from hartree * bohr**6 * a.u.(time) to erg * cm**6 * s
c  just multiply convert with quantity in atomic units to get other units
      convert=4.359748d-11*(5.291772d-09)**6 * 2.418884326505d-17
      open (37,file=filename)
      Write (37,*) '# Gauss-Laguerre integration of NaHe absorption'
      Write (37,*) '# Temp= ',Temp,' Number of GL points= ',epts
      do i=1,Ntot
c convert from nm to cm^-1
           pho(i)=1.e7/(start+(i-1)*interval)
           phonm(i)=start + (i-1)*interval
      end do
      do i=1,Ntot
c  convert pho(i) from wavenumber(cm-1) to hartree
          photon=pho(i)/219474.63068
c  frequency of photon
          freq=2*Pi*sol*pho(i) ! radians / s
      if (phonm(i).gt.587.and.phonm(i).lt.591) then
```

```
                output=0.
                goto 999
        end if
            call gliff_nahe(photon,Temp,nsurf,epts,output)
c output is in atomic units see above
c gomega is in erg * cm**6 * s
999         gomega=output*convert
            alpha = front * freq * (1.-exp(-1.*hbar*freq/kT)) * gomega
        Write (37,1000) pho(i),output,gomega,alpha
1000    Format (1x,4(E15.8,1x))
        end do
        close (37)
        stop
        end
```

gliff_nahe.f

```
        subroutine gliff_nahe (photon,Temp,nsurf,epts,output)
        Implicit Real *8 (a-h,o-z)
        real *8 otwo,output,output3,sumout,output2,en,kT
        integer Jval,sele,epts,pts,ppts,zcount,nsurf
        Dimension Eint(200),x(200),w(200)
        hbar=1.
        fourpiepsn=1.
        Pi=4*atan(1.)
        atomboltz=3.16681520371153e-6 ! hartree/K
        kT=atomboltz*Temp
        atomone=22.989770
        atomtwo=4.0026
        redmass=(atomone*atomtwo)/(atomone+atomtwo)/5.4857990e-4
        thermDB=sqrt(2*Pi*hbar**2/redmass/kT)
        n=epts
        alpha=0.
        call gaulag(x,w,n,alpha)
c  figure out if there is a dead zone
        atomictransition=16967.62607310/219474.63068
        deadzone=atomictransition-photon
        if (deadzone.le.0.) then
```

```
            deadzone=0.
      end if
      intcounter=0
      output3=0.
      do i=1,epts
         en=kT*x(i) + deadzone
         otwo=0.
         mval=0
         tollpercent=0.1
         turn=1.
         do k=1,451   ! changed from 501
            Jval=k-1
            call matrix_nahe(en,photon,Jval,nsurf,turn,outturn,output2)
            turn=outturn
            sumout=(2.*Jval+1.)*output2
            otwo=otwo + sumout
            converge=sumout/otwo*100.
            if (converge.le.tollpercent) mval = mval +1
            if (mval.eq.40) goto 335
         end do
335      Eint(i)=exp(-deadzone/kT)*kT*otwo/fourpiepsn
336      output3old=output3
         output3=output3 + w(i)*Eint(i)
         if (i.gt.40) then
                  diff=abs(output3-output3old)
            if (diff.lt.1e-8) then
                  intcounter=intcounter+1
         end if
         end if
         if (intcounter.ge.30) goto 337
       end do
337    output=hbar*thermDB**3*output3
       return
       END
```

matrix_nahe.f

```
      Subroutine matrix_nahe (energy,photon,J,nsurf,turnin,outturn,
```

```
     + output)
      Implicit Real *8 (a-h,o-z)
      Integer J,points,lolow,lohigh,intstart,sel,ppot,pdip,nsurf
      Real *8 Lowcheck,Hicheck
      Dimension plo(1050000),phi(1050000)
      Dimension Vhigh(1050000),Vlow(1050000)
      Dimension trandip(1050000),x(1050000),y2(1050000)
      Dimension Ghigh(1050000),Glow(1050000)
      Dimension xnodelow(100000),xnodehigh(100000)
c change these if number of points in potential or dipole change
      Parameter (ppot=30,pdip=21)
      Dimension Rpot(ppot),Apot(ppot),Bpot(ppot),Grpot(ppot)
      Dimension Expot(ppot),Dip(pdip)
      Dimension Rdip(pdip),Adip(pdip),Bdip(pdip)
c  Here I have hardwired in my Potential Surface's and
c  Transition Dipole surface's for use with spline later
      Data Rpot/   1.,1.5,2.,2.5,3.,3.5,4.,4.5,5.,5.5,6.,6.5,7.,7.5,8.,
     +   8.5,9.,9.5,10.,10.5,11.,11.5,12.,12.5,14.,15.,16.,17.,19.,20. /
      Data Expot/ ppot*0. /
      Data Apot/   2.76562535,0.958372398,0.298986506,0.0971379567,
     + 0.0388018176,0.0231732823,0.0189425895,0.0167587903,0.0144307489
     + ,0.0119077898,0.00949276165,0.00738218455,0.00563860177,
     + 0.00424734193,0.00316217365,0.00232972877,0.00169984611,
     + 0.00122897403,0.000880823937,0.000626005131,0.000441244452,
     + 0.000308455903,0.000213810724,0.000146886998,4.4667457E-05,
     + 1.8727141E-05,7.02568298E-06,2.020648E-06,-6.12960008E-07,
     + -7.45365014E-07/
      Data Bpot/ 2.69733875,0.938287967,0.281909966,0.0787754358,
     + 0.0188314227,0.0023577089,-0.0014022289,-0.0017660459,
     + -0.0014103944,-0.0010103617,-0.00070060490,-0.00048250115,
     + -0.00033296145,-0.00023089286,-0.00016113323,-0.0001133075,
     + -8.0356503E-05,-5.7503293E-05,-4.1537022E-05,-3.0300905E-05,
     + -2.2336951E-05,-1.6650014E-05,-1.2555143E-05,-9.57862702E-06,
     + -4.548482E-06,-2.91088199E-06,-1.92794803E-06,-1.31564502E-06,
     + -6.59883E-07,-4.81863992E-07/
      Data Grpot/ 2.73381516,0.956943145,0.30227557,0.0990011669,
     + 0.037009445,0.0174928486,0.0104524857,0.00706001695,
     + 0.00489042231,0.0033342449,0.00221179542,0.0014263527,
```

```
     + 0.000895824681,0.000548530382,0.000327124232,
     + 0.000189282033,0.000105441936,5.5688053E-05,2.696694E-05,
     + 1.0932961E-05,2.37560897E-06,-1.885351E-06,-3.74945299E-06,
     + -4.32741899E-06,-3.40781901E-06,-2.47360603E-06,-1.74246E-06,
     + -1.22421201E-06,-6.23933005E-07,-4.55267013E-07/
      Data Rdip/ 3.0,3.25,3.5,3.75,4.0,4.25,4.5,4.75,5.0,5.5,6.0,6.5,
     + 7.0,7.5,8.0,9.0,10.0,11.0,12.0,13.0,14.0 /
      Data Dip/ pdip*0. /
      Data Adip/ 2.1516167,2.1553012,2.1721222,2.1995741,2.2338385,
     + 2.2706806,2.3069016,2.3403384,2.3704835,2.4205249,2.4601838,
     + 2.4925631,2.5193888,2.5414987,2.5593342,2.5838154,2.5968623,
     + 2.6027320,2.6047979,2.6050807,2.6045106 /
      Data Bdip/ 2.6996479,2.6898742,2.6798396,2.6700980,2.6609330,
     + 2.6525204,2.6444580,2.6370604,2.6301830,2.6183212,2.6095147,
     + 2.6036004,2.5996892,2.5980310,2.5971339,2.5970195,2.5978637,
     + 2.5987230,2.5994771,2.6000474,2.6004311/
       hbar=1.
c Na,He specific data
       atomictransition=16967.62607310/219474.63068    ! hartree
       atomone=22.989770
       atomtwo=4.0026
       phottolerance=1e-5
       Pi= 4*atan(1.0)
       redmass=1/5.4857990e-4*(atomone*atomtwo)/(atomone+atomtwo)
       Enlow=energy
       Enhigh=energy+photon-atomictransition
       if (Enhigh.le.phottolerance) then
c         write (6,*) J,Enlow,Enhigh,photon,atomictransition
          output=0.
          outturn=turnin
          goto 1292
       end if
c  this is tolerance for exponential increase of wave function
c  and other parameters for integration
       tolpsi=1.0D250
       DBnum=30.
       final=300.
       cutoff=20.
```

```
c  this determines selection rules for J-J transitions
c  J to J is selection=0.
c  J to J+1 is selection=1.
c  J to J is selection=-1.
       selection=0.
c  choose A state or B state
c  A state is nsurf=0
c  B state is nsurf=anything else (set it as 1)
      if (nsurf.eq.0) then
         do i=1,ppot
            Expot(i)=Apot(i)
         end do
         do i=1,pdip
            Dip(i)=Adip(i)
         end do
       else
         do i=1,ppot
            Expot(i)=Bpot(i)
         end do
         do i=1,pdip
            Dip(i)=Bdip(i)
         end do
      end if
c  define an initial starting point
       turninterval=0.
3457   turn=turnin + turninterval
c   Determine step size want DBnum points per DeBroglie wavelength
c   We use higher energy wave function to determine step size
      if (Enhigh.gt.Enlow) then
         Encheck=Enhigh
       else
         Encheck=Enlow
      end if
      debroglie=hbar/(2.*redmass*Encheck)**(1/2.)
      s=debroglie/DBnum
      rational=(final-turn)/debroglie*DBnum
      points=int(rational)
      if (points.gt.1000000) then
```

```
        Write (6,*) 'ERRORERRORERRORERRORERRORERRORERRORERROR'
        write (6,*) ''
        Write (6,*) 'Enhigh= ',Enhigh
        Write (6,*) 'DeBroglie= ',debroglie
        Write (6,*) 'Turn= ',turn
        Write (6,*) 'Outer= ',final
        Write (6,*) 'stepsize= ',s
        Write (6,*) 'points= ',points
        Write (6,*) ''
        Write (6,*) 'ERRORERRORERRORERRORERRORERRORERRORERROR'
        output=0.
        outturn=turn
        goto 1292
      end if
      do i=0,points
        x(i+1)=turn+i*s
      end do
C Initialize Ground state Potential energy surface
      gr1=(Grpot(2)-Grpot(1))/(Rpot(2)-Rpot(1))
      grn=(Grpot(ppot)-Grpot(ppot-1))/(Rpot(ppot)-Rpot(ppot-1))
      call spline (Rpot,Grpot,ppot,gr1,grn,y2)
      do i=1,points+1
      rad=x(i)
      if (rad.gt.cutoff) then
         Vlow(i)=0.
      else
         call splint(Rpot,Grpot,y2,ppot,rad,en)
         Vlow(i)=en
      end if
      end do
C Initialize Excited State Potential energy Surface
      gr1=(Expot(2)-Expot(1))/(Rpot(2)-Rpot(1))
      grn=(Expot(ppot)-Expot(ppot-1))/(Rpot(ppot)-Rpot(ppot-1))
      call spline (Rpot,Expot,ppot,gr1,grn,y2)
      do i=1,points+1
      rad=x(i)
      if (rad.gt.cutoff) then
         Vhigh(i)=0.
```

```
      else
         call splint(Rpot,Expot,y2,ppot,rad,en)
         Vhigh(i)=en
      end if
      end do
C Initialize Dipole moment surface
      td1=(Dip(2)-Dip(1))/(Rdip(2)-Rdip(1))
      tdn=(Dip(pdip)-Dip(pdip-1))/(Rdip(pdip)-Rdip(pdip-1))
      call spline(Rdip,Dip,pdip,td1,tdn,y2)
      done=Dip(pdip-1)
      dtwo=Dip(pdip)
      rone=Rdip(pdip-1)
      rtwo=Rdip(pdip)
      cthree=(rone**3*(done-dtwo))/(1-(rone**3/rtwo**3))
      dfit=dtwo-cthree/rtwo**3
      do i=1,points+1
      rad=x(i)
      if (rad.gt.Rdip(pdip)) then
         trandip(i)=cthree/rad**3 + dfit
      else
         call splint(Rdip,Dip,y2,pdip,rad,td)
         trandip(i)=td
      end if
      end do
      do i=1,points+1
           al=J
           Glow(i)=2*redmass/(hbar*hbar)*(Vlow(i)-Enlow)
     ++ al*(al+1)/(x(i)**2)
           alhigh=J+selection
           Ghigh(i)=2*redmass/(hbar*hbar)*(Vhigh(i)-Enhigh)
     ++ alhigh*(alhigh+1)/(x(i)**2)
      end do
      plo(1)=0.
      plo(2)=0.0001
      phi(1)=0.
      phi(2)=0.0001
      nodelow=1
      xnodelow(1)=0.
```

```
      nodehigh=1
      xnodehigh(1)=0.
      do i=2,points
      plo(i+1)=(2*plo(i)-plo(i-1)+5*Glow(i)*plo(i)*s**2/6
     ++Glow(i-1)*plo(i-1)*s**2/12)/(1-Glow(i+1)*s**2/12)
      phi(i+1)=(2*phi(i)-phi(i-1)+5*Ghigh(i)*phi(i)*s**2/6
     ++Ghigh(i-1)*phi(i-1)*s**2/12)/(1-Ghigh(i+1)*s**2/12)
      if (plo(i+1).gt.tolpsi) then
         turninterval=turninterval+.1
         goto 3457
      end if
      if (phi(i+1).gt.tolpsi) then
         turninterval=turninterval+.1
         goto 3457
      end if
      testlow=plo(i)*plo(i+1)
      if (testlow.le.0.) then
         nodelow=nodelow+1
         xnodelow(nodelow)=x(i)-plo(i)*((x(i+1)-x(i))
     +/(plo(i+1)-plo(i)))
         nodelowmax=nodelow
      end if
      testhigh=phi(i)*phi(i+1)
      if (testhigh.le.0.) then
         nodehigh=nodehigh+1
         xnodehigh(nodehigh)=x(i)-phi(i)*((x(i+1)-x(i))
     +/(phi(i+1)-phi(i)))
         nodehighmax=nodehigh
      end if
      end do
c  first we find maximum of last peak in wavefunctions
c  ground state
      do i=2,points
      if (plo(i).le.0) then
         goto 456
      end if
      if (plo(i).gt.plo(i+1).and.plo(i).gt.plo(i-1)) then
      if (xnodelow(nodelowmax).gt.x(i)) then
```

```
         amaxlow=plo(i)
         rmaxlow=x(i)
         goto 456
      end if
      end if
456   end do
c  excited state
      do i=2,points
      if (phi(i).le.0) then
         goto 457
      end if
      if (phi(i).gt.phi(i+1).and.phi(i).gt.phi(i-1))
     +then
      if (xnodehigh(nodehighmax).gt.x(i)) then
         amaxhigh=phi(i)
         rmaxhigh=x(i)
         goto 457
      end if
      end if
457   end do
      checklo=sqrt(2*redmass*Enlow/hbar**2)
      checkhi=sqrt(2*redmass*Enhigh/hbar**2)
c changed normalization to use input values of energies
      Enormlow=sqrt(2*redmass/Pi/hbar**2/checklo)
      scalefactorlow=1/amaxlow * Enormlow
      Enormhigh=sqrt(2*redmass/Pi/hbar**2/checkhi)
      scalefactorhigh=1/amaxhigh * Enormhigh
      wavelengthlow=2.*(xnodelow(nodelowmax)-xnodelow(nodelowmax-1))
      wavevectorlow=2.0 * Pi / wavelengthlow
      wavelengthhigh=2*(xnodehigh(nodehighmax)-xnodehigh(nodehighmax-1))
      wavevectorhigh=2.0 * Pi / wavelengthhigh
      Hicheck=abs(checkhi-wavevectorhigh)
      Lowcheck=abs(checklo-wavevectorlow)
      tolerance=0.1
      Tolen=tolerance**2*hbar**2/2./redmass
      if (Hicheck.gt.tolerance.or.Lowcheck.gt.tolerance) then
         Write (6,*) 'ErrorErrorErrorErrorErrorError'
         Write (6,*)  'Energy= ',energy
```

```
         Write (6,*)  'photon= ',photon
         Write (6,*)  'J= ',J
         Write (6,*)  'Hicheck= ',Hicheck**2*hbar**2/2./redmass
         Write (6,*)  'Lowcheck= ',Lowcheck**2*hbar**2/2./redmass
         Write (6,*)  'tolerance= ',Tolen
         Write (6,*) '#ErrorErrorErrorErrorErrorError'
         output=0.
         outturn=0.
         goto 1292
      end if
      do i=1,points+1
         plo(i)=plo(i)*scalefactorlow
         phi(i)=phi(i)*scalefactorhigh
      end do
c now we do the radial part of the transition dipole moment integral
      value=0.0
      do i=1,points
         if (x(i).gt.cutoff) goto 45
         v=plo(i)*phi(i)*trandip(i)*(Vhigh(i)-Vlow(i))
         vplusone=plo(i+1)*phi(i+1)*trandip(i+1)*(Vhigh(i+1)-Vlow(i+1))
         value=value + .5*(x(i+1)-x(i))*(v+vplusone)
      end do
45    continue
      front=2*redmass/hbar**2/(checkhi**2-checklo**2)
      output=(front*value)**2
      outturn=turn
1292  return
      END
```

B.2.3 Free-Bound Broadening of the Na D-line

This is the main program, absorbB1.bound.f, for the calculation of the of the free-bound contribution to the broadening of the Na D-line due to Helium. It requires several subroutines: fb_matrix_nahe.f, which evaluates the transition dipole matrix element; and spline.f and splint.f which are available from *Numerical Recipes*. The program also requires two other files as input: *vibrotlevels* and *BoundWave*. The file *vibrotlevels* contains five columns: rotational quantum number, vibrational quantum number, the overall depth of the energy well, the energy of the state obtained via Numerov-Cooley integration, and the difference

between the the two. The second file *BoundWave* contains the bound-state wavefunctions for each ro-vibrational level and contains two columns: bond distance and value of Psi. This file needs to be be formatted correctly (see subroutine fb_matrix_nahe.f for details). The program is compiled via:
g77 absorbB1.bound.f fb_matrix_nahe.f spline.f splint.f -o ABSORB.B1

absorbB1.bound.f

```
      Implicit Real *8 (a-h,o-z)
      Real *8 ephoton,output,interval,loschmidt
      Dimension pho(1000),pnm(1000)
      integer ivib,irot
      Character *20 filename,filename2
      Write (6,*) 'What output file?'
      Read (5,*) filename
      Write (6,*) 'What output file for vibrational contributions?'
      Read (5,*) filename2
      Write (6,*) 'What Temperature?'
      Read (5,*) Temp
      Write (6,*) 'Careful, bound absorption is not defined for energies
     + greater than the atomic transition'
      Write (6,*) 'How many energies?'
      Read (5,*) Ntot
      Write (6,*) 'Starting Wavelength (nm)?'
      Read (5,*) start
      Write (6,*) 'What interval?'
      Read (5,*) interval
      if (start.le.590) then
      write (6,*) ''
      write (6,*) 'ERROR'
      write (6,*) 'There is no absorption for wavelengths less than the
     +  atomic transition!'
      write (6,*) 'ERROR'
      write (6,*) ''
      goto 1834
      end if
c  constants ( I will use ergs for energy)
c                 1e-7 J = 1 erg
```

```
      Pi = 4*atan(1.)
      h=6.626068d-34 / 1d-7  ! erg*s
      hbar=h/2./Pi
      loschmidt=2.68673d19 ! cm^-3 amagat^-1
      sol=299792458. * 100. ! cm/s
      boltz=1.3806503d-23 / 1d-7  ! erg/K
      kT=boltz*Temp  ! erg
      front= 4.*Pi**2. * loschmidt**2. / 3. / hbar / sol
c  conversion from hartree * bohr**6 * a.u.(time) to erg * cm**6 * s
c  just multiply convert with quantity in atomic units to get other units
      convert=4.359748d-11*(5.291772d-09)**6 * 2.418884326505d-17
      atomone=22.989770
      atomtwo=4.0026
      redma=(atomone*atomtwo)/(atomone+atomtwo)
c  atomic mass units --> me
      redmass=redma/5.4857990e-4
c need to set up photon vector
c need to have loop that adds up all v,J values
      do i=1,Ntot
         pho(i)=1.e7/(start+(i-1)*interval)
         pnm(i)=start+(i-1)*interval
      end do
      open (37,file=filename)
      open (38,file=filename2)
      Write (37,*) '# Free-Bound contribution to B1 absorption'
      Write (37,*) '# Temp= ',Temp
      Write (37,*) '# Photon energy(cm-1),nm,G(omega),A(omega)'
      Write (38,*) '# Contributions from different vib-levels'
      Write (38,*) '# Temp= ',Temp
      Write (38,*) '# Photon energy(cm-1), nm,Sum, v=0, v=1, v=2, v=3, v
     +=4'
      do i=1,Ntot
           ephoton=pho(i)/219474.63068
           write (6,*) 'pho(',i,')',pho(i)
c first do v=0
           vzero=0.
           do j=0,19
              ivib=0
```

```
            irot=j
           call fb_matrix_nahe(ephoton,ivib,irot,Temp,output)
            if (output.lt.0.) then
                Write (6,*) 'Error for ivib=',ivib,' j=',irot
                goto 17
            end if
            vzero=vzero+output
17        end do
c v=1
          vone=0.
          do j=0,15
            ivib=1
            irot=j
           call fb_matrix_nahe(ephoton,ivib,irot,Temp,output)
            if (output.lt.0.) then
                Write (6,*) 'Error for ivib=',ivib,' j=',irot
                goto 18
            end if
            vone=vone+output
18        end do
c v=2
          vtwo=0.
          do j=0,12
            ivib=2
            irot=j
           call fb_matrix_nahe(ephoton,ivib,irot,Temp,output)
            if (output.lt.0.) then
                Write (6,*)  'Error for ivib=',ivib,' j=',irot
                goto 19
            end if
            vtwo=vtwo+output
19        end do
c v=3
          vthree=0.
          do j=0,9
            ivib=3
            irot=j
           call fb_matrix_nahe(ephoton,ivib,irot,Temp,output)
```

```
            if (output.lt.0.) then
                Write (6,*) 'Error for ivib=',ivib,' j=',irot
                goto 20
            end if
            vthree=vthree+output
20        end do
c v=4
          vfour=0.
          do j=0,5
            ivib=4
            irot=j
           call fb_matrix_nahe(ephoton,ivib,irot,Temp,output)
            if (output.lt.0.) then
                Write (6,*) 'Error for ivib=',ivib,' j=',irot
                goto 21
            end if
            vfour=vfour+output
21        end do
c  add em all up and multiply by pre-factors
          sumtotal=vzero+vone+vtwo+vthree+vfour
          vzero=vzero*convert
          vone=vone*convert
          vtwo=vtwo*convert
          vthree=vthree*convert
          vfour=vfour*convert
          freq=2*Pi*sol*pho(i) ! radians / s
          gomega=sumtotal*convert
          alpha=front*freq*(1.-exp(-1.*hbar*freq/kT)) * gomega
       Write (37,*) pho(i),pnm(i),gomega,alpha
       Write (38,10) pho(i),pnm(i),gomega,vzero,vone,vtwo,vthree,vfour
10        FOrmat (1x,8(E15.8,1x))
      end do
      close(37)
      close(38)
1834  continue
      stop
      end
```

fb_matrix_nahe.f

```
      Subroutine fb_matrix_nahe(photon,ivib,irot,Temp,output)
      Implicit Real *8 (a-h,o-z)
      Integer J,points,lolow,lohigh,intstart,sel,ppot,pdip
      integer l,m
      Real *8 Lowcheck,Hicheck,output,kT
      Dimension plo(1050000),phi(1050000),psinorm(1050000)
      Dimension r(1050000)
      Dimension Vlow(1050000)
      Dimension trandip(1050000),x(1050000),y2(1050000)
      Dimension y4(1050000)
      Dimension Glow(1050000)
      Dimension xnodelow(100000)
      Dimension vibrot(0:30,0:30)
c change these if number of points in potential or dipole change
      Parameter (ppot=30,pdip=21)
      Dimension Rpot(ppot),Apot(ppot),Bpot(ppot),Grpot(ppot)
      Dimension Expot(ppot),Dip(pdip)
      Dimension Rdip(pdip),Adip(pdip),Bdip(pdip)
c  Here I have hardwired in my Potential Surface's and
c  Transition Dipole surface's for use with spline later
      Data Rpot/   1.,1.5,2.,2.5,3.,3.5,4.,4.5,5.,5.5,6.,6.5,7.,7.5,8.,
     +   8.5,9.,9.5,10.,10.5,11.,11.5,12.,12.5,14.,15.,16.,17.,19.,20. /
      Data Expot/ ppot*0. /
      Data Apot/   2.76562535,0.958372398,0.298986506,0.0971379567,
     + 0.0388018176,0.0231732823,0.0189425895,0.0167587903,0.0144307489
     + ,0.0119077898,0.00949276165,0.00738218455,0.00563860177,
     + 0.00424734193,0.00316217365,0.00232972877,0.00169984611,
     + 0.00122897403,0.000880823937,0.000626005131,0.000441244452,
     + 0.000308455903,0.000213810724,0.000146886998,4.4667457E-05,
     + 1.8727141E-05,7.02568298E-06,2.020648E-06,-6.12960008E-07,
     + -7.45365014E-07/
      Data Bpot/ 2.69733875,0.938287967,0.281909966,0.0787754358,
     + 0.0188314227,0.0023577089,-0.0014022289,-0.0017660459,
     + -0.0014103944,-0.0010103617,-0.00070060490,-0.00048250115,
     + -0.00033296145,-0.00023089286,-0.00016113323,-0.0001133075,
     + -8.0356503E-05,-5.7503293E-05,-4.1537022E-05,-3.0300905E-05,
```

```
     + -2.2336951E-05,-1.6650014E-05,-1.2555143E-05,-9.57862702E-06,
     + -4.548482E-06,-2.91088199E-06,-1.92794803E-06,-1.31564502E-06,
     + -6.59883E-07,-4.81863992E-07/
      Data Grpot/ 2.73381516,0.956943145,0.30227557,0.0990011669,
     + 0.037009445,0.0174928486,0.0104524857,0.00706001695,
     + 0.00489042231,0.0033342449,0.00221179542,0.0014263527,
     + 0.000895824681,0.000548530382,0.000327124232,
     + 0.000189282033,0.000105441936,5.5688053E-05,2.696694E-05,
     + 1.0932961E-05,2.37560897E-06,-1.885351E-06,-3.74945299E-06,
     + -4.32741899E-06,-3.40781901E-06,-2.47360603E-06,-1.74246E-06,
     + -1.22421201E-06,-6.23933005E-07,-4.55267013E-07/
      Data Rdip/ 3.0,3.25,3.5,3.75,4.0,4.25,4.5,4.75,5.0,5.5,6.0,6.5,
     + 7.0,7.5,8.0,9.0,10.0,11.0,12.0,13.0,14.0 /
      Data Dip/ pdip*0. /
      Data Adip/ 2.1516167,2.1553012,2.1721222,2.1995741,2.2338385,
     + 2.2706806,2.3069016,2.3403384,2.3704835,2.4205249,2.4601838,
     + 2.4925631,2.5193888,2.5414987,2.5593342,2.5838154,2.5968623,
     + 2.6027320,2.6047979,2.6050807,2.6045106 /
      Data Bdip/ 2.6996479,2.6898742,2.6798396,2.6700980,2.6609330,
     + 2.6525204,2.6444580,2.6370604,2.6301830,2.6183212,2.6095147,
     + 2.6036004,2.5996892,2.5980310,2.5971339,2.5970195,2.5978637,
     + 2.5987230,2.5994771,2.6000474,2.6004311/
        hbar=1.
c Na,He specific data
       atomictransition=16967.62607310/219474.63068    ! hartree
       atomone=22.989770
       atomtwo=4.0026
       phottolerance=1e-5
       Pi= 4*atan(1.0)
       redmass=1/5.4857990e-4*(atomone*atomtwo)/(atomone+atomtwo)
CCCCCCCCCCCCCCCCCCCCCCCCCCCCCCCCCCCCCCCCCC
c number of points in bound state wavefunctions
      normpts=100001
      kT=3.16681520371153e-6*Temp
      Jval=irot
      open (2,file='BoundWave',access='direct'
     +,form='formatted',RECL=47)
      open (3,file='vibrotlevels')
```

```
      do i=1,100
         read (3,*) l,m,c,d,e
         if (e.eq.0.) d=0.
         vibrot(m,l)=d
      end do
      close(3)
      Enhighdiff=vibrot(ivib,irot) !Enhighdiff is negative
      Enlow=Enhighdiff+atomictransition-photon
      if (Enlow.lt.1e-5) goto 1234
c  Use direct access to find wavefunctions
      if (ivib.eq.0) nstart=0
      if (ivib.eq.1) nstart=20
      if (ivib.eq.2) nstart=36
      if (ivib.eq.3) nstart=49
      if (ivib.eq.4) nstart=59
      nnstart=(irot+nstart)*100001
c format line for BoundWave is
c1001       Format (1x,D20.10,5x,D20.10)
      do i=1, normpts
            read (2,7,REC=nnstart+i) r(i),psinorm(i)
7           Format (1x,D20.10,5x,D20.10)
      end do
      close(2)
       if (Enlow.le.phottolerance) then
          output=0.
          goto 1292
       end if
c  this is tolerance for exponential increase of wave function
c  and other parameters for integration
       tolpsi=1.0D250
       DBnum=30.
       final=300.
       cutoff=20.
c  this determines selection rules for J-J transitions
c  J to J is selection=0.
c  J to J+1 is selection=1.
c  J to J is selection=-1.
       selection=0.
```

```
       turn=2.
c   Determine step size want DBnum points per DeBroglie wavelength
c   We use ground state energy wave function to determine step size
      Encheck=Enlow
      debroglie=hbar/(2.*redmass*Encheck)**(1/2.)
      s=debroglie/DBnum
      rational=(final-turn)/debroglie*DBnum
      points=int(rational)
      if (points.gt.1000000) then
        Write (6,*) 'ERRORERRORERRORERRORERRORERRORERRORERROR'
        write (6,*) ''
        Write (6,*) 'Encheck= ',Encheck
        Write (6,*) 'DeBroglie= ',debroglie
        Write (6,*) 'Turn= ',turn
        Write (6,*) 'Outer= ',final
        Write (6,*) 'stepsize= ',s
        Write (6,*) 'points= ',points
        Write (6,*) ''
        Write (6,*) 'ERRORERRORERRORERRORERRORERRORERRORERROR'
        output=0.
        goto 1292
      end if
      do i=0,points
        x(i+1)=turn+i*s
      end do
C Initialize Ground state Potential energy surface
      gr1=(Grpot(2)-Grpot(1))/(Rpot(2)-Rpot(1))
      grn=(Grpot(ppot)-Grpot(ppot-1))/(Rpot(ppot)-Rpot(ppot-1))
      call spline (Rpot,Grpot,ppot,gr1,grn,y2)
      do i=1,points+1
      rad=x(i)
      if (rad.gt.cutoff) then
         Vlow(i)=0.
      else
         call splint(Rpot,Grpot,y2,ppot,rad,en)
         Vlow(i)=en
      end if
      end do
```

```
C Initialize Dipole moment surface
      td1=(Bdip(2)-Bdip(1))/(Rdip(2)-Rdip(1))
      tdn=(Bdip(pdip)-Bdip(pdip-1))/(Rdip(pdip)-Rdip(pdip-1))
      call spline(Rdip,Bdip,pdip,td1,tdn,y2)
      done=Bdip(pdip-1)
      dtwo=Bdip(pdip)
      rone=Rdip(pdip-1)
      rtwo=Rdip(pdip)
      cthree=(rone**3*(done-dtwo))/(1-(rone**3/rtwo**3))
      dfit=dtwo-cthree/rtwo**3
      do i=1,points+1
      rad=x(i)
      if (rad.gt.Rdip(pdip)) then
         trandip(i)=csix/rad**3 + dfit
      else
         call splint(Rdip,Bdip,y2,pdip,rad,td)
         trandip(i)=td
      end if
      end do
c now do excited state wave function
      pnorm1=(psinorm(2)-psinorm(1))/(r(2)-r(1))
      pnormen=(psinorm(normpts)-psinorm(normpts-1))/(r(normpts)
     +-r(normpts-1))
      call spline(r,psinorm,normpts,pnorm1,pnormen,y4)
      do i=1,points+1
      rad=x(i)
      if (x(i).le.20.0.and.x(i).ge.2.0) then
         call splint(r,psinorm,y4,normpts,rad,en)
         phi(i)=en
      else
         phi(i)=0.
      end if
      end do
      do i=1,points+1
           al=Jval
           Glow(i)=2*redmass/(hbar*hbar)*(Vlow(i)-Enlow)
     ++ al*(al+1)/(x(i)**2)
      end do
```

```
      plo(1)=0.
      plo(2)=0.0001
      nodelow=1
      xnodelow(1)=0.
      do i=2,points
      plo(i+1)=(2*plo(i)-plo(i-1)+5*Glow(i)*plo(i)*s**2/6
     ++Glow(i-1)*plo(i-1)*s**2/12)/(1-Glow(i+1)*s**2/12)
      testlow=plo(i)*plo(i+1)
      if (testlow.le.0.) then
         nodelow=nodelow+1
         xnodelow(nodelow)=x(i)-plo(i)*((x(i+1)-x(i))
     +/(plo(i+1)-plo(i)))
         nodelowmax=nodelow
      end if
      end do
c  first we find maximum of last peak in wavefunctions
c  ground state
      do i=2,points
      if (plo(i).le.0) then
         goto 456
      end if
      if (plo(i).gt.plo(i+1).and.plo(i).gt.plo(i-1)) then
      if (xnodelow(nodelowmax).gt.x(i)) then
         amaxlow=plo(i)
         rmaxlow=x(i)
         goto 456
      end if
      end if
456   end do
      checklo=sqrt(2*redmass*Enlow/hbar**2)
c changed normalization to use input values of energies
      Enormlow=sqrt(2*redmass/Pi/hbar**2/checklo)
      scalefactorlow=1/amaxlow * Enormlow
      wavelengthlow=2.*(xnodelow(nodelowmax)-xnodelow(nodelowmax-1))
      wavevectorlow=2.0 * Pi / wavelengthlow
      Lowcheck=abs(checklo-wavevectorlow)
      tolerance=0.1
      Tolen=tolerance**2*hbar**2/2./redmass
```

```
      if (Lowcheck.gt.tolerance) then
         Write (6,*) 'ErrorErrorErrorErrorErrorError'
         Write (6,*)  'Energy= ',energy
         Write (6,*)  'photon= ',photon
         Write (6,*)  'J= ',J
         Write (6,*)  'Hicheck= ',Hicheck**2*hbar**2/2./redmass
         Write (6,*)  'Lowcheck= ',Lowcheck**2*hbar**2/2./redmass
         Write (6,*)  'tolerance= ',Tolen
         Write (6,*) '#ErrorErrorErrorErrorErrorError'
         output=0.
         outturn=0.
         goto 1292
      end if
      do i=1,points+1
         plo(i)=plo(i)*scalefactorlow
      end do
c now we do the radial part of the transition dipole moment integral
      value=0.0
      do i=1,points
         if (x(i).gt.cutoff) goto 45
         v=plo(i)*phi(i)*trandip(i)
         vplusone=plo(i+1)*phi(i+1)*trandip(i+1)
         value=value + .5*(x(i+1)-x(i))*(v+vplusone)
      end do
45    continue
      output=(2.*Jval+1)*exp(-Enlow/kT)*value**2
      goto 1292
1234  continue
      output=0.
1292  return
      END
```

Vita

Timothy Carl Lillestolen was born October 23, 1977, in Bridgeport, CT, to Tom and Kathy Lillestolen. After a brief stint in Wyoming, where he was joined by a brother (Jon), the family settled in Knoxville, TN in 1982. In 1990, the family relocated to Växjo, Sweden, where they spent three years. Upon their return to America, they moved back to Knoxville, where the author was enrolled in Bearden High School. After graduating high school in 1996, he enrolled at Presbyterian College (Clinton, SC), where he graduated *thank you laude* with a degree in Chemistry (2000) and a minor in Mathematics. Following this he took up Theoretical/Computational Chemistry in the PhD program at the University of Tennessee, where he studied under the tutelage of Professor R.J. Hinde. The author graduated with a degree in Chemical Physics in August 2005, and probably still hasn't decided what he wants to be when he grows up.